UNIVERSITÀ
DEGLI STUDI
DI PADOVA

Sede Amministrativa: Università degli Studi di Padova

Dipartimento di MEDICINA MOLECOLARE

CORSO DI DOTTORATO DI RICERCA IN: BIOMEDICINA
CURRICOLO: Medicina Rigenerativa
CICLO XXIX

DEVELOPMENT OF A MURINE MODEL FOR THE EXPLORATION OF THE BIOLOGICAL EFFECTS OF EXTERNAL VOLUME EXPANSION

SVILUPPO DI UN MODELLO MURINO PER L'ESPLORAZIONE DEGLI EFFETTI BIOLOGICI DELL'ESPANSIONE VOLUMETRICA ESTERNA

Coordinatore: Ch.mo Prof. Stefano Piccolo
Supervisore: Ch.mo Prof. Vincenzo Vindigni

Dottorando: Luca Lancerotto

INDEX

ABSTRACT

Background: External Volume Expansion (EVE) refers to a class of devices that non-invasively stretch and expand tissue compartments by external application of suction. EVE has been suggested to increase compartments volume and stimulate the formation of a more developed vascular network, leading to less stiff and better vascularized tissues. It is proposed to patients as a method to prepare recipient sites, in particular breasts, in view of a fat grafting procedure, basing on the theory that fat grafts will better survive and retain volume if the recipient site is more vascularized and provides less compression. However, the method requires high patient compliance and no experimental validation for it has been attempted.

Aims: basing on our group's previous experience in downsizing and testing in animal models clinical devices for wound healing, in particular in settings requiring the application of mechanical forces to soft tissues, we proposed to design an animal model for EVE in which to test the validity of the hypothesis of its being beneficial to fat grafting and explore its mechanisms and potentials.

Methods: we designed and built a miniaturized EVE device to be applied to the dorsum of mice. We then designed a series of stepwise incremental studies. We tested the capacity of EVE of inducing angiogenesis and cell proliferation with 28 days long continuous stimulation. We analyzed its effects on tissues in terms of mechanical stretch, hypoxia and ischemia, edema, inflammation, cell proliferation and angiogenesis after a single 2 hours stimulation. We produced a mathematical modeling for the effects of EVE on tissues in relation to fat grafting. We tested if EVE is beneficial to fat grafting and if beneficial effects are maintained also in the setting of chronic radiation damage. We tested if EVE can stimulate adipogenesis and what role inflammation can play in it.

Results: in our series of studies, we successfully designed a miniaturized animal model in which to test External Volume Expansion. We demonstrated that the hypotheses of stimulation of cell proliferation, angiogenesis, and expansion of tissue compartments on which it is proposed as a preparatory method to fat grafting is confirmed in experimental settings. We showed how mechanical stretch of tissues, hypoxia and ischemia, edema, and inflammation are all intervening factors that can contribute to these effects. Our results suggest that pre-stimulation with EVE is successful in achieving increased fat graft weight and volume retention, and that its beneficial effects are maintained also in the setting of recipient sites having sustained radiation injury. We also demonstrated that EVE has a potential for direct stimulation of adipogenesis, and gathered supportive results to a role for macrophages in this.

Discussion: our results validate the technique for its use in the preparatory phase to fat grafting, and can help moving towards making fat grafting a more effective and reliable procedure with improved outcomes for patients. We gathered evidence that help increasing our understanding of how EVE works and what it implies for tissues. This is the basis for optimizing the technique, make it safer, and increase patients' compliance. For example, stimulation patterns can be improved, duration of treatment can be reduced, and practices such as continuation of EVE after fat grafting should be abandoned as detrimental. Our unexpected observations on adipogenesis also open interesting opportunities, such as that of re-starting EVE after fat grafting when this is at the peak of its remodeling phase. And linking this effect with the understanding of the similarity to other conditions in which adipogenesis is seen and desired, such as tissue engineering, or pathological, such as lymphedema, can expand the potential of our animal model to alternative broader fields.

SOMMARIO

Introduzione: Espansione Volumetrica Esterna (EVE) si riferisce ad una classe di dispositivi che distendono ed espandono compartimenti tissutali in modo non invasivo attraverso l'applicazione dall'esterno di suzione. E' stato suggerito che EVE aumenti il volume dei compartimenti tissutali cui viene applicata e che stimoli un arricchimento della rete vascolare, portando a tessuti meno rigidi e meglio vascolarizzati. Viene proposta a pazienti come metodo per preparare un sito ricevente, soprattutto il seno, in vista di una procedura di innesto di tessuto adiposo con la tecnica del lipofilling, sulla base della teoria che l'innesto sopravvivrà' e manterrà il suo volume meglio se il sito ricevente è più vascolarizzato e vi è sottoposto a meno compressione. Tuttavia, il metodo è impegnativo per le pazienti e proposto in assenza di validazione sperimentale delle ipotesi.

Scopi: sulla scorta delle precedenti esperienze del nostro gruppo nel realizzare modelli sperimentali animali per dispositivi clinici nel campo della guarigione delle ferite, e in particolare di dispositivi per l'applicazione di forze meccaniche a tessuti molli in vivo, ci siamo proposti di realizzare un modello animale per EVE in cui testare la validita' dell'ipotesi che possa offrire benefici all'innesto di tessuto adiposo ed esplorarne i meccanismi e il potenziale.

Metodi: abbiamo realizzato un dispositivo per EVE miniaturizzato da applicare al dorso di topi. Abbiamo quindi disegnato una serie di studi con ipotesi e obiettivi incrementali. Abbiamo testato la capacità di EVE di stimolare angiogenesi e proliferazione cellulare applicandola in modo continuo per 28 giorni. Abbiamo analizzato i suoi effetti sui tessuti in termini di stiramento meccanico, ipossia, ischemia, edema, infiammazione, proliferazione cellulare e angiogenesi dopo una singola stimolazione da due ore. Abbiamo elaborato una teorizzazione matematica per gli effetti di EVE sui tessuti in relazione all'innesto di tessuto adiposo. Abbiamo testato se abbia un effetto positivo sull'innesto e se i suoi effetti positivi siano mantenuti nel caso di sito ricevente che abbia sostenuto danno da radiazioni. Abbiamo testato se EVE può stimolare l'adipogenesi e che ruolo possano avere in questo i fenomeni infiammatori.

Risultati: nella nostra serie di studi, è stato realizzato con successo un modello miniaturizzato con cui testare EVE. Abbiamo confermato sperimentalmente le ipotesi che induca proliferazione cellulare, angiogenesi e espansione dei compartimenti tessutali sulla base delle quali viene proposta come metodo preparatorio all'innesto di tessuto adiposo. Lo stiramento dei tessuti, l'induzione di ipossia e ischemia, edema e infiammazione sono tutti fattori che intervengono e possono contribuire a questi effetti. I nostri risultati suggeriscono che la pre-stimolazione con EVE possa essere efficace nell'ottenere un superiore mantenimento di massa degli innesti di tessuto adiposo, e che gli effetti positivi siano mantenuti anche in tessuti che abbiano subito danno da radiazione. Abbiamo inoltre dimostrato che EVE ha il potenziale di stimolare direttamente fenomeni adipogenici, e raccolto evidenze in favore di un ruolo primario dei macrofagi per questo effetto.

Discussione: I nostri risultati offrono supporto sperimentale all'uso di EVE nella fase preparatoria agli innesti di tessuto adiposo, e possono contribuire a rendere l'innesto di tessuto adiposo una procedura più efficiente e prevedibile con maggiori garanzie per i pazienti. Abbiamo raccolto osservazioni che aiutano a comprendere come EVE funzioni e cosa implichi per i tessuti, il che è la base per ottimizzarla, renderla una tecnica più sicura, e aumentare la compliance dei pazienti. Ad esempio, i pattern di stimolazione possono essere migliorati, la durata del trattamento può essere ridotta, e pratiche come quella di riapplicare EVE subito dopo l'innesto di tessuto adiposo dovrebbero essere abbandonate in quanto dannose. La nostra inaspettata osservazione di effetti adipogenici diretti prospetta interessanti alternative, come quella di

riapplicare EVE quando un innesto di tessuto adiposo è al picco della sua fase di rimodellamento. E collegare questo effetto con altre condizioni in cui adipogenesi è desiderata, ad esempio in ingegneria tissutale, o patologica, come nel linfedema, può ulteriormente espandere le potenzialità del nostro modello animale ad applicazioni in campi più vasti.

INTRODUCTION

External Volume Expansion and fat grafting

Free fat grafting was first reported bt Neuber in 1893 and has been sporadically employed throughout the 20th century [1, 2]. A major step forward was the introduction of syringe liposuction in the '80 which allows simple harvesting. Combined with the intuition that fat could be re-grafted similar to skin grafts, it yield to the development of current fat grafting techniques by reinjection [3-5]. Fat grafting has the potential advantages of a physiologic, natural-looking reconstruction of soft tissues deficits or augmentation without the co-morbidity or risk of complications of flaps and implants. It particularly appeals for reconstructive cases and young patients. Investigations led to a better understanding of the evolution of fat grafts and refinement of techniques, and its application to a variety of conditions. Popularization of fat grafting to the breast for volume augmentation or reconstructive refinements was partially impeded by concerns that development of microcalcifications could interfere with radiologic diagnosis of breast cancer, strengthened by a position statement of the American Society of Plastic Surgeons in 1987 [6]. Fat grafting to the breast cautiously continued in European countries and revived in the US after more recent studies failed to detect increased risk of cancer in fat-grafted patients or interference with radiological discrimination of cancer [7-11].

Fat grafting is an attractive alternative. In its current state, however, it remains limited by partial efficiency and is generally considered an unpredictable procedure [12, 13]. Fat grafts have been reported to survive in an unpredictable fashion (30 to 80% take), with inverse correlation to injection volume [12, 14, 15]. This results in the requirement for multiple sessions to achieve satisfactory volumes, in particular if significant volumes are desired such as can be the case with the breast [16, 17]. To be clinically useful, it should yield reliable and consistent results, be safe for patients both in the immediate and long term, and should be performed in a reasonable period of time.

Fat grafting can be considered in four phases: harvesting, processing, re-injecting, and managing the recipient site. Inconsistency of volumetric results is likely due to a failure of multiple variables in the process.

To determine the optimal surgical methods for harvesting, processing, and re-injecting, Gir and colleagues completed an extensive literature review[12]. Their results show the variability of current surgical techniques. Current literature only supports general principles and not any specific technique. Research to date has focused on adipocytes harvest, processing and stem cell enrichment and other ways to manipulate fat itself to improve engraftment. While some discoveries have been promising, few have translated in clinical success. In contrast, maximizing the recipient site has been relatively neglected as an area of investigation.

The experience with skin grafts suggests that improvement of the quality of the recipient site may positively affect the efficiency of graft take. Similar to skin grafts, grafted fat relies initially on diffusion and later on new vessels sprouting from the recipient site. Poor vessel density-to-grafted volume ratio added to high subcutaneous compartment pressures after fat injection are likely factors that negatively affect fat engraftment. Khouri et al initially proposed that an external volume expansion (EVE) system (BRAVA System®, Miami, FL, USA) could be used for non surgical breast augmentation transferring to the breast the principles of tissue expansion [18]. EVE devices mechanically stretch and stimulate tissues by suction in a non-invasive manner (Figure 1). Stretch releases the skin [19] and by direct mechanical action on single

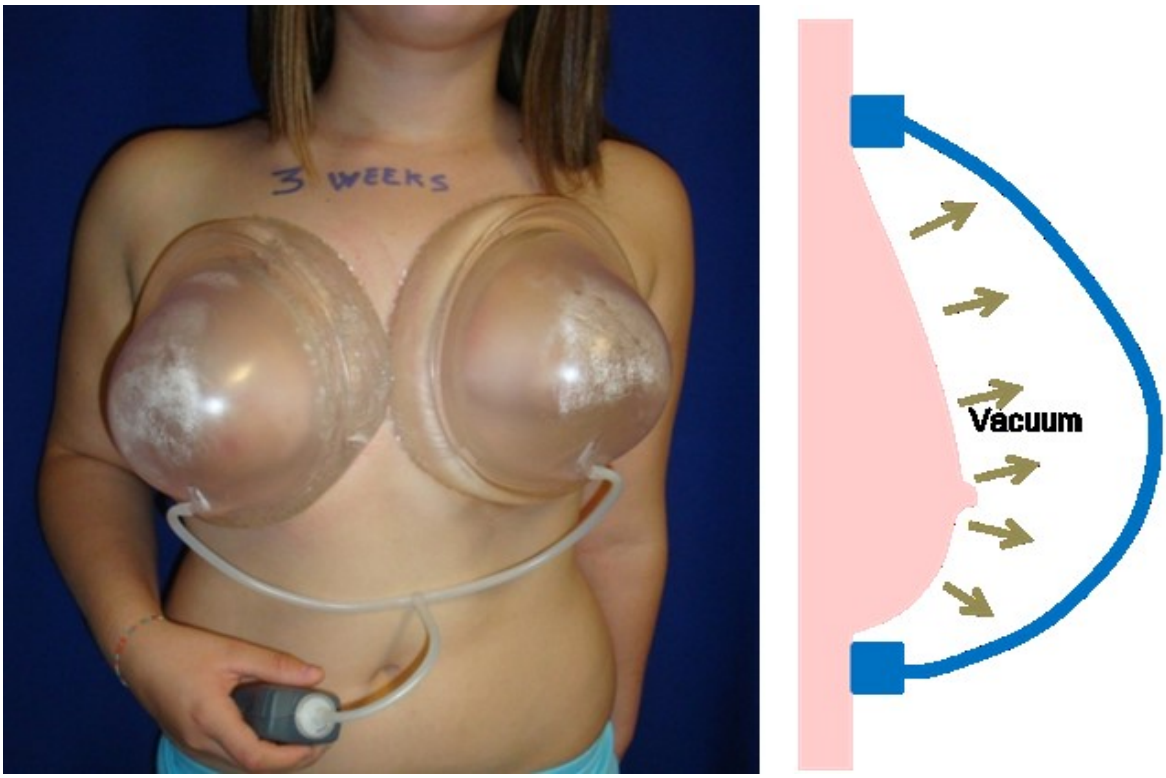

Fig. 1. External Volume Expansion. Rigid cups are applied to the breast and subatmospheric pressure is created inside by suction, resulting in traction force on the skin.

cells [20, 21], induction of ischemia [22, 23], inflammation, and soluble mediators [24] stimulates cell proliferation and, most importantly, vascular remodeling. The latter was the conceptual basis on which after a decade the same started being empirically employed for pre-operative site preparation to fat grafting [25, 26]. In such cases, mega-volume (over 200 cc) fat transplantation is performed following 3 weeks of pre-expansion. With this method Del Vecchio and Bucky reported a 60-200% increase of human breast volume by quantitative MRI after autologous fat injection with long-term consistent increase of 64 ± 13% in volume [27]. Khouri et al reported a 82 ± 18% fat survival at 6 to 12 months in a series of 81 EVE-treated patients enrolled in a multicenter trial which they compared to an average 55±18% of recent published series of non-EVE treated fat grafted breasts [28]. More recently, they reported on having achieved an average 375 ml breast increase in 427 patients after 2.1 operatory sessions/patient in which an average of 225 ml of fat per operation were injected [29].

Although excellent clinical results have been reported, many patients find pre-expansion awkward and both robust clinical studies and mechanistic studies had not been performed before clinical application. As a result, patients were advised on adopting a time consuming and relatively expensive device without proof that a beneficial effect was to be expected. On the other end, limited understanding and testing of the device hampered the possibility of suggesting an optimized treatment protocol.

Mechanical forces in tissue physiology and examples of clinical applications

External Volume Expansion is substantially a method that applies mechanical forces to tissues. Our bodies are constantly subject to a variety of mechanical forces: pressure, compression, gravity, osmosis, surface tension, shear, and tension (figure 2). They come from interaction with the outer world, or within body components in macro or microscopic scale. In addition, other biophysical forces such as electrical, magnetic or electromagnetic have been shown to have biological effects [30].

The ability of mechanical forces to influence cell proliferation and stimulate the expansion of tissues has long been known. In the 19th century, Julius Wolff described the effect of external mechanical forces on the development of bone [31]. In the second half of the XX Century, Ilizarov used these principles to develop the principle of distraction osteogenesis [32], by which through progressive stretching of a bone callus at a fracture site bone lengthening can be induced.

Tissue expansion is a pillar of Plastic Surgery. Balloons are implanted under the skin, inflated, and this stimulates widening of the surface with creation of new tissue. But not all skin components behave the same. The epidermis responds quickly with proliferation in all its elements, ranging from basal cells to appendages to melanocytes. The vascular network also responds with a rapid expansion [33]. On the contrary, the dermis undergoes persistent thinning. Similarly, if the expander is placed either on or under a muscle or bone, the main effect appears to be a form of compression, that induces muscle atrophy, and decrease in bone thickness and volume with unvaried density. As a speculation, these differences could be the consequence of how a mechanical stimulus that is supposed to be uniform is deeply influenced in its local form and application to individual cells by size and microenvironment. In the epidermis the bidimensional stretch is communicated as such via the basal membrane to basal cells, which therefore respond proliferating. In the dermis, the stretch is mainly borne by ECM fibers, that behaving as a tissue mesh become more compact, and compress elements within more than they elongate them. As for the bone, the mismatch in elastic properties and density between bone and expander, which is not fixed on the bone, translate in a purely compressive stimulus. An increase in bone volume and thickness has been observed limitedly to the periphery of the expander. A likely explanation is that in this area, the expansion

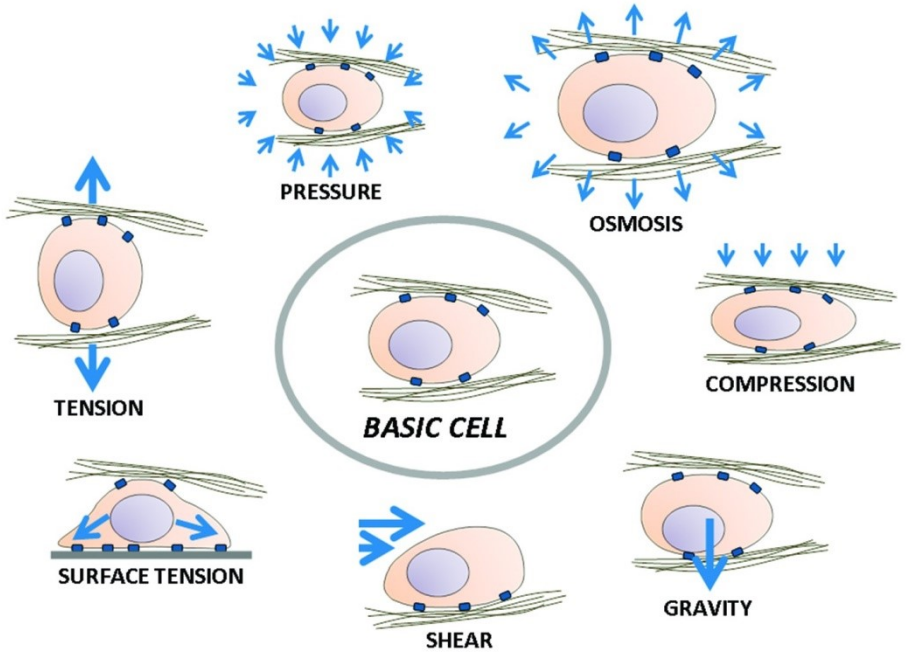

Fig. 2. Mechanical forces in cell biology.

of the tissues at the expander margins transforms in a vertical pulling on the bone, so that only here expansive forces are applied to the bone as well. Tissue expansion inflatable silicone shells were developed simultaneously by Radovan [34] and by Austad [35-37]. Radovan's expansion occurs by periodical injection of saline. Alstad's occurs as a result of osmotic driven accumulation of fluid within the shell. The two methods differ greatly in that Alstad's expansion occurs in a continuous manner, while it is cyclical in Radovan's expanders. Histological examination of expanded skin showed how, in particular in the dermis, the persistence of a continuous pressure beyond 96 hours leads to progressive decrease in mitotic activity [38].

Cell stretch increasing proliferation rate *in vivo* has largely been shown, particularly in the epidermis. In 1968, Lorber and Milobsky showed an increase of tritiated thymidine-labeling of the epidermal cells of the skin of living rats stretched by the insertion of steel pins [39]. MacKenzie described the increase of the proliferative rate of epidermidis stimulated by friction [40], which had been also observed by Bullogh and Laurence in 1959 [41]. Stretching of the skin by tissue expansion in a guinea pig induces an increase of the number of cells in mitosis [42]. Stretching of fibroblasts cultured on a fabric mesh increases the mitotic rate [43]. Squier, implanted a spring in the back of mice showing *in vivo* a hyperplastic response in stretched mouse skin. Later, they demonstrated a transformation of fibroblasts in myofibroblasts under mechanical stresses [44, 45]. A rapid increase in DNA-synthesizing epithelial cells after mechanical stretching was observed also in vitro by Brunette [46].

Angiogenesis is mediated by interactions with the ECM, in which endothelial cells activate, degrade the basement membrane, penetrate by new cell-matrix interactions into the existing extracellular matrix, and establish a new lumen directed by guiding cues. [30] Matrix stiffness is a critical parameter. Endothelial cells self-assemble into capillary tubes and networks when seeded on compliant matrices such as Matrigel. On stiffer surfaces structural organization into tubes does not occur [47, 48]. Endothelial cells can sense differences and alterations in stiffness of the extracellular matrix, as well as tensile forces generated by nearby cells transmitted by the extracellular matrix. Differential stiffness-based reorganization of the cytoskeleton provides directional information by gradient that guide cells in their migration. This principle, for analogy with chemotaxis, is denominated mechanotaxis [49]. Shear stress and circumferential stretch by blood flow on the endothelial surface are also recognized as regulators of vessels biology, and perturbation of the flux by distortion of blood vessels, as occurs with matrix reaction to wounding, adds mechanical cues that potentially contribute to capillary budding. Mechanical forces also act through indirect pathways. Stretching of tissues can result in alterations of the blood flow, with temporary ischemia that activates in nearby cells the HIF-1a pathway, which by releasing VEGF stimulates the proliferation of endothelial cells. These different mechanically-initiated pathways cannot completely be separated in vivo and constitute a known difficulty to researchers approaching this field in human and animal models.

In recent years our group developed multiple models to help estimating the potentials of mechanical forces in vivo and dissect their mechanisms. We first created a model of monoplanar rat ear stretch [50], and later a model in which a selected $1cm^2$ area of the dorsal skin of a mouse could be stretched monodirectionally by a computer-controlled device [22, 24] that allowed versatility of stretch patterns with perfect feedback on time and force intensity.

Fig. 3. In vivo, tensile stimulations affect endothelial cells and induce proliferation and remodeling of blood vessels stimulating capillary budding; *from: G. Pietramaggiori et al, Ann Surg, 2007.*

In these two models we demonstrated how skin stretch, besides stimulating cell proliferation in the epidermis, also induced major remodelling of the vascular network (figure 3). Furthermore, we could appreciate the importance of the pattern of skin stimulation in determining the magnitude of effects, by comparing animals that received a continuous stimulation to animals that were stimulated cyclically. In general, cyclical patterns appeared more powerful than continuous in achieving biological effects.

By PCR we demonstrated a powerful increase in growth factor genes transcription after cyclical stretch, still elevated 2 days after stretch, of growth factors that can contribute to angiogenic and proliferative effects observed. The activated pathways included HIF-1 alpha / VEGF, the main angiogenetic biomolecular pathway, whose main physiologic role is thought to be that of response to hypoxia. Indeed, by

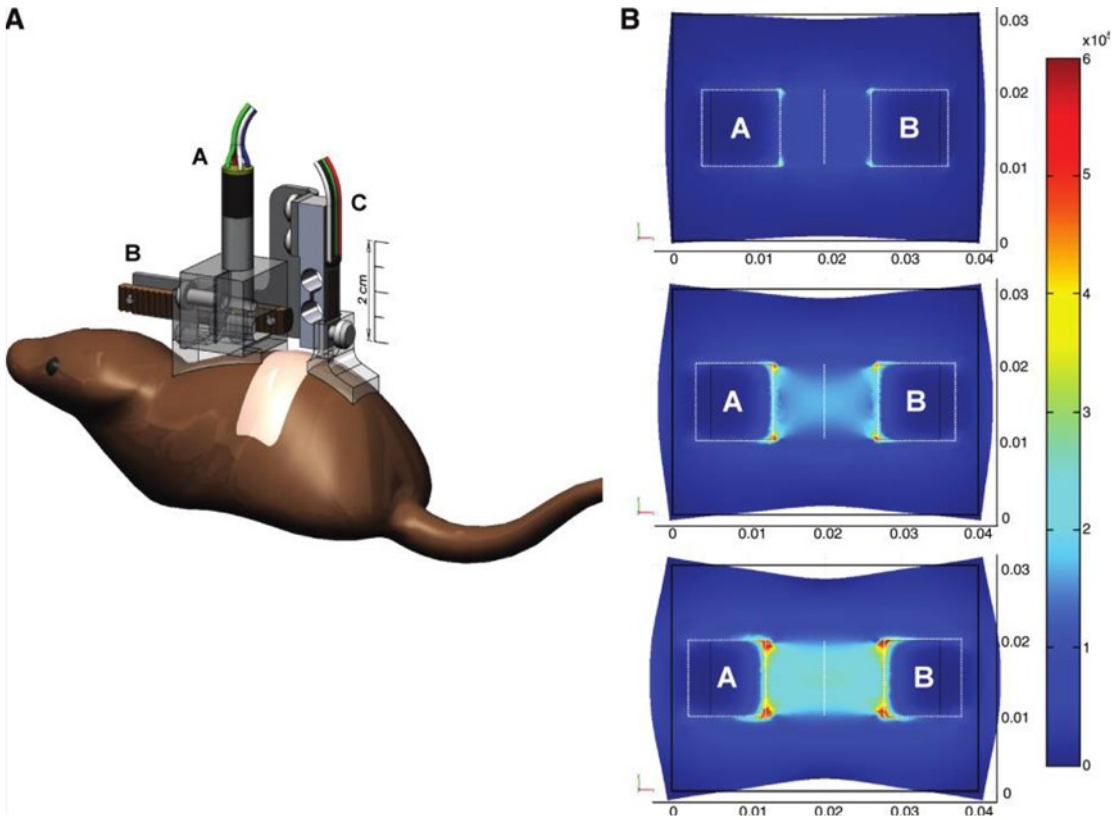

Fig. 4. (A) The stretch device was constructed from a lightweight stepper motor=planetary gear system (A), a rack and pinion transmission (B), and a bar-shaped load cell (C). (B) Finite element analysis. Serial von Mises stress plots predicted nearly uniform stress distribution along the mid-place (indicated as a vertical line) and increasing tension between adhesive pads A and B when they were displaced by 2, 4, and 6mm in the x-direction. Units are in pascals.

hyperspectral imaging we demonstrated how a relative but significant ischemia, in terms of decreased tissue content in haemoglobin, could be detected after cyclical stretch (figure 4).

Mechanical forces have a multi-faced participation in wound healing as well. Wound healing is a complex orchestrated sequence of events that restores the integrity of disrupted skin. It is classically divided in three phases: inflammation, proliferative, and remodelling [51]. Skin interruption causes retraction along anatomic vectors described by Langer [52]. It determines deformation and an elastic reaction of the extracellular matrix that communicates to resident cell. These forces can activate the trandifferentiation of fibroblasts into myofibroblasts. Also, mechanical alterations of the environment can activate proliferative and migratory pathways bringing cells to the wound bed, among which endothelial cells that follow stiffness gradients into the wound margins. The new extracellular matrix deposited in the wound possesses specific mechanical properties contributing to mechanotactic guiding of cells towards the wound and orchestrating their activities and differentiation, especially as in wounds the matrix exhibits well-known chemical, mechanical and density gradients from surface to normal tissues in depth. This process is dynamically mutual and subject to multiple feed-back mechanisms. Restoration of tissue continuity reduces the healing-conductive mechanical conditions of the environment so that stimuli to cell migration and proliferation are removed.

Negative pressure wound therapy (NPWT) is a class of wound healing devices taking advantage of these principles [30, 53]. They apply a highly porous material under suction to the wound surface. NPWT removes fluids and toxins, keep the wound warm and moist, and bring the wound edges together through macrodeformation. The forced contact of the porous material with the wound bed determined by suction also induces microdeformation of the surface which stimulates cellular proliferation (figure 5).

Macrodeformation is the centripetal pulling of wound margins as the interface material collapses with suction. Stretching of the tissues directly stimulates the cells and increases interstitial pressure [54]. Combined with suction at the interface, macrodeformation reduces edema by increasing the differential pressure from the interstitial space to the interface material; it also temporary reduces the blood flow at the wound edges, as observed by Wakenfors et al [55], and confirmed by Kairinos et al. [54, 56, 57] stimulating cell proliferation and angiogenesis through the HIF-1α/VEGF pathway [58]. The deformation is proportional to the level of suction [59], the total volume of the foam, the pore volume fraction of the filler material and the deformability of the surrounding tissues [60]. When exposed to a pressure of -125mmHg, open-pore polyurethane foams decrease in volume of about 80% [61]. From a clinical perspective, understanding the tissue type/macrodeformation relationship is key to a successful use of NPWT. For chronic wounds or wounds in areas with limited skin extensibility such as the scalp, NPWT can be expected to stimulate a healthy wound bed, and permit closure with skin grafts. In areas with large amounts of deformable tissues, such as the abdomen, the shrinkage foam placed in the wound can maximize the reduction of wound size, minimizing the need for additional soft tissue transfer.

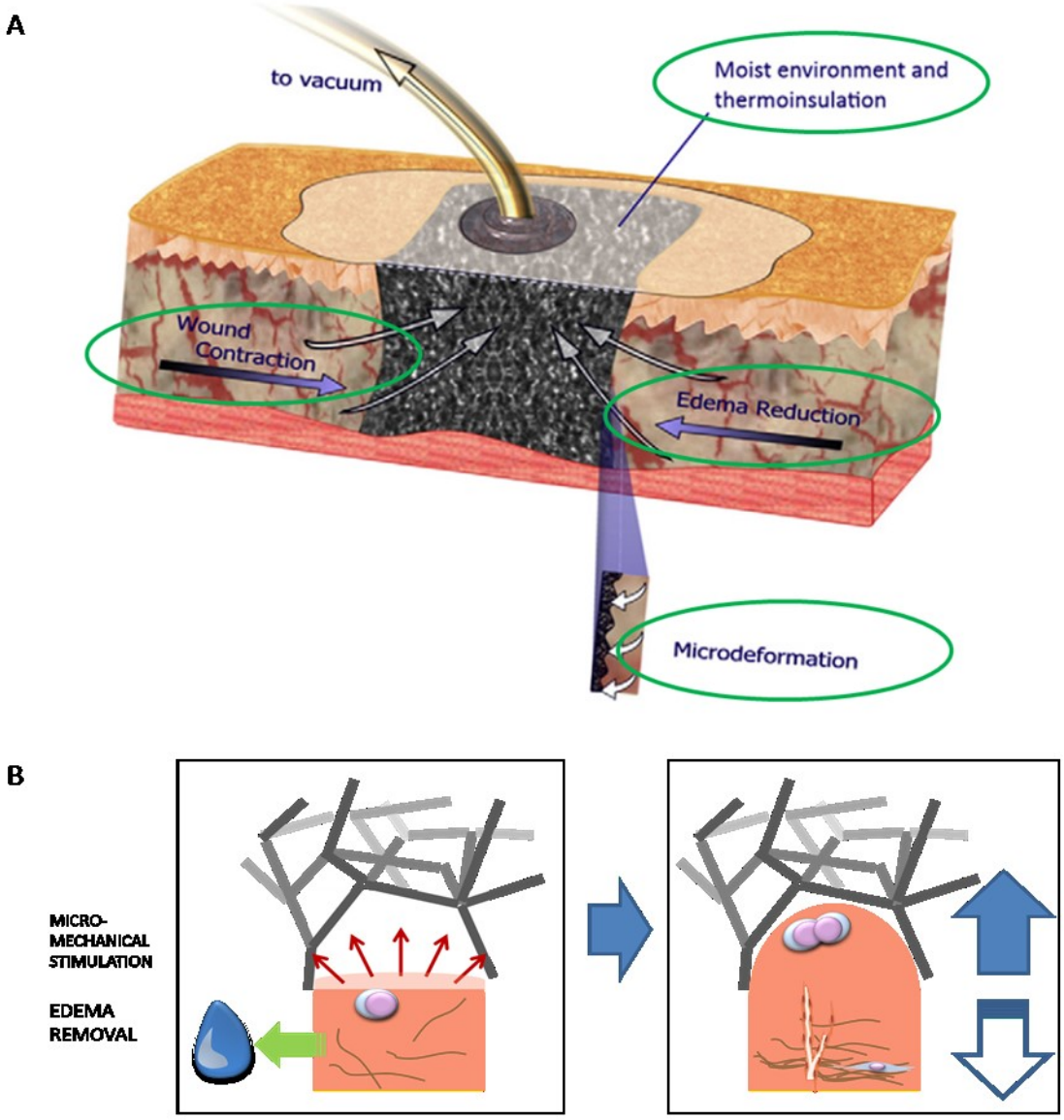

Fig. 5. (A) NPWT combines occlusive dressing, suction and application of foam material. It maintains the wound moist, provides thermoinsulation, removes excess exudates, pulls centripetally the surrounding tissues, increasing interstitial pressure, and mechanically stimulates the wound bed at a micron scale. *Modified from: Orgill et al., J Surgery, 2009*. (B) The combination of compressive forces and tissue pulling into the foam pores by suction determines edema removal and mechanical deformation, that stimulate cell proliferation and angiogenesis.

At the foam-wound interface, wound surface microdeformations occur when suction is applied through the foam. Microdeformations stretch cells, promoting cellular proliferation while creating localized areas of hypoxia stimulating VEGF production. The cell proliferation that results appears as a 3D microdome-like structure to clinicians. Saxena et al. demonstrated on histologic sections an increase of surface length of 22% under typical NPWT conditions compared to areas where suction was applied without the foam interface [21]. By finite element modelling, the microdeformation induced by NPWT was shown to be in the ranges that in vitro studies described as pro-proliferative [62, 63]. Lu et al. applied suction to a deformable fibrin-fibroblast culture apparatus and observed that matrix deformation induced cell proliferation, changes in cell morphology as well as increased expression of bFGF, TGF-β, α-SMA, and collagen 1a1 [64]. In vivo, our group looked at the distinct elements of NPWT in a diabetic mouse model [61]. Foam applied to

the wound without suction significantly stimulated granulation tissue formation and angiogenesis. When suction was added to this (NPWT), the microdeformation at the wound surface was maximized, further increasing the thickness of granulation tissue. The formulated hypotheses was that if the foam, by itself, can have a foreign body effect that stimulates granulation tissue accumulation, NPWT adds microdeformation, which is a direct proliferative stimulus. The effect of mechanical forces at a micro-scale is further potentiated by edema removal that allows full transfer to individual cells. A further study by our group [65] recently demonstrated the importance of pore size in the biological response to NPWT. Larger pore diameters were associated with higher wound surface deformations and were associated with thicker granulation tissue formation, while smaller pore sizes tended to relatively inhibit it, probably because the overall effect becomes more of a compressive type.

As a demonstration of the relevance of microdeformations, when the biological effects of different interface materials as foam, that deforms, are compared with those of gauze, that does not and applies a purely compressive force, inhibition of granulation tissue formation was described with gauze [66].

A clinical consequence of the appreciation of how differently porous materials behave in NPWT is that effects can be modulated and adapted to specific needs by interface choice.

Granulation tissue formation is maximized by a cyclical application of suction [67-69]. The high effectiveness of cyclical regimens reported [55] may be due to a transient hyperfusion of the wound edges that occurs with NPWT is released, paired with the switching between stimulatory phases and phases in which accelerated metabolism is allowed. Dastouri et al. [70] suggest that, at least with pressure cycles in the range of minutes, the shape of the pressure waves may be critical to optimize the effects. Scherer et al showed that repeated brief stimulations (4hrs every other day) with NPWT were enough to induce long-lasting effects [71], while Chen et al [72] observed initial modifications in the capillaries at wound edges and the shape of endothelial cells at TEM after just 2 minutes of NPWT, culminating in capillary budding at 24 hrs, more rapidly than in control wounds. Such reports are in line with the findings of our previously described animal experiment on intact skin, by which it was demonstrated that tensional mechanical stretch elicits growth factor transcription, cellular proliferation and angiogenesis, and that cyclical stimulation is more effective than continuous [22, 24, 50]. NPWT, in particular with cyclical stimulation, has also been shown to affect the local expression of neuropeptides in wounds [73, 74]. It can be hypothesized that higher expression of neuropeptides may result in increased pain, which clinically is a limit to a broader adoption of intermittent NPWT [68], on the other neuropeptides are now recognized as key homeostatic factors for the skin [75] and their secretion may be one of the mechanisms through which NPWT positive effects are exerted.

If tension is good for wound healing, compression might be beneficial to control scarring. Pathologic scarring, keloidal or hypertrophic, occurs by a number of factors but is exacerbated by tension. The examination of the localization and spatial orientation of a large number of keloids allowed the demonstration of the clustering of pathologic scarring to the body areas in which the skin is subject to constant cyclical tension, while areas of loose skin or with minimal tension have no tendency to pathologic scarring [76, 77]. Indeed, most of the traditional techniques of Plastic Surgery deal with scarring minimization or with scar revisions, and the common background they share is the minimization of tension on the wound margins and the reorientation of forces vectors on sutured incisions.

Wound healing should stop when a tissue gap is filled and re-epithelization is concluded. In some cases proliferation proceeds longer than needed leading to elevated scars (hypertrophic) or even scars whose

tissue tends to overgrow into the nearby healthy skin (keloids). Together with a degree of genetic predisposition, a persistent inflammatory status has been called in as a causative mechanism, with particular emphasis on neuroinflammation which we showed is induced by cyclical mechanical stimulation [24, 78]. The fibroblast is considered the pivotal cell in pathologic scarring because of its role in matrix deposition and remodelling. Scar growth is also maintained by the presence and proliferation of a valid vascular network, pathologic scars in their active phase are red and richly vascularized, and the angiogenic-relevant VEGF pathway has been suggested as a potential target for therapy [79]. Scars are hypoxic and have an excess of irregularly shaped endothelial cells [80] and have excess inflammation that is a potent stimulator of angiogenesis. Therapies based on a mechanobiological approach are those proving most effective in the prevention and treatment of exuberant scars. Traditional therapies such as taping, elastic garments, silicone sheets and gels, act primarily by compressing the scars at both a macro and micromechanical level, thus establishing an anti-proliferative and pro-apoptotic environment.

Gurtner and co-workers [81] developed a new mechanomodulating polymer, that in experimental settings was used to overload or offload closed wounds. The device can be applied on sutured wounds in the proliferative/early remodelling phase. The polymer contracts and off-loads the wound margins, transferring mechanical loading to the surrounding skin to which it is attached. Shielding of scars from mechanical stresses successfully antagonized the establishment of a pro-fibrotic environment. To the contrary scar loading resulted in an enhanced pro-fibrotic phenotype of tissues. Developed into a human scar-prevention device, this system obtained positive results in a phase I study.

Mechanical forces in cell biology: the tensegrity model [30]

Several hypotheses have been advanced to explain how tissues and cells sense and respond to mechanical forces. Mechanical stress can open stretch-activated ion channels, distortion can activate cell membrane force-receptors that regulate internally controlled chemical signal cascades, or can induce the release of autocrine / paracrine growth factors [82-85]. These observations suggest that different pathways of mechanical control of cell activity may coexist [86]. However, cells not only sense active mechanical stimulation, but also sense the degree of cell stretch, which is less easily explained by these hypotheses.

Judah Folkman, in studying cancer development, made early observations of the relationship of cell shape and cell function. He noted in tumor growth that cell shape was a critical factor in determining whether cells would proliferate or stay quiescent [87, 88].

A conceptual framework that better encompasses the complexity of the different mechanotransduction pathways was described by Donald Ingber as tensegrity [89, 90]. Tensegrity refers to a building principle in which three dimensional structures composed of rigid elements under compression and elastic elements under tension are maintained stable in an equilibrium of forces (tensional integrity, fig. 6A).

Central to this theory is the observation that the cytoskeleton system transmits forces and interconnects cell structures (fig. 6B). The cytoskeleton is built by filaments and tubules that vary in size and stiffness, some acting more like uncompressible struts, others as elastic strings (Fig. 2, 3). The cytoskeleton is anchored at the inner side of cell membranes at specific sites by interacting with specialized structures, focal adhesions (FA). The focal adhesions complexes are specific membrane molecules that anchor the cell to the extra-cellular matrix (ECM) or other cells. The main component of focal adhesions complexes are

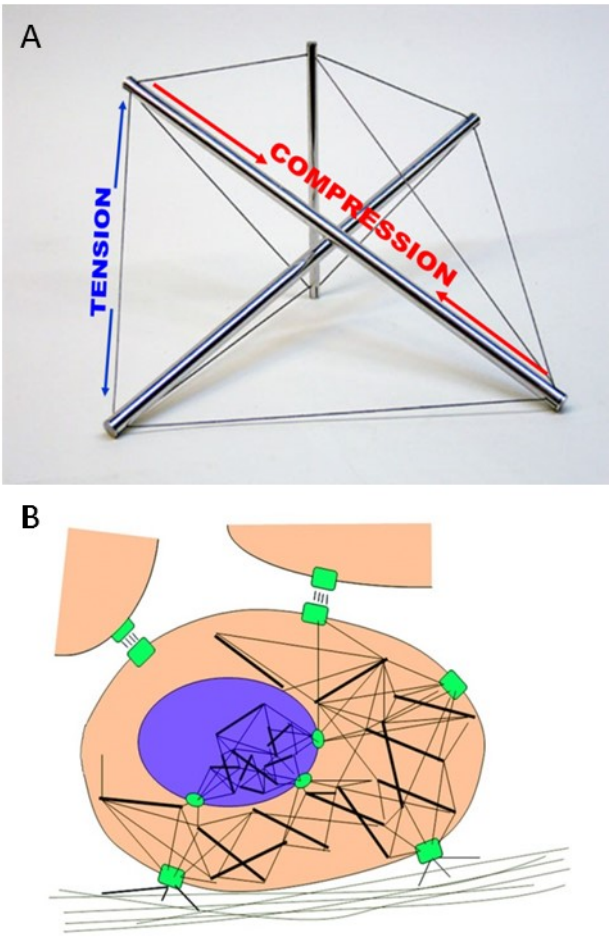

Fig. 6. (A) *tensegrity* is a building principle based on the equilibrium of tensile and compressive forces holding together elements with different stiffness . (*Modified from: X-piece, sculpture by K. Snelson; www.kennethsnelson.net*). (B) according to the *tensegrity* theory also cells are multimodular tensegrity structures. Microtubules, more stiff, behave as rigid struts, and microfilaments and intermediate filaments as strings. The cytoskeleton is anchored at the inner side of focal adhesions, membrane complexes receptors for the ECM and nearby cells, that behave as preferential pathways for mechanical forces transmission. In this way amounts of energy are stored in the equilibrium of the cytoskeleton; forces altering this equilibrium change the global shape of the cell, move and deform all inner organels and molecules anchored to the cytoskeleton, and affect cell function.

transmembrane proteins (such as integrins), which internally function as anchorage for the cytoskeleton. Other proteins such as protein kinases and stress-activated channels that can act as alternative force receptors also gather at focal adhesions. In this way, a preferred FA-cytoskeleton filaments pathway of mechanical forces transmission is built. Of notice, all molecules and organels inside a cell are not freely floating, but also anchored to the cytoskeleton.

The cytoskeleton has the capacity to store energy distributed throughout its various components in equilibrium of tensile and compressive forces. The energy stored in the cytoskeleton derives from the balance of multiple forces, those applied from the outer environment (ECM and other cells), those produced inside the cell (actomyosinic apparatus and cytoskeletal remodelling) and osmotic and gravitational forces, which are thus effectively integrated. Additional external or internal forces alter the established state of cytoskeletal elements with a shifting of the reciprocal position transmitted globally inside the cell. The shape and relative position of all molecules and organelles connected to the cytoskeleton are affected, changing the likeliness of reactions to occur and providing a mechanism to transform resting tension and its perturbations into biochemical signals. Cells then adapt to new states of mechanical stress by activating internal and external mechanisms that establish a new equilibrium. For example, a new steady state can be achieved by cytoskeleton reorganization or by secreting proteins such as matrix-metalloproteinases that modify the surrounding extracellular matrix or producing new ECM structural molecules.

This theory has been tested in a number of in vitro models in which cells were pulled, stretched, compressed, or maintained in mechanical isolation, proving how the “mechanical state” of a cell, whether it is under mechanical stimulation or not, can act as gatekeeper on all other types of chemical and physical signals. In simpler words, the mechanical state of a cell is able to determine whether a cell will respond, and how, to additional stimuli. And will therefore be a critical factor in deciding the fate of that cell, whether it will undergo differentiation, proliferation, or face apoptosis [20, 62, 91].

AIMS OF THE PROJECT

Having observed the lack of experimental validation with which External Volume Expansion devices were introduced in clinical practice, we set on establishing a mouse model for it building on our previous experience in designing small animal models to test and validate clinical technologies and therapies. We initially aimed at testing the hypotheses of tissue expansion and angiogenic effects on which it was proposed to patients. We then proceeded stepwise by progressive adaptations of the model, to assess factors that potentially played a role in determining these effects, to establish if EVE had an effect on fat graft volume retention, to establish if its angiogenic potential was maintained in skin with chronic radiation injury, and if it could affect fat graft retention in such setting. We also incidentally observed that in our animal model EVE seemed to induce a deposition of adipocytes, and therefore tested the hypotheses that EVE has adipogenic effects, and then the role of macrophages in inducing adipogenesis in EVE. We are now exploring the correlation of the EVE model with lymphedema to test if it ca be adopted as a model for lymphedema/lipedema transition.

AN ANIMAL MODEL FOR EXTERNAL VOLUME EXPANSION

Basing on the above mentioned experience of our group, it was apparent that the mouse was a suitable species for an in vivo animal model to test in controlled experimental settings the properties and effects of EVE.

Compared to larger mammals, it had the significant advantages of less developed nervous system, easier manipulation, increased control over the experimental settings, less regulation not being USDA controlled, reduced costs. It also was a model with which we had large familiarity and in which many forthcoming issues could be readily predicted or easily faced. Its main downsides were the need of major downsizing of the device, and most importantly the different anatomical and mechanical properties in the skin. Rodent skin is much looser and elastic than human skin, limiting the possibility of directly translating results to the human model in particular with regards to magnitude. It also presents an extremely thin subcutaneous tissue. This was a reason why it was decided in several cases to use the dermis as target tissue for examining some effects which would be clinically relevant in the subcutaneous tissue, such as changes in vascular network density. This issue had already been object of discussion in previous model, but it is generally accepted that such general effects as those for which such process of trans-tissue analysis approach was adopted are similarly elicited across different tissues and therefore, provided this limit is understood, the method is accepted. On the other end a thin subcutaneous tissue allowed the perception of some effects such as edema and adipogenesis that would likely have been lost in thicker subcutaneous tissue layers. And full excisional biopsies of the stimulated areas could be analyzed, reducing issues with bias in tissue sampling.

Downsizing of the device was performed aiming at a miniaturized device that maintained the main aspects of clinically available EVE devices with reference to expected effects on tissues. That is, allows the reproduction of a close chamber in which vacuum can be induced when applied to the skin. The main tissue expansion effect was to remain at a macroscopic scale. A dome-shaped structure with a circular caliper at the base of 1cm was adopted basing on the experience with previous models that showed such a size of target skin to be suitable for the chosen animal model [22, 61]. Previous experience also allowed to expect that the device would have been possibly been worn by animals for a prolonged time without significant interference in their activities and that the animals could be maintained connected to an external vacuum source while awake in their cages through thin flexible tubing [61]. Silicone dome structures were obtained by modifying commercially available baby nipples. The silicone wall of such devices proved strong enough to avoid collapse at adopted pressures and a sufficiently flexible and adhesive border to be worn by animals without gluing. The width of the silicone border in contact with the skin, to which specific attention was paid in the clinically available model [18], was disregarded in the present animal device as due to downsizing and different characteristics of murine skin which greatly reduced the issue of shear induced skin lesions. Pilot experiments revealed that the range of pressure suggested for clinical use was well tolerated by mice. Much higher pressures (-50 and -75 mmHg) induced high rates of skin ulcerations consistently with clinical experiences, lower pressures (<20 mmHg) did not allow self-adherence of the device to the skin in short application experiments. A setting of -25 mmHg was adopted as target setting for most experiments.

GENERAL METHODS

Unless indicated otherwise, the following methods apply to individual studies which follow.

Device: *A dome-shaped rubber device obtained by modification of baby nipples with an internal diameter of 1 cm and an internal volume of 1 ml was designed, fabricated, and connected by flexible 2mm rubber tubes to a suction pump (VAC Instill®, KCI, San Antonio, TX, USA) set at a pressure of -25 mmHg (Fig. 7). The device was applied to the dorsal skin of mice 5cm cephalad to the tail and 3 cm lateral to the midline spine without fixatives. The skin around the device was stabilized by a semi-rigid rubber doughnut-shaped frame, with internal diameter of 2.5 cm.*

Histology and Immunohistochemistry: *Tissues were harvested en block, fixed in 10% neutral-buffered formaldehyde for 24 hours and stored in 70% ethanol at 4°C. Samples were embedded in paraffin and cut into 5 µm sections. Hematoxylin and Eosin staining was performed according to standard protocols. For immunhistochemistry, sections were de-paraffinized in xylene and re-hydrated in graded ethanol series. Antigen retrieval for Ki67, PCNA, pimonidazole hydrochloride, and Perilipin-A was accomplished by microwaving in 10mM sodium citrate (pH 6.0). Sections for endothelial cell marker platelet endothelial cell adhesion molecule 1 (CD31 / PECAM-1) and pan-leukocyte marker CD45 were treated with 40 µg/ml Proteinase K (Roche Diagnostics Corp.) for 30 min at 37°C. PECAM-1, CD45 and Ki67 and Plin-A primary antibodies were incubated at 4°C overnight. Signal was intensified using the tyramide amplification system (Perkin-Elmer, Boston, MA, USA) and positive staining was detected with DAB (Dako North America Inc., Carpinteria, CA, USA)*

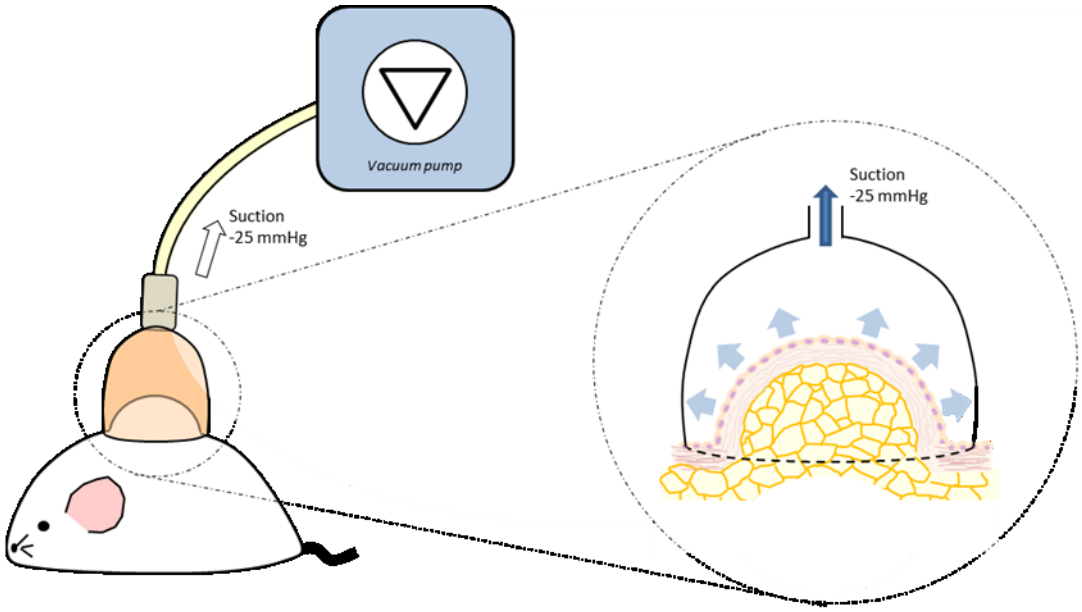

Fig. 7. Miniaturized EVE device applied to mouse dorsum

Primary and secondary antibodies

Antibody	*Company*	*Code*	*Dilution*
Ki67	Thermo Scientific	RM-9106-S	1:200
CD31	BD Pharmigen	553370	1:100
PCNA	Dako Corp.	M0879	1:50
CD45	BD Pharmigen	550539	1:100
Hypoxyprobe1 MAB1	HPI Inc.	HP1 200 Kit	1:250
Perilipin-A	AbCam	Ab3526	1:2000
CD68p	AbCam	Ab125212	1:200
Biotinylated anti-rat IgG	Vector Lab	BA-4001	1:100
Biotinylated anti-rabbit	Thermo Scientific	TR-125-BN	Ready to use

Data representation and Statistical analysis: *Results are expressed as mean ± standard deviation in text and figures. A p value less than 0.05 was considered statistically significant.*

PROOF OF CONCEPT: CONTINUOUS EVE EXPANDS STIMULATED TISSUES AND ENRICHES THE VASCULAR NETWORK [92]

The cornerstones of clinical External Volume Expansion as a recipient site preparation method prior to fat grafting are the hypotheses that it expands tissue compartments and increases the vascular network. Our first study aimed at proving the feasibility of the animal model we proposed, and in parallel providing preliminary insight into these two cornerstone issues.

MATERIALS AND METHODS

Study groups and model

A total 20 adult wild-type mice (strain C57BL/6), of female sex and 8 weeks old (Jackson Laboratory, Bar Harbor, ME, USA), were housed in an Association for Assessment and Accreditation of Laboratory Animal Care–certified facility under an approved protocol. The mice were randomly assigned to two groups and treated with either suction device (S, n = 10) or occlusive dressing alone - Tegaderm™ (3M Health Care, St. Paul, MN, USA) - (C, n = 10). The device was applied to the dorsal skin of the mice, 3cm cephalad to the tail and 0.5 cm lateral to the midline spine, and stabilized with adhesive tape (Tegaderm™). Mice (n = 6 per group) were treated for 28 days continuously and sacrificed (Fig. 8).

Macroscopy

Digital photographs captured on days 7, 14, 21 and 28 were compared with photographs taken on day 0 by two independent, blinded observers.

Magnetic resonance imaging

MRI scans of the treated area were performed for 4 mice of the suction group and 4 controls on day 0, 7, 14, 21 and 28 on a 3 Tesla GE HDx scanner (GE Medical Systems, Waukesha, WI, USA). Thin section T1 and T2 weighted images were obtained using a transmit and receive 6 cm surface coil. The mice were anaesthetized with 60 mg/kg body weight pentobarbital (Nembutal®, Lundbeck Inc., Deerfield, IL, USA). During imaging procedures the physiologic body temperature of the mice was maintained with warm gel packs. The sequences were analyzed by two independent, blinded observers.

Histology

Cross-sections of the treated areas were stained with Hematoxylin and Eosin. Digital images were acquired with an Olympus BX40 microscope.

Immunhistochemistry

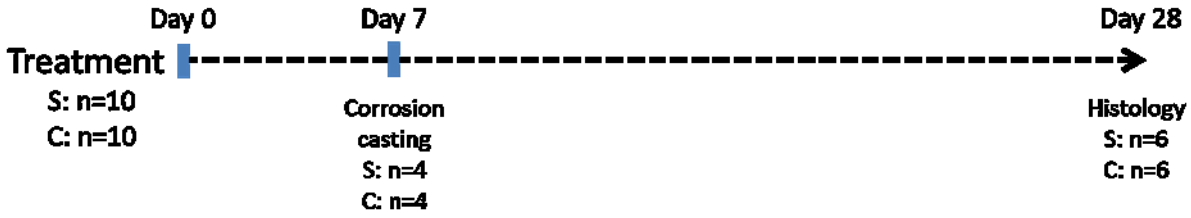

Fig. 8. Study design

Stainings were performed for proliferating cells nuclear antigen (PCNA) and for endothelial cell marker platelet endothelial cell adhesion molecule 1 (PECAM-1). PCNA staining was performed using Vectastain ABC Kit (Vector Laboratories, Burlingame, CA, USA). Positive staining was detected using the Liquid DAB + Substrate Chromogen System (Dako North America Inc., Carpinteria, CA, USA) and counterstained with Hematoxylin. Images were acquired using an Olympus BX40 microscope. Cell proliferation was assessed by cell counting in 40x fields of treated areas using Adobe Photoshop software and expressed as ratio PCNA+ nuclei/total nuclei. Blood vessel density is expressed as number of PECAM-1 stained vessels identified in 40x fields. For each slide three 40x fields were quantified by three independent observers and results are expressed as averages +/- SD.

Corrosion casting on day 7 post-suction

For spatial evaluation of changes in the skin microvasculature, 4 mice of the suction group and 4 of the negative control group were perfused on day 7 in deep anesthesia (120 mg pentobarbital/kg bw; Narcoren, Merial, Germany). Vascular access was established by cannulating the ascending aorta after systemic heparinization and thoracotomy with an olive-tipped needle (Acufirm 1428LL; Dreieich, Germany). After flushing with body warm saline and fixation with 10ml of 2.5% glutaraldehyde in Ringer's saline solution, the vascular system was perfused with 10-15 ml of a polyurethane based casting resin (PU4ii; VasQTec, Switzerland). After polymerization and dissection, the dorsal back of the mouse was immersed in 5% KOH to digest all tissues around the vessel casts. After freeze-drying, the specimens were mounted with conductive bridges on stubs and coated with gold in an SCD 040 sputter-coater (BAL-TEC AG, Leica Microsystems). The specimens were visualized using a Philips XL30 ESEM scanning electron microscope (Philips, Eindhoven, The Netherlands).

Statistical analysis

A MANOVA test (IBM® SPSS®, IBM Corp., Armonk, NY, USA) was used to determine the significance of differences between the suction group and the control group.

RESULTS

Gross and Imaging Analysis

The model was effective in applying to tissues a mechanical, multi-directional, expansive and non-invasive stimulation driven by suction for a prolonged time. All animals were able to complete the expansion program according to the study design.

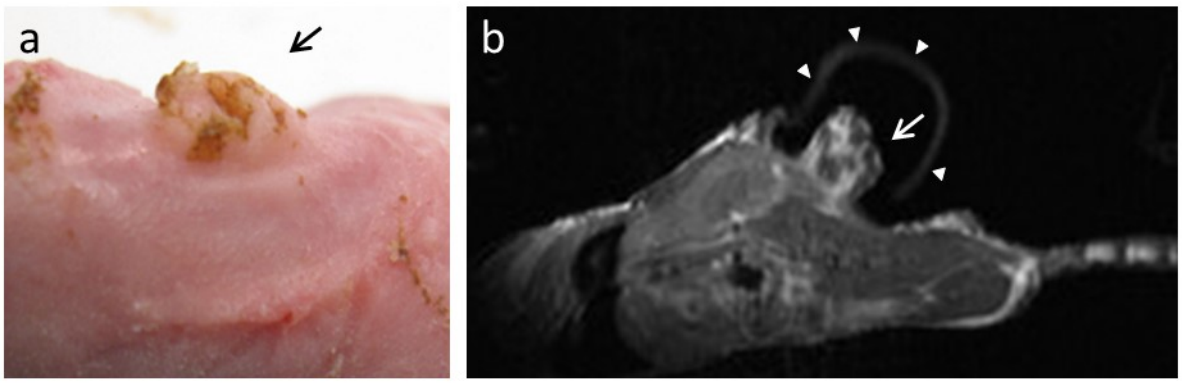

Fig. 9. Tissue expansion induced by EVE (a) macroscopically evident at EVE removal (b) during EVE at MRI

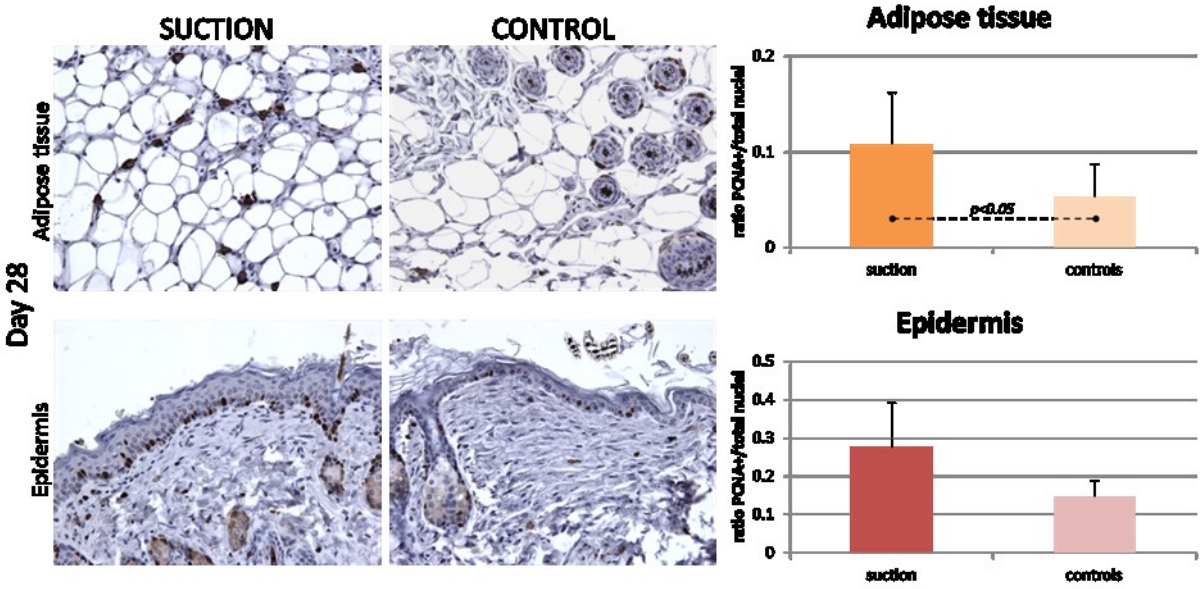

Fig. 10. EVE induced a significant increase in cell proliferation rate in both epidermis and hypodermis

Grossly, treated areas by the EVE device demonstrated a local swelling. This swelling was evident by 21 days and not seen in the control group. No signs of infection or tissue damage were detected (Fig.9a). MRI scans at 28 days confirmed the development of tissue swelling in the experimental group with low-density T1 signal. The sequences were compatible with fat tissue (Fig. 9b).

Cellular proliferation

EVE treatment using 25 mmHg continuous suction for 28 days induced a significant 2-fold increase of ratio of proliferating nuclei/total nuclei in the subcutaneous tissue ($p<0.05$). The proliferating rate of cells located in the epidermis was 1.9 times greater than controls ($p=0.08$; Fig. 10).

Vascular Remodeling

Compared to controls, in 28 days suction-treated tissues we detected a 1.9–fold increase of subcutaneous tissue blood vessel density ($p=0.01$, Fig. 11b and 11c). Mechanical stimulation resulted in changes of the microvascular architecture on day 7: intense remodeling of vessels with re-orientation and increase of luminal diameter were seen by scanning microscopy of the casts (Fig. 11a).

DISCUSSION

We developed a miniaturized, murine EVE device, using continuous suction and demonstrated expansion of tissue compartments, stimulation of cell proliferation and changes in the vasculature with remodeling phenomena and increase in density of the capillary network. The results are consistent with previous *in vitro* and *in vivo* findings of mechanotransduction in biological tissues.

There are differences in our model as used in this proof of concept study from the clinically available EVE system. For simplicity we used a continuous application of the device for 28 days rather than a periodic application of 6-10 hours a day for 21 days. In biology, most systems have a more robust response to periodic or cyclical application of mechanical forces [22, 30]. In addition, as discussed above force

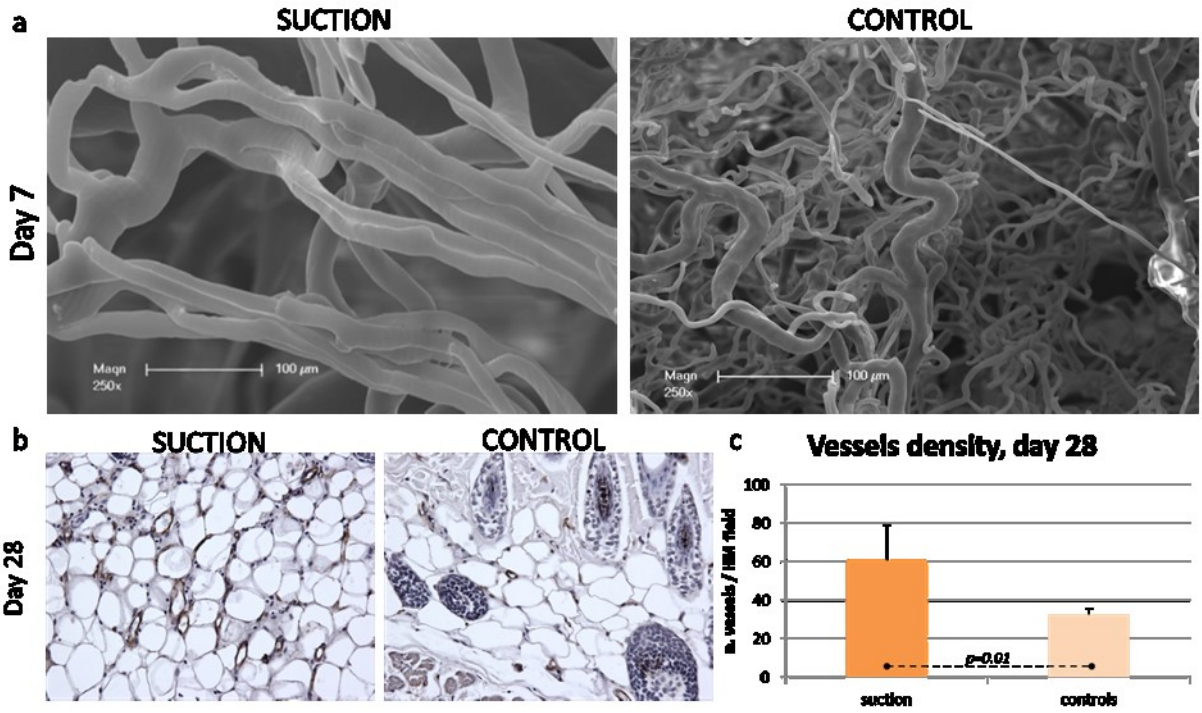

Fig. 11. EVE induced remodeling of the vessel network and a significant increase in vascular density in the hypodermis

transmission might be different due to the mobility of mouse skin and the scale of the model. Some of the excess thickness observed may have been due to recruitment of adjacent skin into the device.

However, our preliminary results from this study provide experimental support to the hypotheses that EVE has the capacity of stimulating an enhancement of tissues vascular network, and might indeed be a useful tool if employed with this aim in the preparation of recipient sites to fat grafting.

EFFECTS AND MECHANISMS OF EXTERNAL VOLUME EXPANSION

Having demonstrated proliferative and vascular remodeling effects with a 28 days continuous stimulation, we set on better understanding the direct effects on tissues of External Volume Expansion and characterizing the mechanisms likely involved in the observed outcomes. Our group showed in both a rat ear stretch [50] and a murine skin stretching model [22, 24] that tensile forces have proliferative and vascular remodeling effects on skin. These models showed a 1.8 to 2.0-fold increase of epidermal proliferation rate after just 4-hours of application of tensile forces [22]. By RT-PCR and hyperspectral imaging, we observed that cell proliferation and vascular remodeling are likely to be induced by a combined action of transmitted forces on cells as well as transient ischemia which activates HIF-1α [93].

We adopted a similar approach in designing a new set of experiments, consisting in applying a single short 2 hours EVE stimulation and analyzing stepwise its effects on tissues during stimulation and over the following 48 hours.

MATERIALS AND METHODS

Study design

A total of 24 male, 8 week old SKH1-E hairless mice (Charles River Laboratories, Wilmington, MA) were used in an AAALAC–certified facility and in accordance with our Institutional Animal Care and Use Committee guidelines under an approved protocol. Eighteen were treated for two hours with the EVE device set at a pressure of -25mmHg; 6 were used as untreated controls. At the end of treatment mice were euthanized immediately (2h group, n=6), one hour (2h+1, n=6) or two days (2h+48, n=6) after the removal of the device. Tissues were harvested with a 10mm biopsy punch.

Hypoxia

Pimonidazole hydrochloride staining was used to identify hypoxic cells. Pimonidazole selectively binds to thiol-containing proteins in cells with with pO_2 < 10mmHg and was injected intraperitoneally (70 mg/kg) in the 2h EVE and untreated groups 30-60 minutes prior to sacrifice.

Hyperspectral Imaging

Spatial maps of tissue perfusion and oxygenation were generated using a medical hyperspectral imaging system (OxyVu-2, HyperMed Inc., Greenwich, CT). The optical properties of this device have been described.[94] Briefly, this device uses optical hardware to collect images of a sample over a 20 second period at select wavelengths between 500- and 660-nm. Diffuse reflectance tissue spectra were determined for each pixel within this collection of images using proprietary algorithms. Mean oxy-hemoglobin (OxyHb) and deoxy-hemoglobin (DeoxyHb) values were obtained by decomposition from a 79-pixel diameter region of the images corresponding to the stimulated area using standard spectra for OxyHb and DeoxyHb. Perfusion was measured as total hemoglobin (tHb), calculated as the sum of OxyHb and DeoxyHb. Tissue oxygenation (StO_2) was calculated as OxyHb divided by tHb. Hb values are reported in arbitrary units that have previously been shown to correlate with in vivo molar concentrations [95].

Prior to imaging, the system was calibrated to a standard pixel reflectance. Imaging was performed with mice under anesthesia, at standard room temperature, and respiratory motion-artifact was corrected with the use of a fiducial target. A baseline scan was obtained from all animals immediately before EVE on Day 0. Treated areas in mice of the 2h+1 and 2h+48 groups were scanned at multiple timepoints for one hour after removal of the EVE device. Mice of the 2h+48 group were further scanned 4 hours, 1 day and 2 days after the end of stimulation.

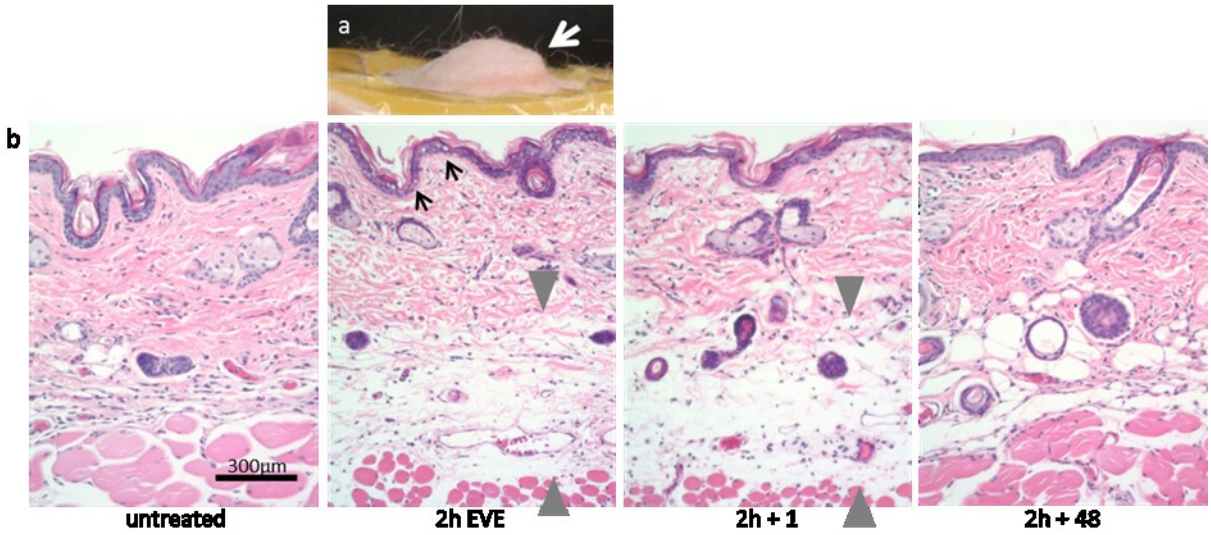

Fig. 12. a) macroscopically evident development of tissue swelling (white arrow) in EVE treatment areas at the removal of the device; b) histologically this corresponds to accumulation of intense edema in the deep dermis and hypodermis (between grey arrowheads), which is still present one hour after the end of the stimulation. Isolate nuclear vacuolization is seen in some epithelial cells at the end of treatment (black arrows). Normal microscopic anatomy is restored two days after EVE treatment. Hematoxylin and eosin staining, 10x magnification.

Histology and immunohistochemistry

Sections were stained for proliferating cells nuclear antigen (PCNA), endothelial cell marker platelet endothelial cell adhesion molecule 1 (PECAM-1), pimonidazole hydrochloride and pan-leukocyte marker CD45. Images were acquired using a Nikon E200 microscope.

Quantifications

Cell proliferation in the epidermis and in the deep dermis was assessed by cell counting in 40x fields of treated areas with Adobe Photoshop software and expressed as ratio PCNA+ nuclei/total nuclei. Epithelial appendages were excluded from counting. The same method was used to quantify the ratio of inflammatory cells to total cells in the deep dermis. Blood vessel density was quantified as number of PECAM-1 stained vessels identified in 10x fields. For each slide, three fields/staining were evaluated by three independent observers.

Statistical analysis

Differences in hyperspectral imaging features between time points were evaluated using general mixed linear models [96] with pairwise comparisons using Fisher's LSD multiple comparisons procedure without multiplicity adjustments (Proc Mixed procedure of the SAS® Statistical Software package, SAS Institute Inc., Cary, NC). For quantitative immunohistochemistry, one-way analysis of variance (Anova, WinStat®) with Tukey post-hoc correction was used to determine the significance of differences.

RESULTS

At the end of the EVE cycle, the treated area developed local swelling (Fig. 12a). Swelling was reduced but persistent at 1 and 4 hours post-stimulation. At histological examination gross edema was evident in the deep dermis/hypodermis and was unvaried between the end of treatment and one hour aftermath; the

superficial dermis was less affected. Epidermal cells showed focal vacuolization. By two days post-stimulation, normal histological architecture had been restored (Fig. 12b).

Tissue hypoxia

The staining for pimonidazole hydrochloride showed diffuse positivity of the majority of cells in the dermis and epidermis of EVE treated skin compared to rare positive cells in untreated skin, demonstrating presence of hypoxia in EVE treated tissues (Fig. 13a).

Hyperspectral imaging

OxyHb levels in stimulated samples were similar to pre-treatment baseline levels between 5" and 3'30" after removal of the EVE device. By 6' following stimulus cessation, OxyHb levels were significantly decreased and remained such for 1h. Normal OxyHb levels were restored by 4h (Fig. 13b). In parallel, DeoxyHb was significantly decreased at all timepoints between 40" and 1h. A non-significant trend towards lower DeoxyHb levels was observed at 4h post-EVE, with normal levels restored on day 1 (Fig. 13c). Total Hb content of the stimulated tissue was lower than baseline at all timepoints from the end of treatment up to 1h (Fig. 13d), while StO_2 was reduced between 6' and 1h post-treatment. Representative hyperspectral imaging acquisitions are found in Suppl. Figure 1.

Inflammation

EVE treated tissues displayed a significantly increased inflammatory infiltrate by the end of the two-hours stimulation. Inflammation tended to resolve over time, but was still elevated above baseline levels by two days (Fig. 14).

Cell proliferation

Two days after stimulation, the proliferation rate was 1.4 and 1.7 fold higher in the epidermis ($p<0.05$) and dermis ($p<0.01$) of treated skin versus untreated skin, respectively (Fig. 15a and 15b).

Vessel density

The skin of EVE-treated samples from the 2h+48 group had a significantly higher vascular density than samples from the untreated, 2h and 2h+1 groups. No difference in vascular density was observed when comparisons were made between samples from the untreated, 2h and 2h+1 groups (Fig. 14c).

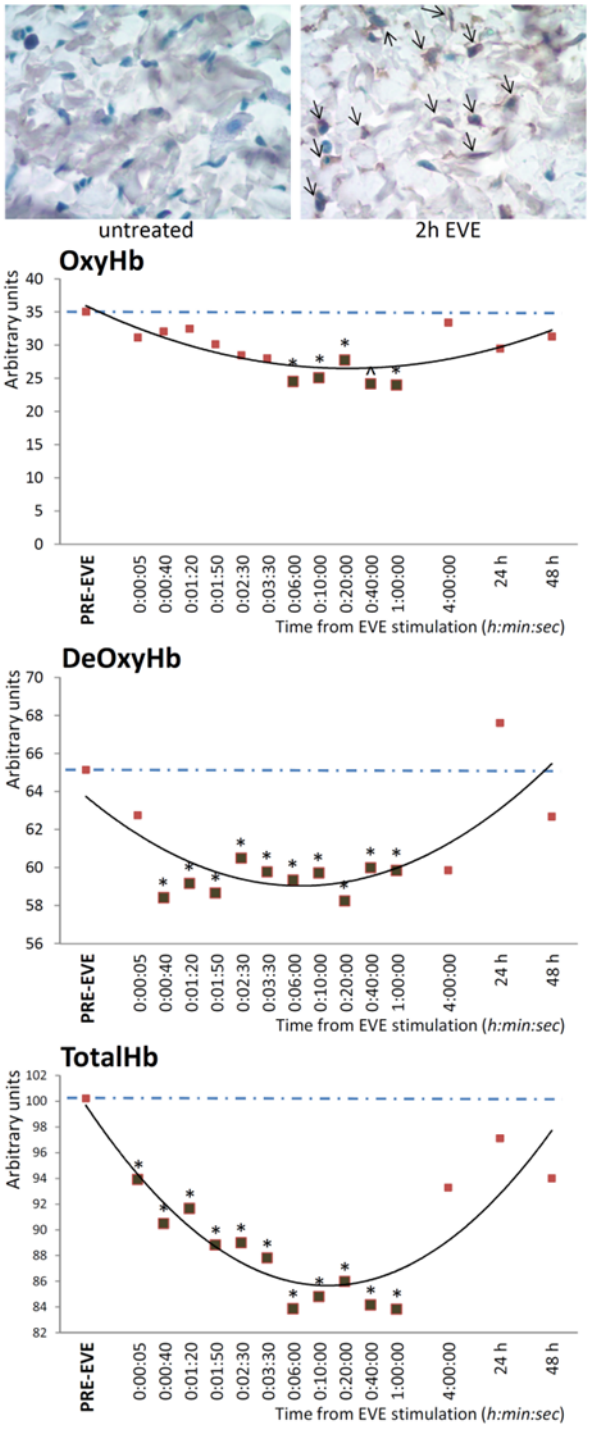

Fig. 13. a) IHC staining for pimonidazole hydrochloride demonstrates numerous hypoxic cells (arrows) in EVE-treated areas which are not found in untreated controls. B, c and d) hyperspectral imaging of treated areas demonstrates decreased tissue content in OxyHb after EVE treatment starting from 6 minutes after release of suction. DeOxyHb is significantly decreased from 40 seconds after removal of EVE at all timepoints up to one hour. TotalHb, which is the sum of the previous two, is decreased at all timepoints from EVE release to 1 hour post-EVE. All are normalized at the four hours timepoint and in the following two days. ^ p<0.05, * p<0.01 versus pre-EVE baseline. Notice that the timepoints indicated correspond to the beginning of a 20" imaging caption cycle.

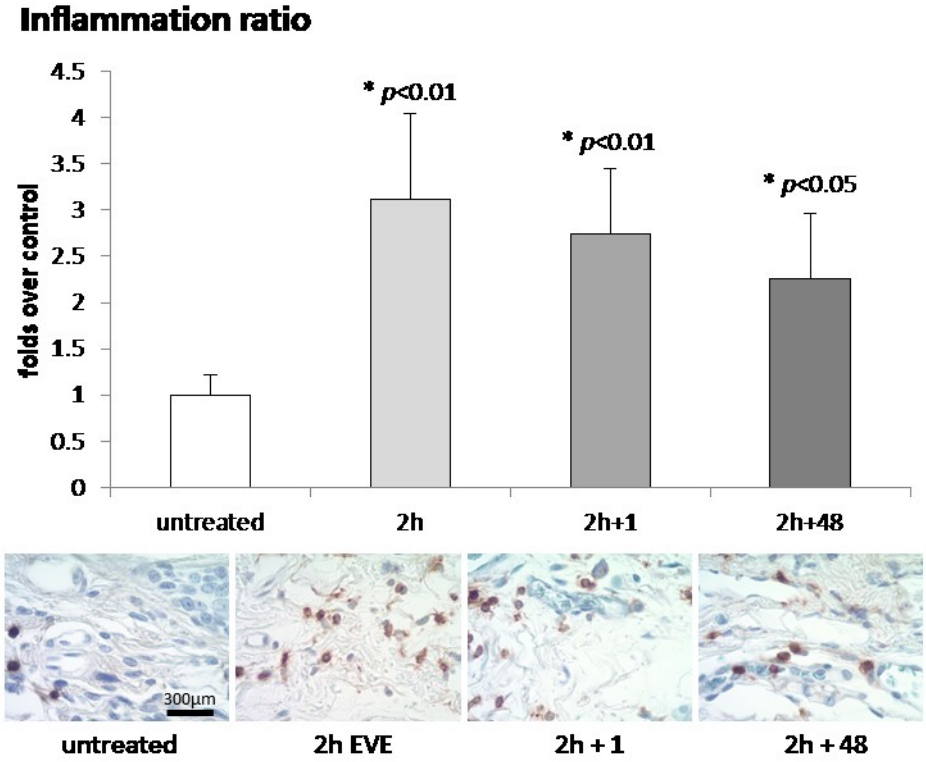

Fig. 14. Semiquantitative analysis of slides stained for pan-leukocyte antigen CD45 demonstrates significant 3-fold increase of density of inflammatory cells in EVE treated skin at the removal of the device. Inflammation decreases over time but is still significantly higher than baseline two days after treatment.

DISCUSSION

Our results demonstrate that the three-dimensional mechanical forces that EVE exerts on tissues activate multiple pathways ultimately responsible for proliferative, vascular and possibly even adipogenic responses (fig. 16). It is likely that the induced extracellular matrix (ECM) deformation, which in our model is evident from the macroscopic appearance of treated tissues, translates to an increase of the micro-mechanical strain on the single cells anchored to ECM fibers at focal adhesion sites. This has largely been shown *in vitro* to induce a pro-proliferative state by acting as a gate-control signal on global cellular activity mediated by the cytoskeleton [20, 97]. On a different scale, blood vessel deformation by EVE likely obstructs blood flow either through kinking or stretching which reduces the cross-sectional area and increases vascular resistance. Reduction of the interstitial pressure favors accumulation of edema and increases cell-to-vessel distance, decreasing mass transport due to diffusion. Pimonidazole hydrochloride stainings show that pO_2 is diffusely reduced during EVE stimulation. As we have demonstrated, edema is not immediately reabsorbed at the removal of EVE and generates a sustained physiological response to its presence. In addition, with the removal of the external sub-atmospheric pressure that stimulates tissues, edema transforms into a relatively compressive force on individual cells and blood vessels. This proposed relationship of edema and tissue perfusion is further supported by our hyperspectral imaging observations. The OxyHb content of tissues depends on systemic and local factors. In unmodified systemic conditions, OxyHb concentration is affected principally by the quantity of blood that passes through the capillaries in a unit of time (blood inflow). On the other end, DeoxyHb reflects both the local tissue metabolism at cellular level, and the time red blood cells need to pass through capillaries during which oxygen is exchanged with local tissues. In our case, the prolonged decrease in OxyHb we measured between 6 and 60 minutes

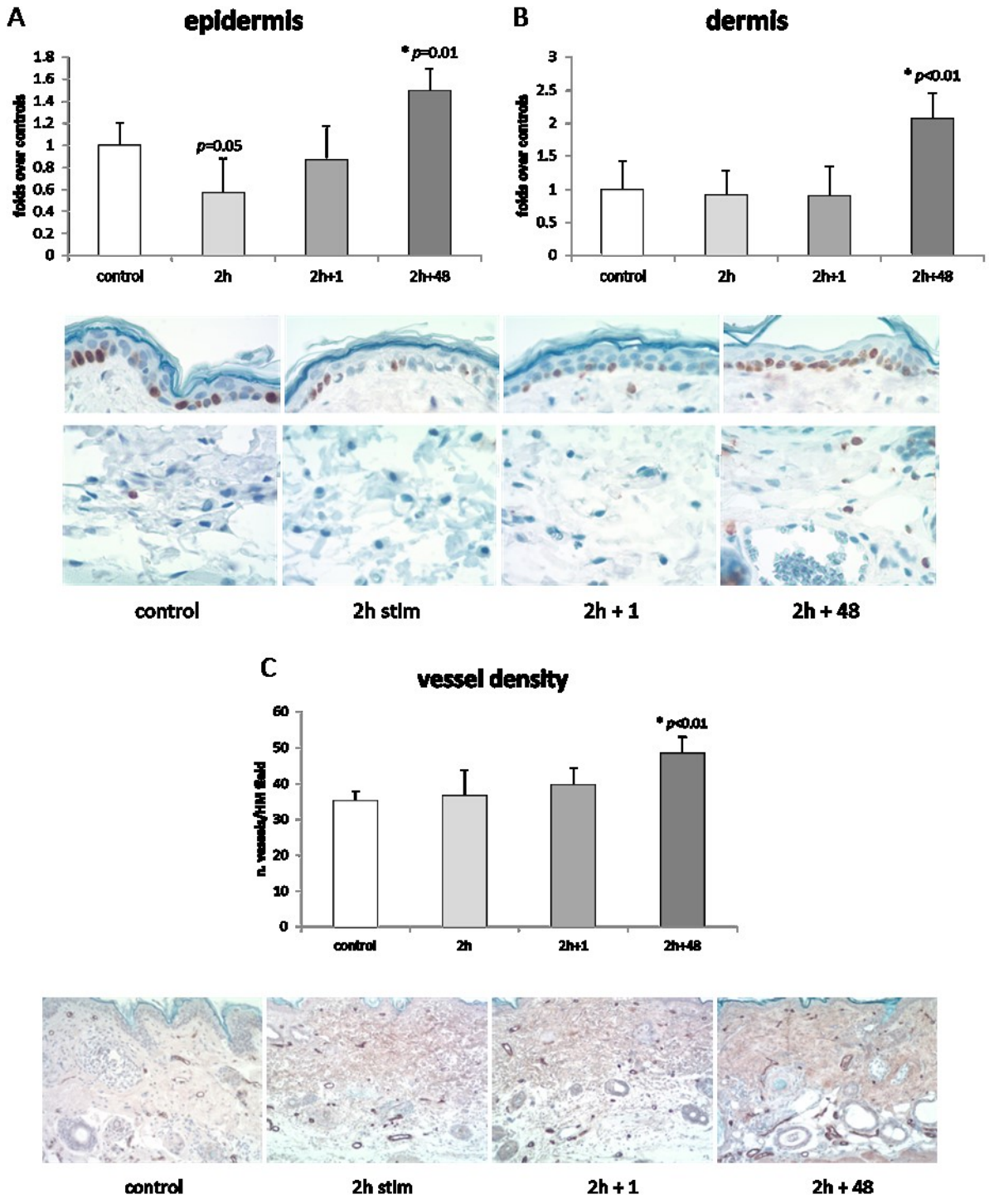

Fig. 15. a and b) EVE induces significant increase in cell proliferation rate by two days after treatment in the epidermis (a) and deep dermis/hypodermis (b), as evaluated by cell counting in PCNA-stained slides; results expressed as fold-increase over untreated skin c) EVE-treated skin exhibits higher density of PECAM-1 positive vascular structures two days after stimulation; results expressed as number of vessels/field.

following EVE removal suggests a relatively reduced blood inflow, possibly attributable to reactive vasoconstriction secondary to stretch. Decreased levels of DeOxyHb and TotalHb are suggestive of the absence of significant venous stasis as well as absence of vessels damage with extravasation of RBC in the interstitium. A limit of the hyperspectral imaging as employed in this study is the time needed for signal acquisition (20") and processing (20") that does not allow for true real-time imaging, and impedes detailed

exploration of the initial physiology after EVE release. The combination of pimonidazole observations that show hypoxia during stimulation, with normal OxyHb levels along with decreased DeoxyHb and total Hb after ceasing stimulation are suggestive of a behavior mildly reproducing hypoxia-reperfusion models. The likely peak in blood flow within the first seconds which can be expected basing on those models is probably lost in our analysis because of the limits of the technique. A prolonged state of relative ischemia is established after EVE release that is likely maintained by the combination of likely vasoreactions (not explored in our study) and compression by edema. While the mechanical stimulus of EVE ends abruptly with cessation of sub-atmospheric pressure, relative ischemia and hypoxia seem to last at least one hour beyond the stimulus and normalize by four hours. We also observed that an equally powerful stimulus, inflammation, appears to last well-beyond the immediate hours following EVE cessation. We observed the onset of inflammation having already occurred after two hours of EVE stimulation, and persistance through 48 hours post-EVE albeit in a progressively decreasing state. Ischemia/hypoxia are well known triggers of cell proliferation, as well as the best known stimulus of vascular remodeling and neo-angiogenesis via activation of the HIF-1a/VEGF pathway.

A significant question that this study generates is whether post-fat grafting EVE, as some authors have reported [28], is clinically appropriate. Indeed, while EVE may release positive pressure from the engrafted fat, it also induces intense levels of edema that may decrease diffusion of metabolites critical to fat survival during the first days, hampering rather than improving fat survival. For the same reason, an interesting approach may be to re-initiate EVE stimulation *after* the first week post-engraftment – when graft take can be expected to have already occurred - to maximize the adipogenic potential of the grafted tissue that is undergoing remodeling during that period.

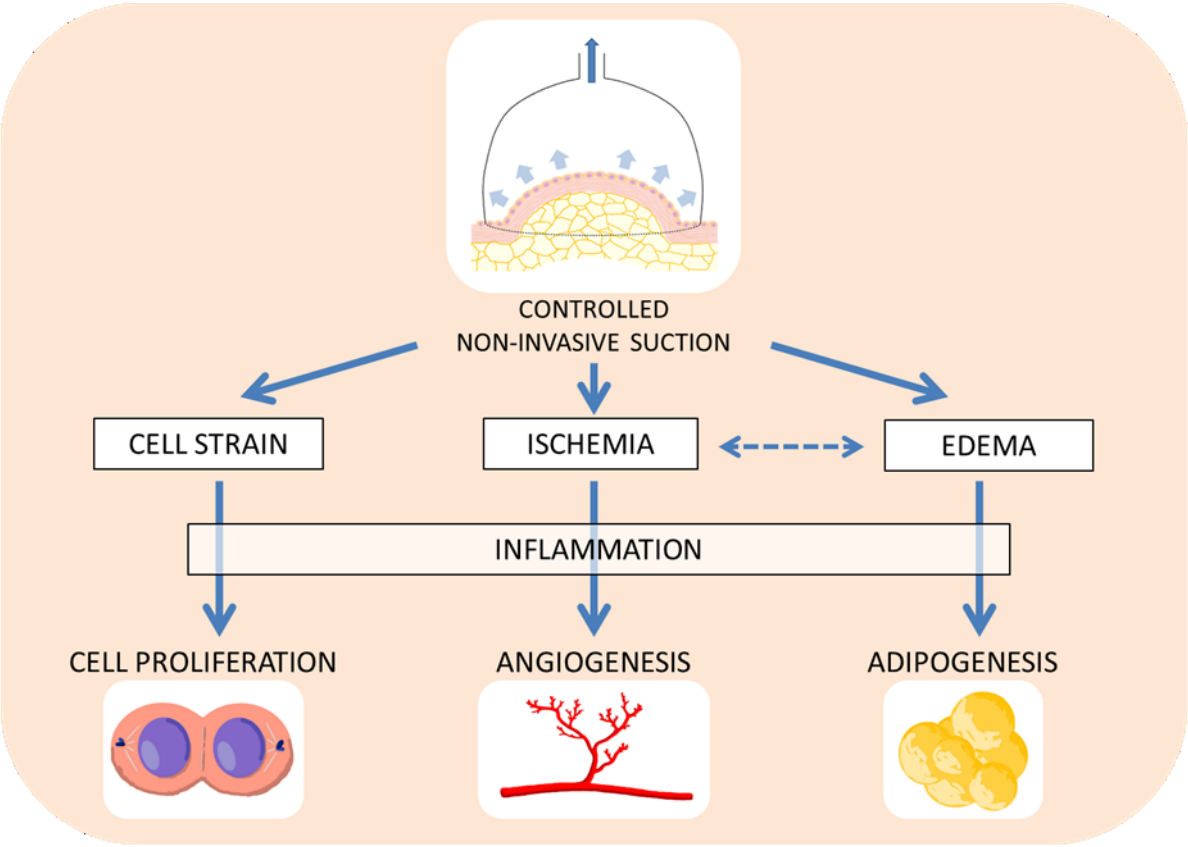

Fig. 16. Mechanisms and effects of External Volume Expansion summarized.

MODELING DIFFUSION AND PERFUSION IN FAT GRAFTING AND EXTERNAL VOLUME EXPANSION

Modeling has been critical for many advances in plastic surgery. Our group has previously modeled the effects of mechanical forces on skin expansion and Vacuum Assisted Closure devices before [21, 22]. The papers derived from these modeling efforts have greatly enhanced our understanding of the biological effects and medical uses of mechanical forces. Modeling provides the theoretical framework for testing theories. This study aimed to characterize which aspects of the microenvironment surrounding a fat graft affect retention and to create models to serve as a scientific basis to analyze the variables related to graft retention.

Grafted fat initially lacks vascular support and must receive oxygen and other nutrients by diffusion from nearby capillaries until neovascularization occurs. Oxygen appears to be the critical molecule required for cell survival. Low oxygen partial pressures in the center of the graft can lead to necrosis. Attempts to improve graft retention have largely been based on the "cell survival theory," which states that long-term graft volume consists primarily of grafted adipocytes that have survived the entire procedure[98]. This theory has generally been accepted and has directed most efforts to maintaining adipocytes viability through improved harvesting, processing, and re-injecting techniques. Studies supporting the cell survival theory claim that the "viable zone" (40% adipocyte survival) reaches as far down as 0.2 cm from the periphery of the grafted tissue [99]. These conclusions are based mostly on morphological observations with H&E staining. However, judging adipocyte health by shape or nuclear appearance can be misleading, and histologic sections are too thin to show most nuclei of healthy adipocytes [100]. Moreover, the "cell survival theory" may fail to get to the complex phenomena occurring in fat grafting. Fat grafts are not pure aggregates of adipocytes, but a mixture of adipocytes, preadipocytes, endothelial cells, pericytes, stem cells, fibroblasts, inflammatory cells, and matrix.

Using immunostain for perilipin, a reliable method for determining adipocyte viability, Eto and colleagues tested the cell survival theory and concluded that a dynamic remodeling of grafted adipose tissue (AT) occurs [100]. In hypoxic cell cultures, they demonstrated that adipocytes cannot survive more than one day of severe ischemia-mimicking conditions (1% O_2 with no serum), while adipose-derived stromal cells (ASCs) remained viable for up to 72 hours. In a second experiment, the inguinal fat pad of a mouse was grafted to the scalp. Only the peripheral area (surviving zone; <0.03 cm from the edge) of the graft had a high survival rate of both adipocytes and ASCs. In a deeper (regenerating zone), most adipocytes did not survive more than one day, but ASCs survived and eventually provided new adipocytes. By day three, the number of proliferating cells increased, and by day seven, they found an increased thickness of the zone with viable adipocytes. At the center of the graft, no AT survived; this was named the "necrotic zone."

Recent studies support this "host replacement theory." Rigamonti and colleagues suggest that 4.8% of preadipocytes are replicating at anytime, and 1-5% of adipocytes are replaced each day [101]. When mouse AT oxygenation reaches less than 65% of baseline, adipocytes undergo apoptosis in 24 hours; however, ASCs can survive for multiple days in severe hypoxia [102]. Hypoxia is known to enhance ASC proliferation [103]. Damaged adipocytes release fibroblast growth factor-2, which stimulates ASC proliferation and hepatocyte growth factor, contributing to the regeneration of AT [104]. The retention of grafted fat largely depends on the distance metabolites must travel to reach the center of the graft and on the depths of the surviving and regenerating zones.

MATERIALS AND METHODS

We studied the peer-reviewed literature to determine which aspects of the microenvironment surrounding a fat graft affect retention. Based on these findings, we created three models. The "Micro-Ribbon Model" relates the radius of a given fat injection to the oxygen concentration and cellular composition at various depths within the graft. The "Fluid Accommodation Model" relates the interstitial fluid accumulation to interstitial fluid pressure (IFP) and capillary perfusion. The "EVE Effect Model" predicts how preoperative external volume expansion (EVE) alters the microenvironment to allow for greater graft retention.

RESULTS AND DISCUSSION

The thickness of the exterior rim of viable cells in multi-cell spheroids increases linearly with the theoretical oxygen diffusion distance [105, 106]. The core principle of fat graft survival is that oxygen concentration at any point in a graft is a function of the oxygen concentration of the surrounding capillaries, the diffusion rate of oxygen to reach that point in the tissue, and the metabolic rate. In other words, at every point in a fat graft, there is a race between the rate at which oxygen is being consumed by the cells and the rate at which oxygen is being delivered by the capillaries and diffused through the AT.

The metabolic rate of a given section of AT is directly proportional to its volume (V). However, the diffusion rate of any substance is directly proportional to the surface area (SA) over which diffusion takes place, and the SA:V ratio of any interior section of a cylinder is (2/radius). Therefore, as the radius of a cylindrical injection of AT increases, the SA:V ratio decreases, and oxygen's diffusion rate cannot meet the tissue's metabolic needs.

Using diffusion and metabolism equations and known biological and physical constants [105, 107-109], we modeled the theoretical borders between the surviving, regenerating, and necrotic zones for fat grafts of different radii (Figure 1). This Micro-Ribbon Model predicts that the largest fat micro-ribbon with no necrotic zone would have a radius of 0.16 cm. Such a graft would have a surviving zone of only 0.03 cm and a regenerating zone of 0.13 cm. As graft radius increases beyond this critical point, the necrotic zone grows rapidly.

The following formulas model O_2 diffusion into a metabolizing cylinder of tissue[107]:

1.) $C = C_0 - (M/4D)[(R^2 - r^2) - a^2 \ln(R^2/r^2)]$

2.) $a^2 = [1 + \ln(R^2/a^2)] = R^2 - (R_{crit})^2$

3.) $R_{crit} = \mathrm{sqrt}(4DC_0/M)$

$C = [O_2]$ at a radial distance (r) cm from the center of a cylinder.	*(µmol/mL)*
$C_0 = [O_2]$ at the surface of a cylinder of radius R cm.	*(µmol/mL)*
C_S = min $[O_2]$ at which ASCs can survive.	*(µmol/mL)*
C_A = min $[O_2]$ at which adipocytes can survive.	*(µmol/mL)*
M = metabolic rate.	*(µmol/(mL*min))*
D = O_2 diffusion coefficient.	*(cm^2/min)*
R_{crit} = largest radius (R) such that ASCs survive throughout the graft.	*(cm)*
a = max radial distance (r) at which $[O_2] = 0$ when R > Rcrit.	*(cm)*
r_{ma} = min distance from center (r) at which adipocytes can survive.	*(cm)*

—The effective O_2 diffusion constant in AT (D) = $9.42*10^{-4}$ cm^2/min [105].

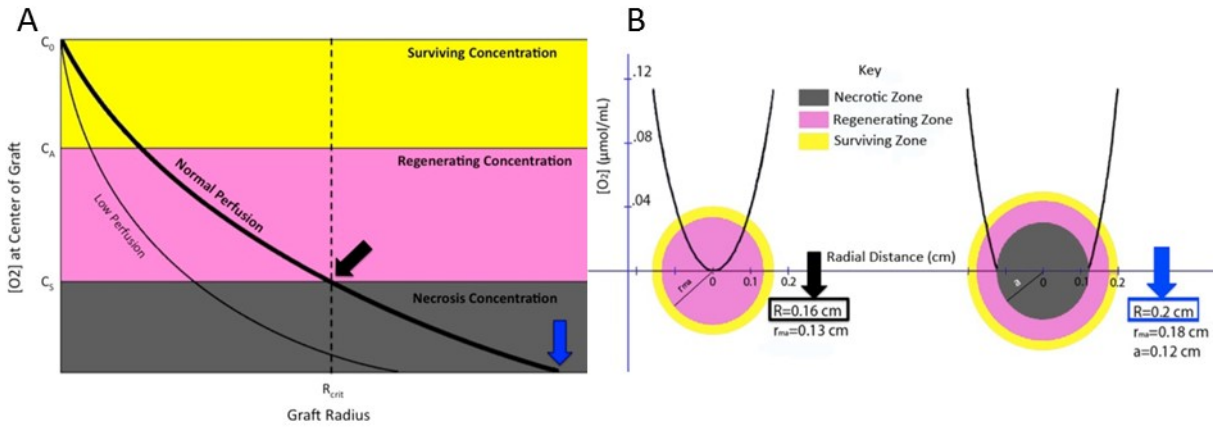

Fig. 17. A, Theoretical representation of oxygen concentration at the center of a fat graft as a function of its radius. There are 3 zones of oxygen concentration. The surviving zone has $C > C_A$. The regenerating zone has $C_A > C > C_S$. The necrotic zone has $C < C_S$. B, Cross-sectional views of cylindrical fat injections, showing $[O_2]$ as a function of radial distance. a, Cylindrical injection with $R = R_{crit}$. Adipocytes only survive in the outer 0.03 cm. ASCs survive throughout. b, Cylindrical injection with $R > R_{crit}$. Adipocytes only survive in the outer 0.02 cm. ASCs only survive in the outer 0.08 cm. No cells survive in the inner 0.12 cm.

—The maximum normal blood oxygen concentration (C_0) = 0.115 μmol/mL [108]. Because the mean number of capillaries per adipocyte in lean patients is 1.77 [27], we assume the graft is adequately surrounded by capillaries.

*—The baseline AT O_2 consumption in lean patients is 1.78 μmol/(100g AT * min) [107]. Assuming mean AT density is 0.95 g/mL [109], O_2 consumption in lean patients (M) = 0.0169 μmol/(mL tissue * min).*

*Using these values, equation 3 gives **R_{crit} = 0.16 cm**. This suggests the largest injected cylinder of fat should have a radius of 0.16 cm. Assuming adipocytes cannot survive oxygen concentrations below 0.075 μmol/mL (65% of C_0) [101], equation 1 predicts that when $R = R_{crit}$, r_{ma} = 0.13 cm (0.03 cm from the periphery), and viable ASCs will be found throughout the cylinder. If $R > R_{crit}$, the oxygen gradient creates three zones: the surviving zone (0.115-0.075 μmol/mL) in which all AT remains viable, the regenerating zone (0.075-0.01 μmol/mL) in which only ASCs remain viable, and the necrotic zone (0.01-0 μmol/mL) in which no AT survives (Fig. 17).*

The Micro-Ribbon Model correlates well with experimental data. When multi-cell spheroids were cultured in excess medium, the spheroids ceased to expand at a radius of 0.15 cm [110]. Long-term fat graft retention requires small volumes of AT to be diffusely distributed as "micro-ribbons" into a well-vascularized recipient site through well-separated tunnels; If too many micro-ribbons are injected into a recipient site of limited size, they will coalesce, forming particles too wide to survive. While the width of individual fat micro-ribbons can be determined by the surgeon, independent of the recipient site, the number of micro-ribbons that can be injected without coalescing is determined by the volume and compliance of the recipient site.

Fat graft survival has also been shown to significantly increase with improved recipient site vascularity in animal and human studies [111]. Therefore, recipient site vascularity, volume, and compliance are the essential microenvironment variables that determine oxygen delivery via diffusion, and thus, graft retention.

Several surgeons have suggested that injecting too much AT into a given recipient site can increase IFP enough to constrict capillaries and reduce oxygen delivery to the grafted tissues. Guyton demonstrated

that, for up to a certain volume, interstitial fluid can accumulate in a tissue without a significant IFP increase, but beyond that range, any additional fluid causes drastic IFP increases[112], quickly reaching levels associated with compartment syndrome. Milosevic and colleagues also demonstrated that capillary radius and perfusion decrease with increasing IFP [113]. Using these relationships, we modeled the change in relative capillary blood flow as a function of IFP and interstitial fluid accumulation (Fig. 18).

The model by Milosevic and colleagues suggests:

$$(\text{capillary radius}) = f(\text{intracapillary pressure} - \text{IFP} + 3)^{0.1},$$

and

$$(\text{flow rate}) = f(\text{capillary radius})^{4}.$$

Therefore,

$$(\text{flow rate}) = f(\text{intracapillary pressure} - \text{IFP} + 3)^{0.4}.$$

According to this Fluid Accommodation Model, a given tissue compartment can accommodate about 60% of its weight in interstitial fluid before reaching a critical IFP (IFP_C) of 9 mmHg, beyond which, any additional fluid causes a drastic IFP increase and capillary perfusion decrease. This IFP_C closely correlates with recent suggestions of IFP-based fat grafting stop points of 10 mmHg [114] and 9 mmHg[115, 116]. Clearly, the relative amount of fluid a given tissue can accommodate before reaching IFP_C also depends on its compliance, which can vary greatly between patients. In addition to decreasing capillary perfusion, increased IFP may also inhibit retention of grafted cells by mechanical compression, which induces apoptosis and regulates cytokine release [117]. Therefore, interstitial volume and compliance also determine how many micro-ribbons of fat can be dispersed before reaching IFP_C, reducing perfusion and cell survival.

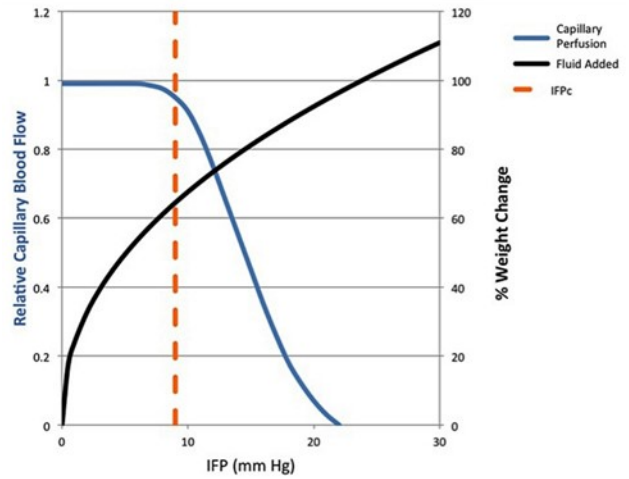

Fig. 18. IFP as a function of percent change in leg weight by saline injection in isolated dog hindleg (black). Mathematical model of relative capillary blood flow as a function of IFP (blue). IFP_C = IFP at which perfusion becomes compromised quickly; fat grafting should be stopped at this point.

Mechanical forces can induce angiogenesis and increased subcutaneous tissue thickness and compliance (Figure 3) [22, 28, 92, 118, 119]. In our previous studies we concluded that the macroscopic swelling is likely due to the deformation of the extracellular matrix (ECM). Micromechanical strain is transferred to the cytoskeleton, where it acts as a gate-control signal to induce proliferation[20]. Ischemia induced by EVE activates the HIF-1α/VEGF pathway to induce vascular remodeling, angiogenesis, and cell proliferation[119]. These processes are all promoted by inflammation (Figure 4).

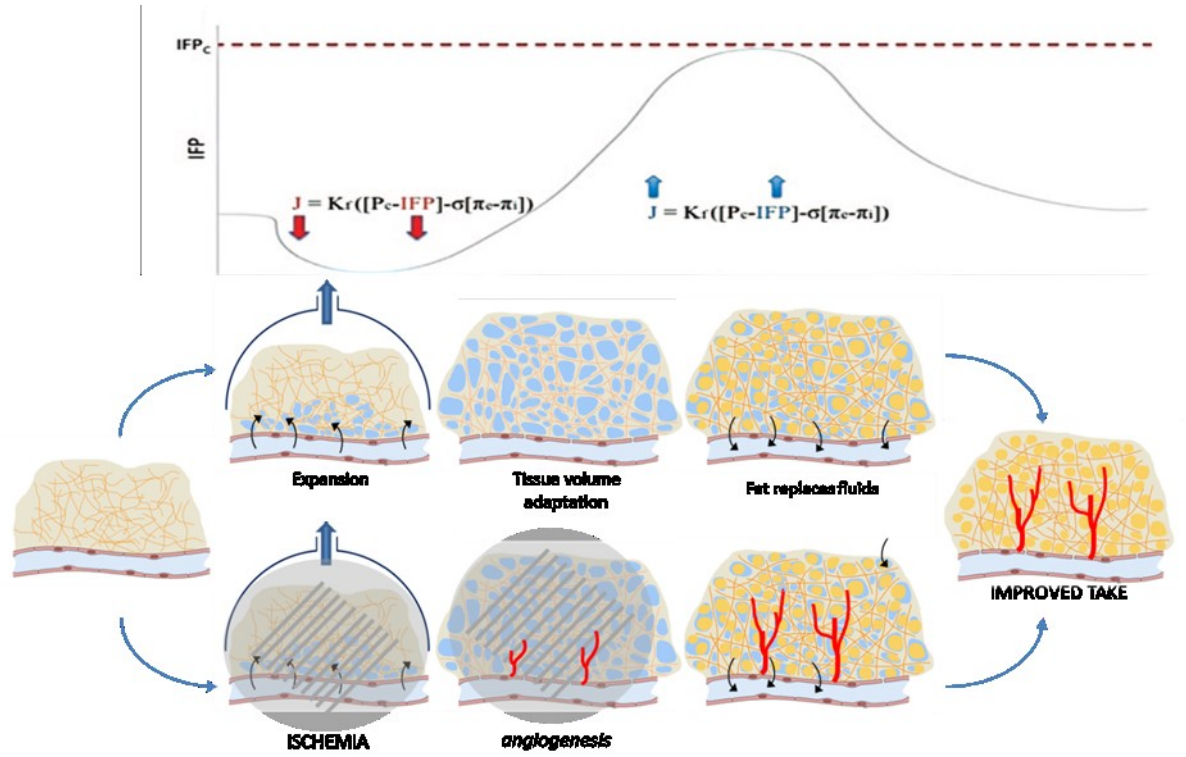

Fig. 19. Relative IFP throughout fat-grafting process with EVE. Long-term EVE expands tissues and causes an influx of edema, according to the Starling equation. Because the tissue is pre-expanded, as fat is injected, less coalescence occurs and more fat can be grafted before IFP reaches IFP$_C$. As pressure increases, edema quickly leaves the tissues, allowing pressure to return to baseline levels. Further, temporary ischemia stimulates angiogenesis achieving a more vascularized recipient site. The two effects combined improve chances of graft take.

With clinically available EVE breast pre-expansion and resultant augmentation had a strong linear correlation (R^2 = 0.87), and pre- expansion allowed significantly more AT to be grafted and retained than what was reported in a meta-analysis of six other published reports on fat graft breast augmentation without pre-expansion ($p < 0.00001$) [28].

In order to understand the effectiveness of fat grafting using EVE devices, we must consider the ratio of grafted fat to recipient site volume. If the original recipient site is only 100 mL and noncompliant, and the volume of AT to be grafted is 30 mL, there is no need for pre-expansion because, with a 30% increase, the AT can be diffusely micro-injected. If the original recipient site is 100 mL, and the volume of AT to be grafted is 90 mL, this 90% increase cannot be done without overcrowding, which would cause coalescence, increased IFP, reduced perfusion and oxygen delivery, thinner surviving and regenerating zones, and significant volume loss. However, our EVE Effect Model predicts that a tight 100 mL recipient site can be transformed into a compliant 300 mL site and, according to the Starling equation, cause an influx of edema. Because the fat micro-ribbons can be diffusely dispersed into the pre-expanded tissue, less coalescence occurs and more AT can be grafted before reaching IFP$_C$. As IFP increases, the Starling equation dictates that interstitial fluid is reabsorbed, allowing IFP to quickly return to baseline levels (Fig. 19).

Our EVE Effect Model also predicts that the pre-operative cyclical negative pressure treatment increases the host vascular density, increasing total blood flow and oxygen delivery, decreasing the mean distance each molecule of oxygen must diffuse to reach a grafted cell, and accelerating graft revascularization: a major determinant of volume retention (Fig. 20) [120].

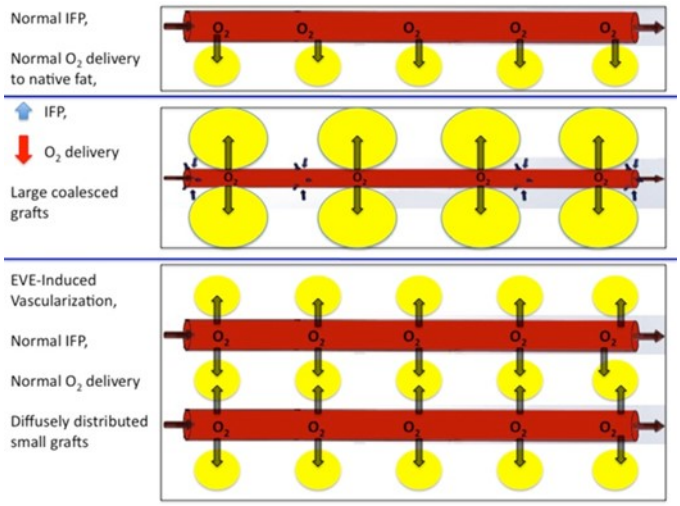

Fig. 20. A, At baseline, IFP is at basal state, so capillary radius is at basal state, and native fat receives sufficient oxygen delivery. B, When large volumes of fat are grafted without pre-expansion, fat particles coalesce and IFP increases, causing decreased capillary radius and oxygen delivery to grafted fat. C, When the same volume of fat is grafted with pre-expansion, fat particles remain diffusely distributed and IFP remains below IFP_C, so capillary radius remains uncompromised, and the grafted fat receives sufficient oxygen delivery.

The vascularity, volume, and compliance of the recipient site determine fat graft retention by regulating oxygen delivery via blood perfusion and molecular diffusion. Our theoretical analysis points to the potential of EVE devices to increase the recipient capacity for fat grafting. Increasing the volume and compliance of the recipient site allows thin injections of fat to be diffusely distributed. Thin injections have higher SA:V ratios, decreasing the distance oxygen must diffuse to reach the center. Diffusely injecting AT also avoids reaching high IFPs that may constrict capillary radii and reduce oxygen delivery. Increasing the vascularity of the recipient site increases the total oxygen delivery, decreases the mean distance oxygen must diffuse to reach each particle of AT, and accelerates revascularization.

EXTERNAL VOLUME EXPANSION INCREASES FAT GRAFTS VOLUME RETENTION

Our previous studies showed that EVE expands tissue compartments by 3D stretching and increases their vascularity [92, 119]. The next question was whether this is beneficial to fat grafting. We added to the model by performing grafting by injection of human gat after EVE stimulation, as would be expected in patients. In order to allow survival of the fat without rejection phenomena we switched to immunodeficient mice as animal model. We also integrated the study with data acquired in parallel studies aiming at optimizing stimulation parameters (unpublished data).

METHODS

Study Design

34 female, 12-week old NOD SCID Gamma Immune-deficient mice (NOD.Cg-Prkdc^{scid} Il2rg^{tm1Wjl}/SzJ, Jackson Laboratories, Bar Harbor, ME) underwent moderate-intensity intermittent EVE on the left dorsum during the course of 5 days. The choice of the stimulation pattern was based on a previous parallel study by our group in which we observed that 0.5-hour long stimulations separated by 1-hour long breaks repeated 6 times a day for 5 days, optimized the vascular density of target skin while limiting cutaneous complications. We obtained fat as lipoaspirate from discarded panniculectomies from two non-smoking, non-diabetic patients with similar demographics and processed it according to the standard Coleman's technique. Use of human tissue was performed according to existing regulations and approved by Institutional Review Board. On post-stimulation day 5 (PSD 5) 6 animals were sacrificed as baseline and the other 28 were grafted 1 cc of fat at the stimulated area and 1 cc at the contra-lateral not stimulated control area. On PSD 19 (Medium-term follow-up, n = 14) and PSD 47 (Long-term follow-up, n = 14) grafts were harvested en bloc using standardized 2 x 2 cm biopsies (including the graft, the overlaying/surrounding full-thickness skin and the panniculus carnosus). Fresh samples were weighted with a precision scale (OHAUS Corporation, NJ), then fixed in 10% neutral-buffered formaldehyde and stored in 70% ethanol before processing for microscopic analysis.

Microscopic Analysis

Samplese were stained with hematoxylin and eosin. Image acquisition and analysis (thickness of subcutaneous tissue, cross-sectional area of adipose grafts) was also performed according to our previously established methods. A qualitative analysis of the morphology of the grafts was also performed to evaluate presence of cyst and vacuoles.

Statistical Analysis

One-way analysis of variance (SPSS Statistics 20, IBM, NY) with Tukey post-hoc correction was used for means comparison.

RESULTS

Graft weight

Fat grafts in EVE-treated areas had a significantly higher weight that control grafts at both medium-term follow-up (2.2 ±0.2 vs 1.9 ±0.2) and long-term follow-up (2.0 ±0.2 1.6 ±0.2) with average fold increase over

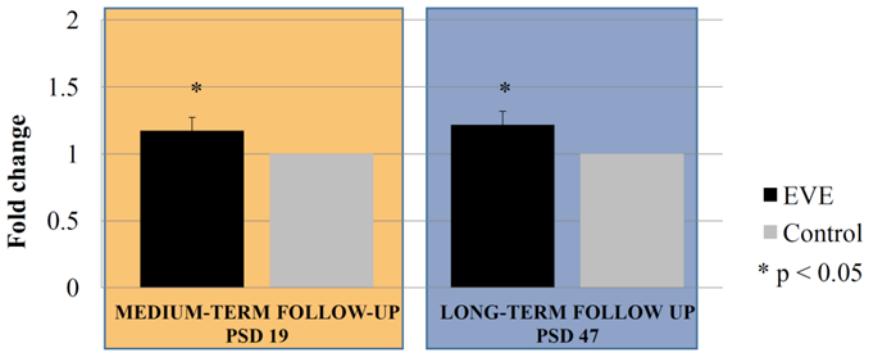

Fig. 21. Human adipose tissue xenografted in immunodeficient mice achieved better weight retention when grafted in areas pre-treated with External Volume Expansion at 2 and 6 weeks from grafting

control: 1.2 ± 0.1 ($p < 0.05$) (Fig. 21). Partial graft reabsorption was observed between medium-term and long-term follow-up within groups ($p < 0.05$).

Morphology

Both grafts at EVE treated sites and control grafts showed similar characteristics at H&e stainings. An inflammatory reaction was present at 2 weeks from grafting, consistent with graft remodeling. Adipocytes presented a regular morphology and were present throughout the graft at 6 weeks, at which timepoint some areas of fibrotic substitution and vacuoles could be equally appreciated in EVE treated animals and controls.

DISCUSSION

These results should be interpreted with extreme caution and not directly translated into clinical significance. The animal model, an immunodeficient mouse, presents several limitations and differences from the human setting. Besides already discussed anatomical characteristics, immunodeficiency implies a different inflammatory reaction to the graft even compared with autologous grafting and may have an impact on survival. However, the results support the hypotheses that EVE pre-treatment increases fat graft retention. Considering the two main mechanisms normally proposed, compartment expansion with decreased pressure on graft and increase in vascular density, it can be hypothesized that due to the relatively looseness of mouse skin the first factor should not have played a significant role in our model. Increase in vascular density may have, by itself, determined the increased retention of fat volume reducing its reabsorption.

EXTERNAL VOLUME EXPANSION IS EFFECTIVE IN IMPROVING FAT GRAFT RETENTION IN IRRADIATED TISSUES

Breast reconstruction following radiation therapy continues to be a challenge. While autologous and implant-based strategies present plausible options, a debate still exists in the setting of radiation injury as the risks of intra and post-operative complications increase dramatically [121-123]. As discussed before, fat grafting has recently emerged as a potential adjunct which may benefit many breast reconstruction patients. It can be used to improve the results achieved with either microsurgical or implant-based reconstructions, or even be the sole plan for total breast reconstruction in the form of large-volume fat grafting. In parallel, it has been speculated that stem cells present in fat can improve tissue trophism and skin appearance after radiation injury, furthering interest in the procedure for post-radiation breast reconstruction [124, 125].

However, several questions remain with regards to fat grafting in the setting of radiation fibrosis [126]. In the first few days after grafting, adipose tissue relies on oxygen exchange by diffusion with the recipient site, which in turn depends on nurturing from an underlying vascular network. As we and others showed, radiation induces a chronic state of fibrosis that deteriorates the vascular network of tissues [127, 128]. At an irradiated site, long term graft retention and quality would likely be negatively affected by the poor vascular bed [129].

We previously developed a mouse model of chronic radiation injury localized to a 0.8 cm diameter dorsal skin area. In this model we demonstrated how tissues developed after a single 50 Gray dose a state of reduced perfusion (-21% to baseline, $p<0.001$) (fig. 22) and decreased vascularity (1.7 fold reduction in density, $p<0.001$) (fig. 23) [127].

We also showed how an ischemic state develops early after injury, and monitoring deoxygenated hemoglobin by hyperspectral imaging we showed how its levels over the first three days correlated with irradiation dose in the spectrum 5 to 50 Grays (fig. 24), and how dose and deoxyhemoglobin levels correlated with entity of vascular density decrease at 28 days [128].

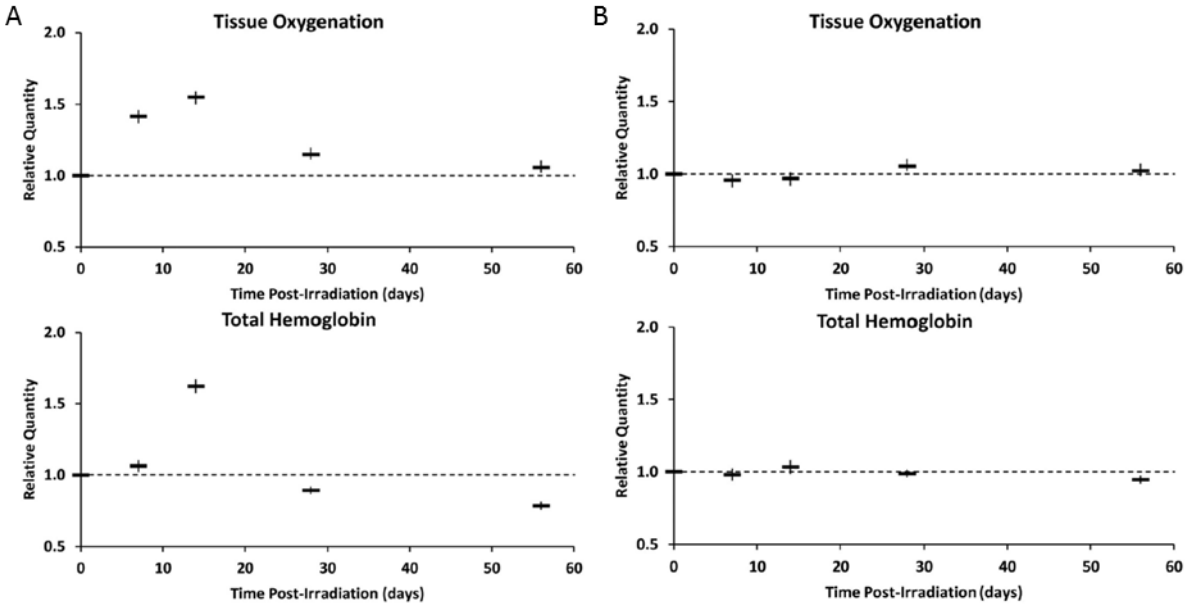

Fig. 22. Mean oxygen saturation (above) and total hemoglobin (below) in irradiated skin (A) and non irradiated skin (B) as a function of time after irradiation. Dahed lines represent baseline in each plot.

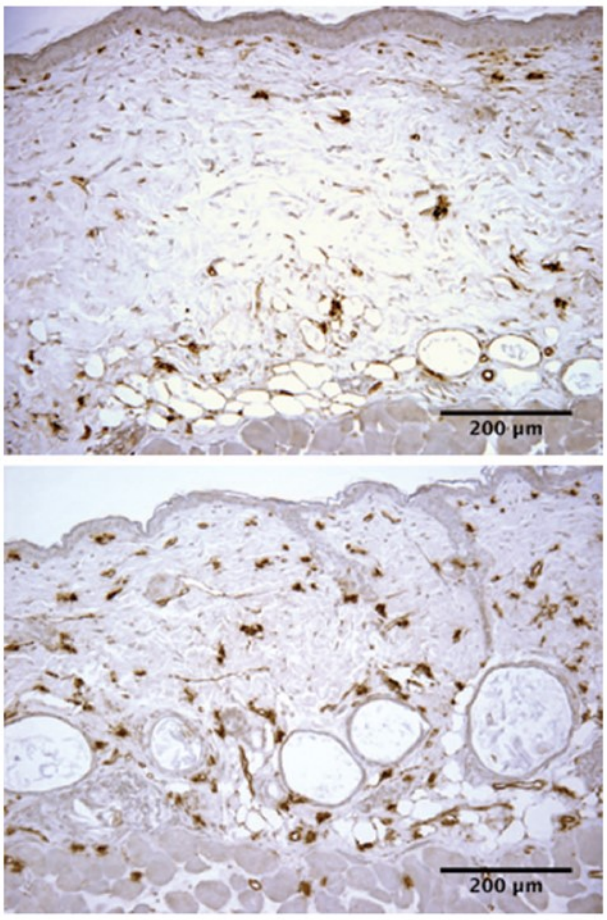

Fig. 23. Significant reduction (p<.001) in blood vessel density in irradiated skin (above) versus non irradiated skin (below)

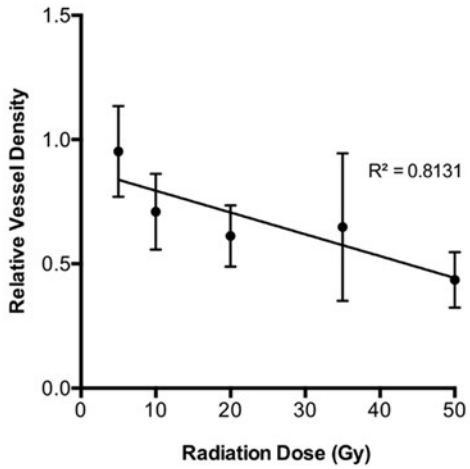

Fig. 24. Decrease in blood vessel density is directly proportional to radiation dose

EVE may offer an option to improve the vascularity of recipient sites even in a setting of radiation fibrosis.

A further recent work of our collaborators at the University of Massachusetts demonstrated how, despite the deleterious effects of radiation in soft tissues (fibrosis, hypo-vascularity, ulceration), pre-conditioning with External Volume Expansion can effectively induce an angiogenic stimulus even in this setting, increasing the subcutaneous vasculature density by 37%. Similarly it induces a strong proliferative effect, increasing the epidermal thickness by 37% and epithelial cell proliferation by 45% compared to irradiated but non pre-expanded skin (fig. 25) [130].

Building on the animal models already developed for skin radiation fibrosis and for EVE, we now focused on assessing 1) the capacity of tissues with chronic radiation injury to act as recipient sites to fat grafting, and 2) the capacity of external expansion to improve the take of fat grafts in tissues with radiation fibrosis. Thus, we hypothesized that pre-conditioning of the irradiated area will create a richer recipient site, which will improve volume preservation and long-term results, mitigating the damage caused by radiation.

METHODS

A total of thirty CD-1 athymic nude mice were used and allocated into 3 study groups. This strain has been selected from previous pilot studies due to the absence of rejection of human xenografts and an otherwise preserved immune system that allows radiation-related changes to occur (inflammation-ulceration-healing-fibrosis). Dorsal skin areas to be studied were tattooed with a needle and permanent ink in order to allow the identification of the area of interest at all times.

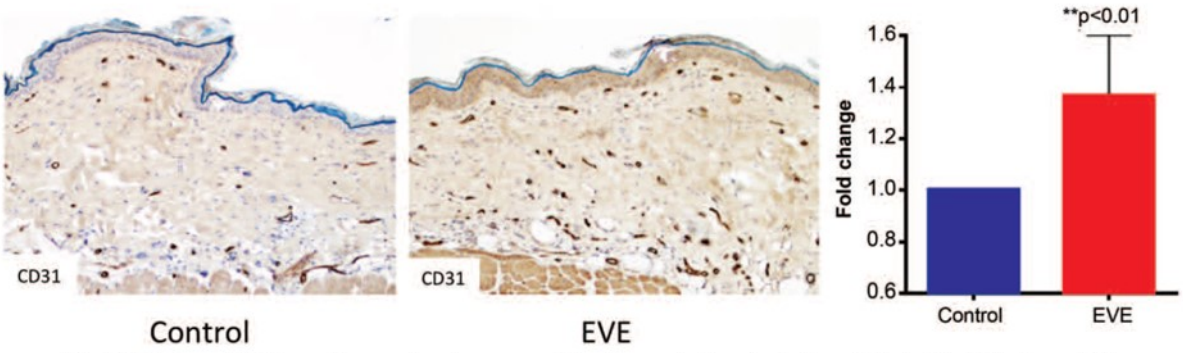

Fig. 25. External Volume Expansion increases blood vessel density in irradiated skin (+37%, p<.01).
Reproduced from: Chin MS et al. External Volume Expansion in Irradiated Tissue: Effects on the Recipient Site. Plast Reconstr Surg. 2016 May;137(5):799e-807e.

Group 1 (n=10) received a single exposure of radiation and served to validate the effectiveness of irradiation-fibrosis/hypoperfusion evolution in this study. Group 2 (n=10) received only fat grafting without radiation, to evaluate the take rate of fat under native conditions in this model. Group 3 (n=10) received bilateral radiation exposure, followed by a course of external volume expansion in one of the sides as described in our previous work, leaving the contralateral side unexpanded. Both sites then received fat grafts and allowed assessment of the effect of radiation injury on fat grafting and the effect of pre-treatment with EVE respectively (fig. 26).

Radiation Exposure

Radiation source was handled and supervised by experts in the radiation oncology department at the University of Massachusetts Medical Center. Groups 1 (n=10) and 3 (n=10) received a unilateral or bilateral exposure respectively of 50Gray of radiation using a 1cm-diameter topical beta-source placed 5 cm lateral to the spine. This dose is the equivalent to the average cumulative dose received by breast cancer patients at our institution. Dosing and radiation source protocol has been established based on our previous studies. It affects up to the superficial 2mm of skin without underlying organ damage. Over the following 8 weeks, we expect all mice to develop a sequence of inflammation-dry desquamation-ulceration-fibrosis.

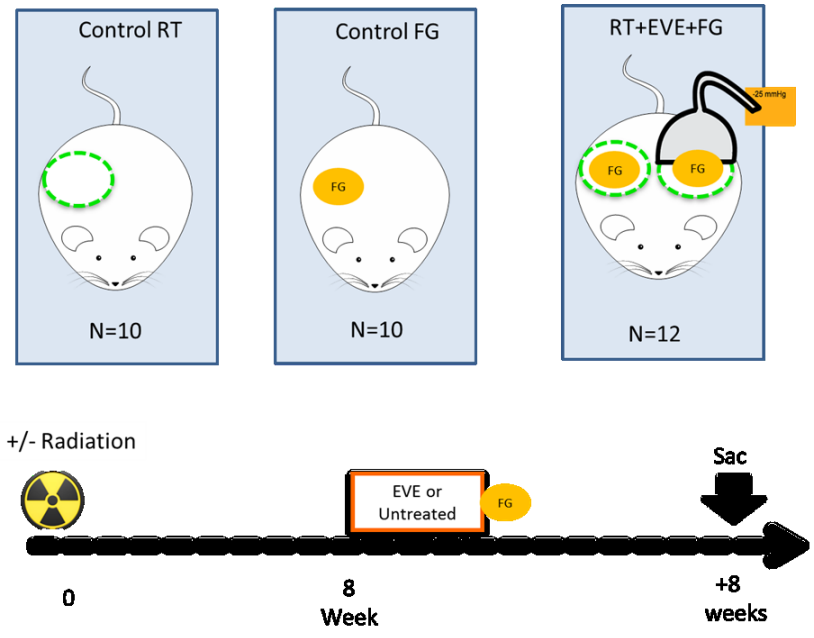

Fig. 26. Study design

Radiation-induced ischemia was confirmed by the use of the HyperSpectral Imaging device Oxy-Vu (Hypermed, MA) used by our group in previous studies [127]. The fold change relative to the contralateral non-irradiated side was used as main unit of comparison. The perfusion values were followed up during the first 8 weeks of the study and trends were captured in a graph.

External Volume Expansion

Expansion was performed for 6 hours daily for 5 days, following the protocol of stimulation of our collaborators previous study on irradiated skin [130].

In these studies we saw that irradiated tissues treated with EVE remain hypoxic and underperfused for up to 5 days. This may have negative impact in the graft survival. Similarly, we found that in irradiated tissue a robust angiogenic response is seen by 2 weeks after the last day of expansion. Basing on these combined observations we selected day 14 post-EVE stimulation as an ideal time in our model to perform fat grafting.

Fat grafting

Adipose tissue was obtained from discarded material from one panniculectomy performed at UMASS, under an approved IRB. In order to counter issues of variability in donor and fat characteristics, all grafts were derived from same donor. Fat was extracted by manual liposuction with multiple passes using a 3mm cannula and dry technique, and centrifuged to eliminate oil.

Fat grafts were performed under sterile conditions using a 16G IV cannula. The cannula was inserted at a distant site, the tip was advanced to reach the previously irradiated area or the selected untreated site depending on group assignment, subcutaneous fibrosis was released by blunt dissection, and fat was injected in single-bolus. A total of 0.3 ml of fat was injected basing on previous pilot studies performed to

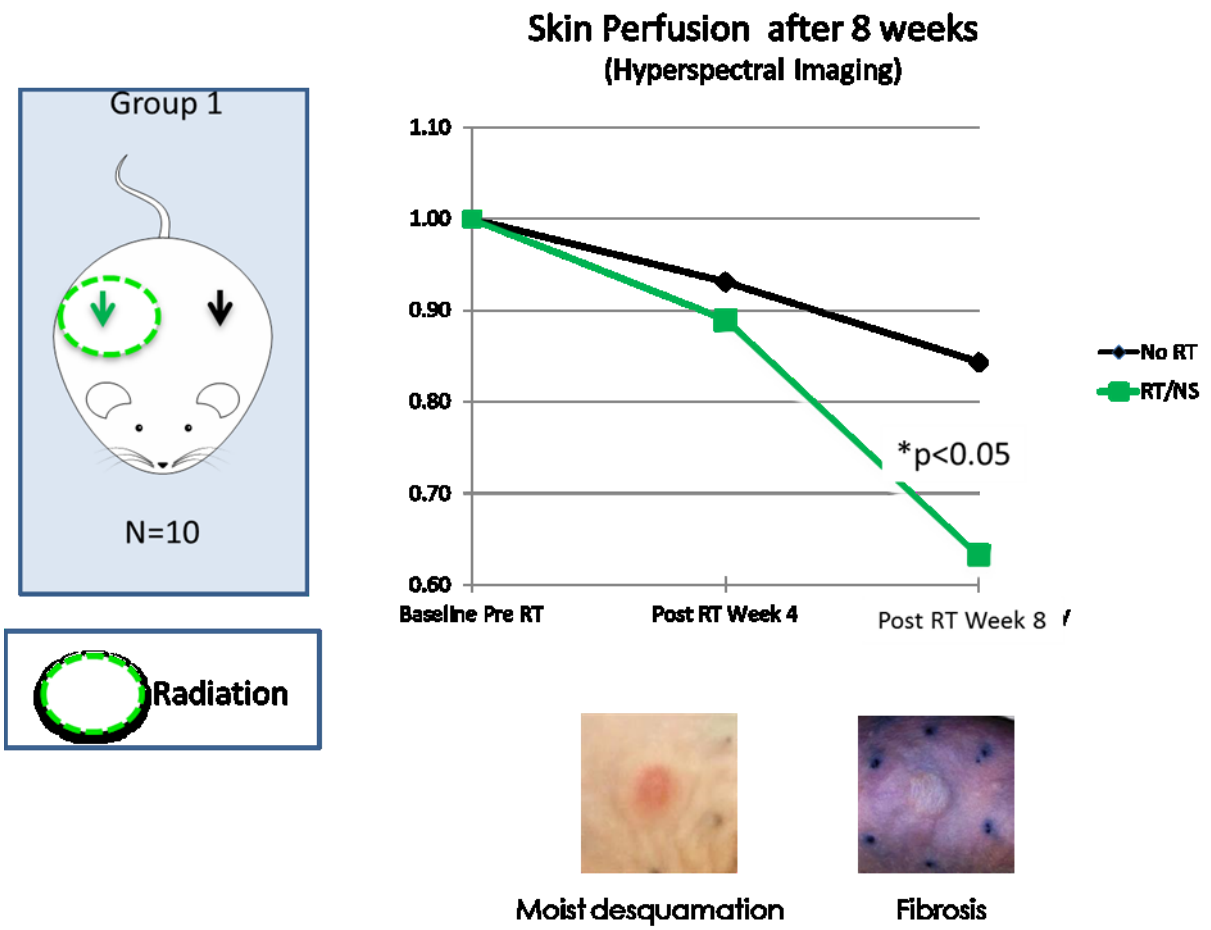

Fig. 27. Animals in group 1 were monitored by Hyperspectral Imaging to confirm the development of chronic radioinduced injury in irradiated sites. Irradiation induced a sugnificant decrease in tissue perfusion by 8 weeks.

establish a reasonable injection volume that would allow achieving a reproducible subcutaneous fat mass of size still compatible with the development of the graft evolution zones as modelled by Yoshimura's group. Then a rubber donought-shaped splint of 1.5 cm internal diameter was positioned on the skin to surround the grafted area, protecting and preventing fat graft displacement for the first 2 weeks. Mice were monitored daily during the first 2 weeks and then once a week for the remaining time of the study. At 8 weeks mice were sacrificed and tissue was collected for histology.
Volume Quantification

Micro-CT was performed at at the Musculoskeletal Imaging core facility of our institution for small animals. Mice that underwent fat grafting were imaged 2 days postoperative fat graft injection for baseline volume. The grafted mice then underwent imaging at week 8 to calculate final volume retention as compared to baseline.
For micro-CT scans, the mice were anesthetized with isoflurane. Anesthesia was maintained by mask inhalation of isoflurane vaporized at concentrations of up to 5% in the induction phase and at 2% during acute imaging procedure. Imaging was performed with animals in the dorsal position using a Scanco vivaCT 75 microCT system scanner (Scanco Medical, Switzerland). The effective voxel size of the reconstructed images was 40. A global threshold (170) was applied to remove soft tissue background for 3D image reconstructions.
Fat grafts were reconstructed in three-dimensions by contouring regions of fat as seen on the microCT images. All reconstructions were performed by two independent investigators to avoid single observer bias. Fat volume was calculated using the distance transformation function of the Scanco Medical 3D analysis software.

Histology

Transversal sections through the center of the samples were stained with hematoxylin and eosin according to standard protocols and by immunohistochemistry for CD31 and Perilipin-A.

RESULTS

Irradiation

After radiation exposure, all mice went through the expected course of erythema, moist desquamation, ulceration and fibrosis. All wounds were completely healed by 8 weeks after radiotherapy, resulting in a velvet-like skin surface appearance indicative of fibrosis..

Concurrently, Hyperspectral imaging confirmed a decrease in Total-Hb in irradiated side compared to the non irradiated contralateral side ($p<.05$), and a (decrease compared to baseline measurements ($p<.05$), confirming the ischemic damage and vessel obliteration seen in our previous studies (fig. 27).

EVE

After a course of uncomplicated External Volume Expansion for 5 days, tissues were visibly expanded and swollen, although the outer fibrotic appearance of radiated skin was still present and unchanged. Swelling had reabsorbed after 14 days, when fat grafting was performed (fig. 28A).

Fat grafts

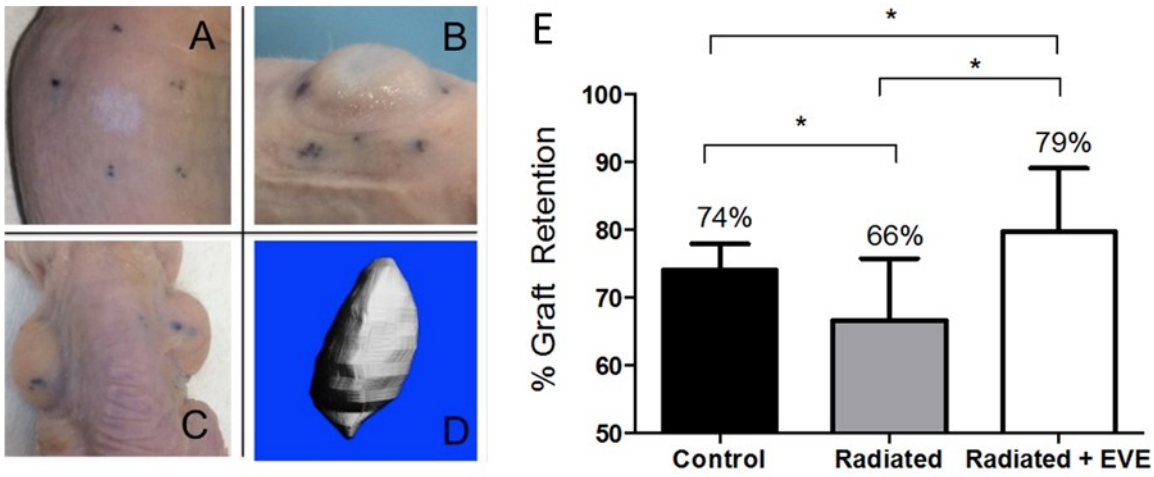

Fig. 28. Irradiated skin areas (A) received 0.6ml fat grafts (B) and were followed up for 8 weeks (C). Volume reconstruction from CT-scans (D) allowed comparison of fat grafts volumes (E).

Adipose tissue was grafted without complications on mice from groups 2 and 3. No evidence of rejection reactions was appreciated during the subsequent 8 weeks of monitoring.

By the end of this period, grafts presented as well-defined dome-shaped soft masses at the injection sites (fig. 28C).

By Micro-CT volumetric analysis (fig. 28D) we established that the fat grafting/non-irradiated group had a 74% graft volume retention after 8 weeks. Fat grafts performed at a previously irradiated site displayed a retention of 66% by the end of the same time period ($p<.05$). When fat grafts were performed to irradiated sites prepared by a cycle of external volume expansion, grafts showed a 79% retention by 8 weeks ($p<0.05$) (fig. 28E).

Histology

Samples presented similar features at H&e stainings. Some oil cysts were present along with some signs of fibrous substitution. CD31 positive structures were present throughout the grafts. Perilipin-A staining showed almost uniform positive staining, with occasional non-staining adipocytes localized in the central areas of the grafts, sign of still ongoing remodeling. No significant differences could be perceived between groups.

DISCUSSION

Radiation therapy has been a key contributor to the increased survival of breast cancer patients and modern protocols allowed a paradigmatic shift in the approach to breast cancer from radical mastectomies to breast conserving surgeries. This responds to and helped developing a more mature sensibility to the concept of restorative surgery not limited to curing the disease but aiming at maximizing life quality. The downside is that, despite improved protocols minimizing acute side effects of radiation therapy, irradiated tissues still undergo chronic changes that, among others, negatively impact reconstructions. Autologous reconstruction with flaps can face higher rates of wound healing issues, fat necrosis, stromal/flap atrophy and contour deformities requiring a revision rate up to 62% of cases in comparison to non-irradiated breasts. On the other hand, implant based reconstruction carries higher rates of infection, capsular

contracture and implant extrusion with reconstruction failure in up to 77% of cases [122, 131, 132]. Even nipple reconstruction suffers of higher complications rate in presence of previous radiotherapy [133].
Recently fat grafting emerged as a tool that can be useful in addressing tissue quality related issues following radiation therapy. It can provide a thicker protective layer around implants, soften atrophic irradiated tissues, and improve contour deformities. Further, some evidence suggests a regenerative potential of adipose tissue, possibly due to the reservoir of stem cells present in the stroma. Animal studies demonstrated improvement of skin quality achieved by fat grafting after irradiation [134, 135] in a laboratory setting, and have been successfully translated into clinical settings with burns or radiation dermatitis [129, 136]. It is believed that a combination of growth factor secretion through paracrine action is and differentiation of mesenchymal cells to vascular or epithelial lineages may be the contributors to clinical improvements demonstrated on these reports [137].

Therefore, breast reconstruction in presence of radio-dermatitis could potentially benefit from fat grafting for both a restoration and reshaping of volume missing secondary to breast parenchyma resection and for a mitigation of the cutaneous damage caused by radiation.

We and others have demonstrated that external radiation causes obliteration and fibrosis of blood vessels of the targeted area leading to vessels deprived tissues [127]. It was confirmed in this study by reproducing previous results that showed the establishment of a localized fibrotic hypoperfused environment following irradiation. This underperfused state could potentially compromise the survival of grafted fat. Our results indeed demonstrate that previous irradiation of the recipient site determined a significant reduction of 11% of volume of the final grafted fat mass, at comparison with volumes achieved in not irradiated sites. It confirms the assumption that radiated tissues, as well as being less good sites for traditional autologous or prosthetic reconstructions, also offer a sub optimal recipient site to fat grafts. Clinically, it potentially translates in higher number of procedures needed, higher fat necrosis with calcifications or oil cysts, more inflammatory reactions with reabsorption, less visible results, and overall less patient and surgeon satisfaction with the procedure.

Basing on current theories on the relationship between fat graft take and recipient site vascularity, increasing the density of the vascular network might restore the potential of irradiated tissues to act as adequate recipient sites.

We previously tested whether the angiogenetic potential of EVE was still significant in presence of fibrotic irradiated tissues. EVE displayed the capacity of inducing a 37% enrichment of the capillary network density of previously irradiated tissues at two weeks from stimulation [130].

We now showed that EVE preparation of the recipient site is effective in reversing the negative impact of previous irradiation on fat graft survival, achieving a 20% increase in retained fat volume at comparison with non-EVE treated sites. This is even a 6.5% higher retention volume than standard fat grafting to non-irradiated tissues.

Interestingly, these results offer further support to the outcome of our previous study in which we demonstrated a positive effect of EVE pre-treatment in retaining fat grafts mass in normal, non-irradiated tissues.

In conclusion, we confirmed that previous irradiation has a deleterious effect on fat grafting, but our results also suggest that preparing the recipient site by increasing its vascularity with EVE can be a rescue technique that significantly impacts the fate of the graft.

EXTERNAL VOLUME EXPANSION DIRECTLY STIMULATES ADIPOGENESIS

In contrast to the unidirectional tensile stimulation on underlying tissue of our pre-EVE mechanobiological studies [22, 50], the miniaturized EVE device provides a more complex three-dimensional array of mechanical forces that include tension, compression and shear depending on the location of the tissue within the device. As EVE using suction induces a transient decrease in interstitial pressure facilitating transport of fluids into the extracellular space, a potential further effector may be localized edema.

Edema has been suggested to stimulate adipogenesis. In particular, lymphedema is often accompanied by an accumulation of fat tissue in the affected body part [138, 139], but the underlying mechanism is still unknown. Harvey et al. demonstrated in an in-vivo model that deficiency in the Prox1 allele lead to the development of obesity with increased subcutaneous tissue based on defective lymphatic system and generalized edema [140]. Lymphatics drain from the extracellular space proteins and lipids that leak from capillaries [141, 142], and lymph stasis may signify local accumulation of molecules with lipogenetic or adipogenetic effects. Application of suction to wounds suggests a direct relationship between edema, inflammation and cell proliferation, with reduction of edema being accompanied by decreased inflammation and proliferation[53, 143]. Edema increases the distance between cells and blood vessels distance which can generate a hypoxic or inflammatory environment.

Indeed, the development and introduction of EVE devices into the plastic surgery and breast augmentation markets was guided by the idea that three-dimensional tensile forces could be employed to directly stimulate breast growth and induce non-surgical breast enlargement (Brava® Breast Enhancement and Shaping System, Brava LLC, Miami, FL) [18].

In the initial clinical experience with the device, most users achieved an average of one-cup size increase after several months of EVE usage by receiving stimulation for up to 10 hours daily. Although these findings were in agreement with accumulating *in vitro* [63, 91] and *in vivo* evidence [22, 32, 50] of the role played by mechanical forces in tissue augmentation, the device was highly patient compliance-demanding and did not achieved widespread use for breast augmentation alone due to the inconsistence of the results. Only years later began the clinical interest in adopting the device as a preparatory approach for fat grafting to the breasts which we discussed as motivating reason for our previous studies [144].

In our first proof of concept EVE study reported above we also analyzed changes in the fat composition of the hypodermis [92].

METHODS

For study design see "proof of concept" section

Adipocytes quantification

Measurements were made in H&E stained sections of tissue thickness and of the number of adipocytes in vertical columns between panniculus carnosus muscle and the dermis, in three random spots per sample (Image J, NIH, Bethesda, MD, USA). The number of adipocytes and the subcutaneous thickness were plotted together to generate a two-dimensional graph.

RESULTS

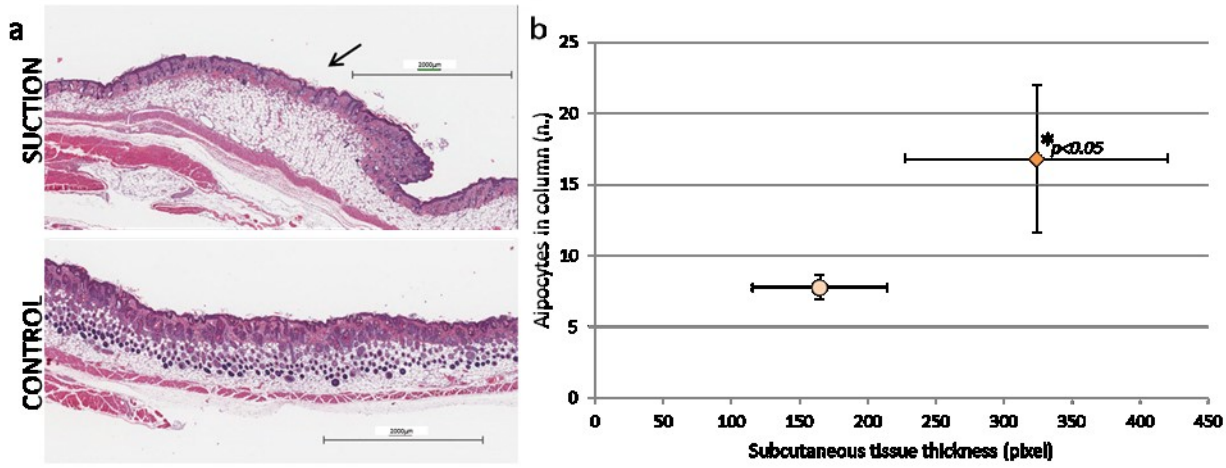

Fig. 29. 28 days EVE induced accumulation of fat in the subcutaneous tissue (A) with significant increase in both subcutaneous tissue thickness and in number of adipocytes in vertical columns (B)

Microscopy (Fig. 29) showed a 2-fold increase of the subcutaneous thickness ($p<0.01$), with an average 2.2 times more adipocytes in columns (S: 17±5.1; C: 7.8±0.9; $p<0.05$) compared to the controls at day 28. The thickness of the dermis was not affected by treatment (data not shown).

Based on our studies, it appears all four factors 1) micro-mechanical stimulation, 2) edema, 3) hypoxia/ischemia and 4) inflammation likely contribute to cell and vessels proliferation (Figure 5). Importantly, previous studies suggest that both edema and inflammation, acting in a coordinated fashion, have pro-adipogenic effects. In an elegant series of studies, Morrison and colleagues demonstrated that the presence of an empty proteic matrix [145-148] in contact with a fat mass [149, 150] provides signals for cellular differentiation and attracts cells from blood vessels that are induced to differentiate into adipocytes, promoted in part by inflammation [151]. The model, which may have close similarities with the "empty space" filled with edema in EVE-treated tissues, is now being translated from animals to clinical applications [152].

The idea that EVE stimulation may have adipogenic effects is intriguing. Mature adipocytes generally are believed not to proliferate. Adipogenesis is thought to result from stem cells commitment to the adipocyte lineage, proliferation of preadipocytes, their recruitment, and terminal differentiation into mature adipocytes.

Building on the evidences collected in our previous work, we designed a study aiming at specifically assessing the hypothesis that EVE stimulations can directly induce adipogenesis, independently from fat grafting [153].

MATERIALS AND METHODS

Animal model

Under a protocol approved by the local Institutional Animal Care and Use Committee, twenty-eight male SKH1-E hairless and euthymic mice (Charles River Laboratories, Wilmington, MA) were stimulated for 2 hours/day for either 1 (EVE1) or 5 (EVE5) consecutive days. These patterns were designed basing on our previous studies with EVE models and on a feasibility pilot, in order to establish single-stimulation effects and explore the kinetics of ciclicity remindful of clinically adopted daily wearing of EVE systems. Half of the

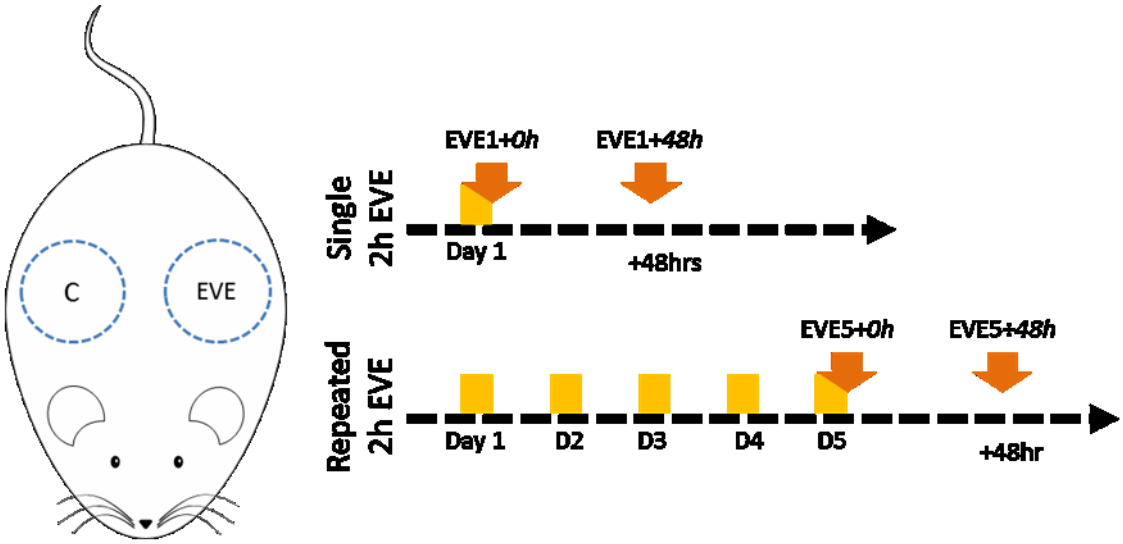

Fig. 30. ***Left:*** **A selected area of mouse dorsum lateral to the spine was stimulated (EVE); the contralateral area was left untreated as internal control (C).** ***Right:*** **Animals were distributed into 2 groups. Group 1 received one single stimulation of 2hrs (EVE1). Group 2 received a daily stimulation of 2 hrs repeated for 5 consecutive days (EVE5). The animals were euthanized immediately after the last session of stimulation (+0h, n=7/group) or 48hr after the last session (+48h, n=7/group).**

animals receiving either treatment pattern were euthanized immediately after completing stimulation (+0h) to evaluate early effects of EVE, and the other half 48hrs after stimulation (+48h) (Figure 30).

The treated site and the non-treated contralateral skin were harvested with a 10-mm punch biopsy tool. One half was snap frozen and preserved at -80°C for protein analysis; the remaining half was mounted on cardboard, fixed in 10% formaldehyde for 24 hours for histology and stored in 70% ethanol at 4°C.

Histology and immunohistochemistry

Sextions were stained for Hematoxylin and Eosin, Perilipin-A and pan-leukocyte marker CD45. One animal in the EVE1+48h group was excluded from examination due to sample labeling issues, and one in the EVE5+48h due to sample loss in processing.

Adipocyte quantification

Adipocyte number was selected as the primary outcome of our study. Viable adipocytes were identified in sections stained for the specific marker Perilipin-A (PLIN-A), which is a protein coating lipid droplets in adipocytes that protects them against lipases [154]. Oval structures with positivity for antigen expression around the membrane were considered as mature adipocytes.

Quantification of the number of adipocytes in the subdermal adipose layer, superficially to the panniculus carnosus muscle was performed in the EVE1+48h and EVE5+48h groups. Counting was done on entire sections scanned at 40x magnification with the aid of ImageScope software (Aperio, Vista, CA, USA) by three investigators and confirmed by blinded manual counting by independent investigators. The results were normalized as number of adipocytes per mm basing on section length as measured in the scanned slides, and expressed as fold-increase of treated sides over internal controls. Adipocyte counts in animals from the +0h groups was not performed, as edema and tissue distortion impeded adequate staining and identification of structures.

Qualitative assessment of tissue

The architecture of epidermis, dermis and subcutaneous tissue was analyzed on H&E stained slides, paired with the macroscopic appearance, and reviewed by 2 independent examiners.

Inflammation

CD45 positive cells density in the EVE1+48h and EVE5+48h groups was quantified over three representative 10x fields of each stained section by three independent observers with the aid of Image J software (Image J, NIH, Bethesda, MD).

Protein Expression

Western Blots were performed on samples of EVE5+0h and EVE5+48h (n=4 each) for Peroxisome Proliferator-Activated Receptor Gamma (PPAR-γ) and Preadipocyte Factor 1 (Pref-1, also called DLK1) under similar protocols.

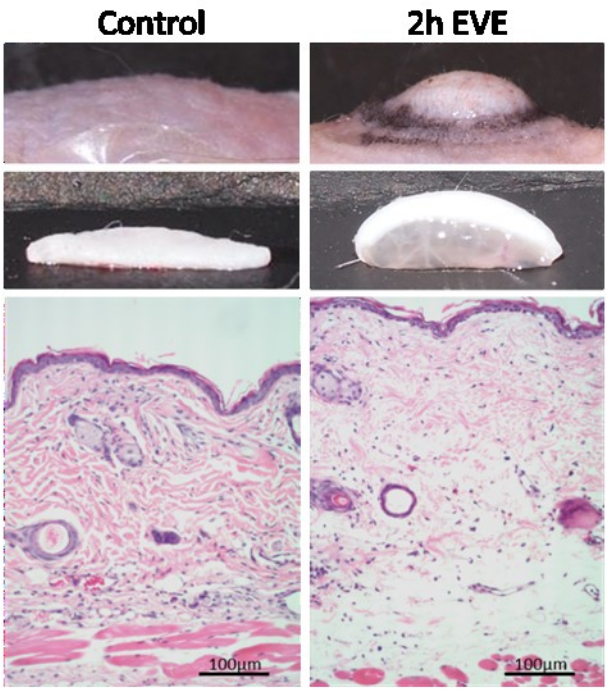

Figure 31: Acute effects of EVE on stimulated tissues. Immediately after ceasing stimulation, tissues were macroscopically swollen (*top*). This was confirmed by cross sectional biopsy (*center*) and at histological analysis showing interstitial fluid accumulated in the dermis and hypodermis (*bottom*).

Tissue samples were placed in T-PER Pierce/Thermo scientific Protein Extraction Buffer (Thermo Scientific) that contained complete Mini EDTA-free proteinase-Inhibitor cocktail (Roche). Samples were then lysed on ice by means of motorized pestle.

Protein concentrations were measured using the standard BCA protein assay method (Pierce) and UV spectrophotometer (NanoDropTM ND-2000, Thermo Scientfic). Gel electrophoresis was performed using precast Ready Gel® Tris-HCl 4–12% Gels (Biorad). Tris/glycine/SDS buffer (Biorad) served as running buffer. Equal amounts of protein (15–30 µg) were loaded in each lane, and the gel was run at 180 V for one hour. Polyvinylidene difluoride (PVDF) membranes (Biorad) were briefly incubated in 100% methanol, quickly rinsed and then incubated in 20% methanol containing Tris-glycine transfer buffer. Next, proteins were transferred onto PVDF membranes at 25 V for 50 min using transfer buffer and a Trans-Blot Semi-Dry System (Biorad). PVDF were then blocked with 5% milk in Tris-buffered saline (TBS)-Tween (TBS-T) for 90 min at room temperature. The primary antibody was diluded in 5% milk in TBS-T. PVDF membranes were incubated in the primary antibody solution at 4°C overnight on an orbital shaker. PVDF membranes were washed three times with TBS-T and then incubated in the secondary antibody solution (also in 5% milk in TBS-T) for 45 minutes at room temperature followed by three washes. Thermo Scientific™ Pierce™ ECL 2 Western Blotting Detection reagents (Thermo Scientific) served as the chemiluminescence kit. Semi-quantitative imaging analysis was performed using Image J (National Institutes of Health).

Statistical Analysis

A paired two-tailed Student's t-test was performed to compare means of EVE-treated vs control tissues within the same animals and at the same time points using PRISM software. Means between groups at

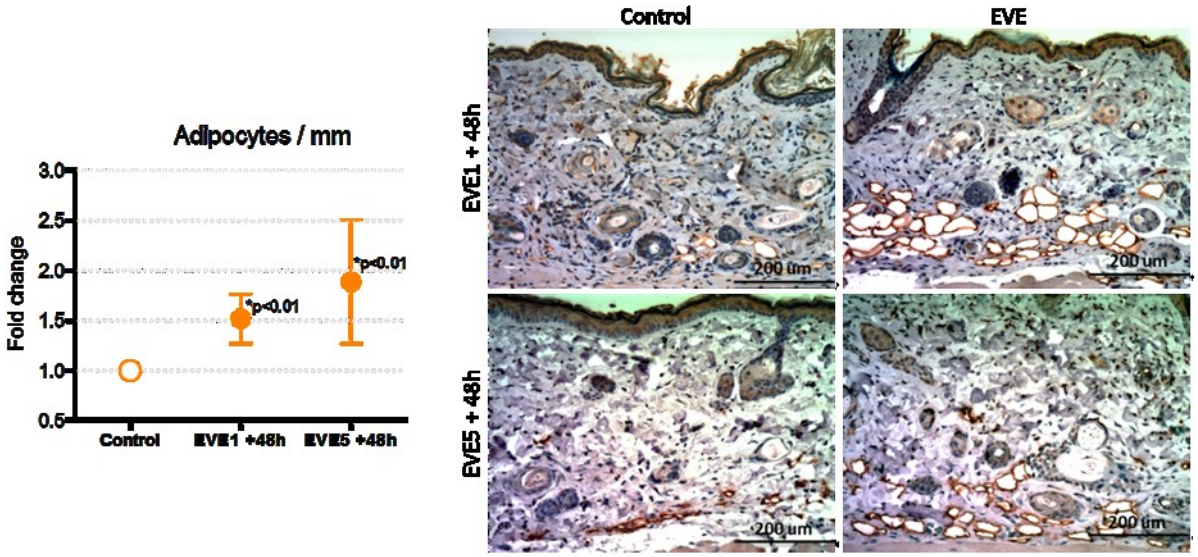

Figure 32: Adipocytes (Perilipin-A+ oval-shaped structures) were identified in the subdermal layer above the panniculus carnosus muscle, and their number/mm over entire section and surface percentage in standard 40x fields were quantified. Resuls are expressed as fold increase over controls. P values refer to the comparison of each stimulated group with its internal controls from the same animals. Differences in fold increase between the EVE1+48 and EVE5+48 groups did not reach significance for either adipocyte numbers and area.

different time points were compared with a two-tailed Student's t-test for independent samples with equal variance.

RESULTS

Adipocyte quantification

An increased density of subdermal adipocytes in EVE-treated sites was detected at microscopic evaluation of H&E stained slides, and confirmed by quantitative analysis of slides stained for Perilipin-A (fig. 32). Two days after a single stimulation for 2hr (EVE1 +48h), tissues presented a 1.5-fold (+/- 0.25) increase in number of adipocytes per linear millimeter of tissue compared to non-stimulated (NS) tissue (p<0.01). Treatment for 5 consecutive days (EVE5 +48h) yielded to a 1.9-fold (+/- 0.6) increase in adipocytes in the subcutaneous tissue compared to NS skin in the control side (p<0.01) (Figure 3). The difference in fold increase between time points was not significant.

Qualitative Assessment of tissue

Immediately after EVE, both with single 2h stimulation (EVE1 +0h) and with a 5-day course (EVE5 +0h), tissues appeared macroscopically swollen (Figure 31). Histological evaluation of H&E slides confirmed a large amount of interstitial fluid having accumulated, in particular into the hypodermis. A normal histologic architecture was restored in samples collected 48 hours after treatment, when tissue swelling was no longer evident at examination

Inflammation

EVE stimulation induced an inflammatory response, with a 2.2 (+/-0.9) (p<0.01) and 1.8-fold (+/- 0.7) (p=0.01) increase over controls in CD45 positive cells density in both EVE1+48h and EVE5+48h respectively. (Figure 33).

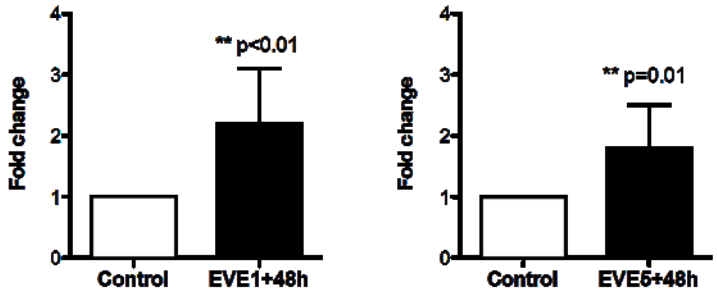

Figure 33: Inflammatory cells (CD45+) in EVE1 and EVE5 respectively, 48hr after treatment. Results are expressed as fold-increase over controls.

Western Blot

Western blot analysis revealed that immediately after 5 days of stimulation (EVE5+0h) relative PPAR-γ expression was significantly increased in stimulated skin when compared to non-stimulated (1.0 ± 0.17 vs. 0.24 ± 0.05, p<0.01, N=4). This effect, though to a lesser degree, was still detectable 48h later (EVE5+48h, 0.75 ± 0.04 vs. 0.43 ± 0.08, p<0.05, N=4). In samples analyzed for Pref-1, no difference was found between EVE and NS sites after 5 days on the immediate sacrifice group (EVE5+0h) (p=0.88). The samples from animals sacrificed 48hr later (EVE5+48h) showed no difference in Pref-1 expression, (0.81 ± 0.20 control vs 0.40 ± 0.01 EVE (p=0.12, n=4). (Figure 34).

DISCUSSION

The results from this study support the hypotheses that EVE possess an intrinsic pro-adipogenic potential, showing in our model an increased number of adipocytes after a period of recovery of 48 hours, even from

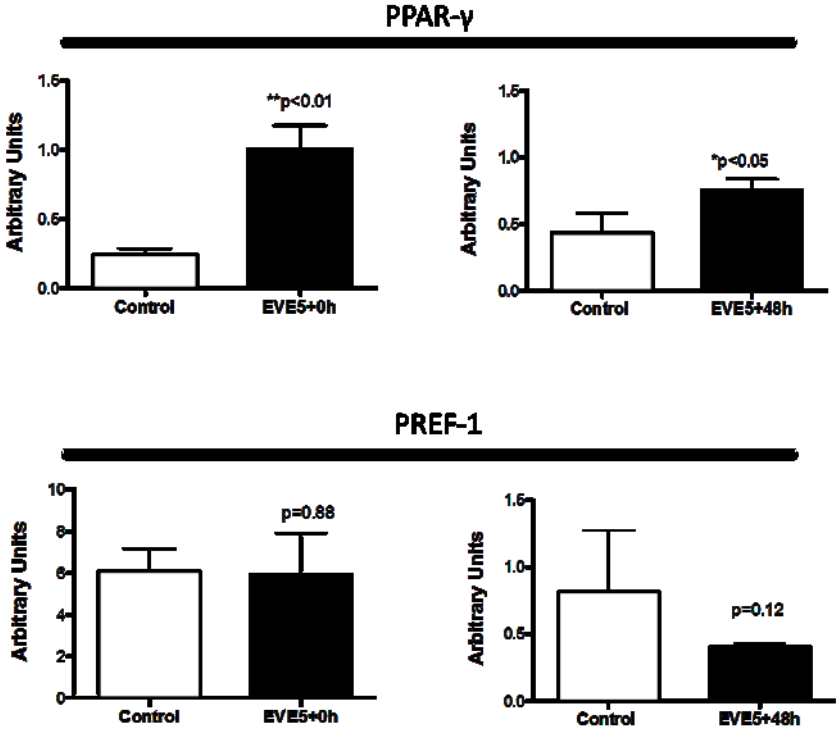

Figure 34: Expression of PPAR-γ and PREF-1 evaluated by Western Blot in animals treated with 2h stimulation repeated for 5 days, immediately after sacrifice (EVE5+0h) and 48 hours later (EVE5+48h).

a single 2h stimulation. This potential seems to elicit its effect via the establishment of a pro-adipogenic edematous, inflammatory environment.

Peroxisome Proliferator-Activated Receptor Gamma (PPAR-γ) is a ligand-activated transcription factor expressed chiefly in adipocytes and macrophages [155, 156]. This transcription factor has been demonstrated as the main initiator and orchestrator of adipogenesis [156, 157]. PPAR-γ activation initiates pre-adipocyte expansion *in vitro* [158], and induces adipogenesis *in vivo* [159], while in its absence, adipose tissue fails to develop [160]. In our study, we found that a pro-adipogenic environment is induced, as demonstrated by an increased expression of (PPAR-γ) signaling pathway..

In parallel, Pref-1 is a specific marker of preadipocytes, acting as a gatekeeper in the process of adipogenesis. Pref-1 acts as an autocrine/paracrine factor, inhibiting adipocyte differentiation [161]. As differentiation occurs, Pref-1 expression decreases to undetectable levels, reflecting the degree of maturation and differentiation [162]. This marker in EVE-treated tissue after 48hrs showed a tendency to reduced expression, which did not reach significance. However, this may be attributable to our small sample size due to technical problems and tissue loss or to inappropriate choice of the timepoint for this effect.

EVE creates mechanical tension and induces edema and inflammation; each of which, independently, have been found to trigger adipogenesis (Figure 35). Inflammation up-regulates PPAR-γ [151] and promotes M2 macrophage activation [163]. In the matrigel chamber with arteriovenous loop model, inflammation was key in formation of adipose tissue, which could be blunted by macrophage depletion [151, 164-166]. Furthermore, adipose tissue formation has been noted in lymphedema as a result of chronic inflammation in patients [138, 139, 167] and replicated in animal models [141, 142]. In agreement with this, we found in our recently published model that inflammation was significantly increased by the end of a 2hr EVE treatment [119] and remain elevated for at least two days. In the aforementioned studies, inflammation and edema are chronic elements that remain consistently present, while in the present study, they are acute phenomena, which regress over the course of hours for edema and days for inflammation [119].

Mechanical stimulation is also a potential independent player in the observed adipogenic effects. We and others have established its pro-proliferative and pro-angiogenic effects *in vitro* [63, 91] and *in vivo* [22, 50]. Moreover, static mechanical traction induces a pro-adipogenic effect [168-170]. Our model is in agreement with these observations, as the stimulation applied resembles periods of static tension through an externally-applied source repeated over several days.

Hypoxia is known as an anti-adipogenic factor, as Hypoxia-Inducible Factor 1 (HIF-1) downregulates PPAR-γ expression [171]. We previously showed transitory presence of hypoxia and ischemia during EVE treatment [119]. Moreover the transitory inhibitory effect of hypoxia is likely overcome by the aforementioned factors, but its potentially negative role should be taken into account when developing clinical protocols of stimulation with EVE.

While our results demonstrate the capacity of EVE alone to induce a pro-adipogenic environment and increase adipocytes number, previous clinical experience attempting to increase breast mass with this strategy alone has been less satisfactory. This can be explained by multiple reasons. Our results are from histological analysis at microscopic level, while volume augmentation of a larger mass likely takes more time and factors to occur to a perceivable extent. However, our model is suggestive of a trend towards superior number of adipocytes gained as the number of sessions of stimulation increases. Cyclical external

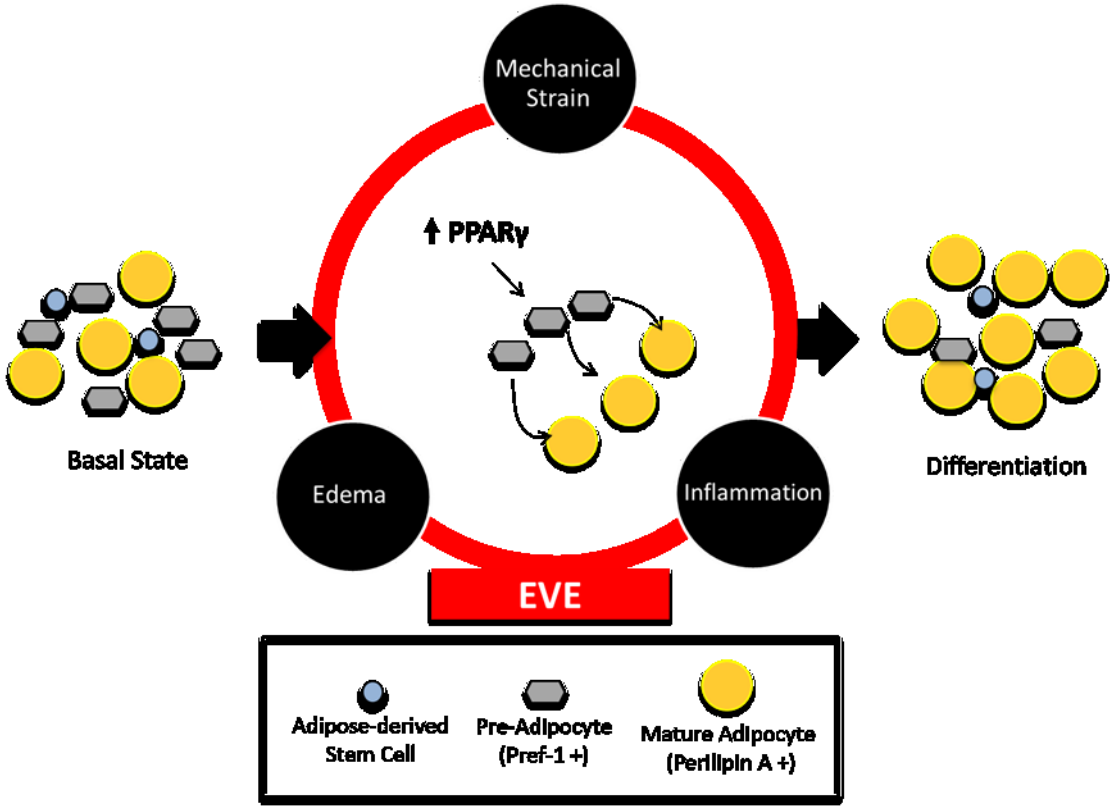

Figure 35: A theorical model for adipogenesis induction by EVE. The combined effects of mechanical stimulation, edema and inflammation may stimulate differentiation of commited pre-adipocytes present in the tissue. This overall results in accumulation of mature adipocytes.

forces have demonstrated a greater regenerative effect than constant forces (9). Therefore, the kinetics of repeated stimulations should still be assessed for maximum gains. The mouse and human models present significant differences [172, 173]; however, similar mechanisms, even if of different magnitude, could reasonably be expected to be at play.

According to recent theories that are gaining sound experimental support, much of the retained fat mass after fat grafting may not be due to adipocytes survival, but to repopulation by surviving adipose derived stem cells in the empty scaffold left by dead mature adipocytes [100, 174, 175]. As we demonstrated in earlier work, application of EVE prior to fat grafting expands the recipient site, reducing the compression on the graft, while stimulating the formation of a rich vascular network, key elements for fat graft survival [176]. Another option suggested by our results may be to clinically employ EVE after fat grafting as well, with the intention not of "stabilizing the graft" [144, 177], but rather to specifically stimulate a pro-adipogenic environment that may increase stem cells commitment to adipocytic differentiation in the scaffold repopulation phase. Such a strategy may help reducing scarring and reabsorption in fat grafts, leading to an overall quantitatively as well as qualitatively improved yeld. Several elements need to be looked into before this is safely proposed, in particular timing and pressure levels. Moreover, EVE may find application in tissue engineering to drive the development of new adipose tissue within a scaffold, combining its adipogenic with its angiogenic potentials. Morrison's group recently published their experience in moving from the mouse to humans in testing the in vivo tissue engineering chamber for breast regeneration they developed. In their study, they moved to the breast area a small amount of fat vascularized by the thoracodorsal pedicle and covered it with their chamber. At six months one patient had developed a satisfactory if not perfect fat mass, while in other 5, even if signs of fat depositions were observed, most of the newly formed tissue was essentially fibrous. As they suggest, combination of their

model with an EVE stimulation might help overcoming the difficulty they experienced in translating to a larger model their previously successful and promising technique. [178, 179] Further experiments are needed to identify the nuances of the mechanical forces and the specific timeframe in which an EVE-based adipogenic approach can be of most benefit post-grafting and even potentially tailored to multiple uses.

However, caution should be exercised when attempting to translate the results of this animal model to clinical significance, as important intrinsic differences are present that could affect the relative contribution of the different factors we have identified. In particular, human tissues are stiffer and less deformable than those in the mouse, which affects both the stretch imposed at a given pressure and the amount of edema which can accumulate in the third space. Furthermore, the adipogenesis shown in our previous study resulted from continuous EVE that maintains a stable level of edema remindful of lymphedema and of Morrison's chamber model. In contrast to this static state of edema, current clinical EVE utilizes cyclical wear patterns (6 to 10 hours daily) that generate transient periods of edema formation and subsequent absorption. This can be expected to lead to in/out-flux of metabolites, and more closely reflects the design of this study. While the proposed non-surgical EVE methods have yielded but a limited degree of breast enlargement [180-183], the possibility that continuous wearing of EVE may overcome this barrier shown with cyclical EVE appears an appealing hypothesis to evaluate.

THE ROLE OF INFLAMMATION IN THE ADIPOGENIC EFFECTS OF EXTERNAL VOLUME EXPANSION

Several models point to edema, ischemia and catabolites accumulation as factors determining a pro-adipogenic environment in which mesenchymal stem cells are stimulated to preferentially undertake the adipose cell differentiation pathway [138, 141, 142, 146, 147]. However, several models also suggest that inflammation is a key effector in this process [151, 166].

We showed inflammation to be a common denominator to EVE stimulation as well, and this factor alone could potentially all of the observed effects in terms of cell proliferation, increase in vascular density, and adipogenesis. Macrophages, in particular M2, play a pivot role in switching mesenchymal stem cells fate. Previous experiments in other models showed that macrophages depletion could prevent adipocytes deposition [151, 164].

We therefore set on testing the role of macrophages in determining EVE induced effects, and in particular adipogenesis, by undertaking a new study in which EVE was applied to animals in which macrophages response was hampered by macrophages depletion.

Clodronic acid, or clodronate, is a drug of the biphosphonates family routinely used in the treatment of multiple myeloma, primary hypothyroidism, osteoporosis, tumoral osteolysis, due to its inhibitory effect on bone reabsorption [184]. It acts by antagonizing osteoclasts, bone macrophages cells which are specialized differentiated cells of the monocyte-macrophage lineage [185].

Experimentally, clodronate can be included within liposomes in high concentrations, and clodronate liposomes can be employed as a strategy to induce macrophages depletion in animals. Liposomes are phagocytated by macrophages as part of their natural scavenger activity. Liposomes are broken down in cell lysosomes, liberating relatively high concentrations of clodronate that are toxic to the macrophage and induce its apoptosis [186, 187]. This method demonstrated high safety profiles for the animals, and has been used also in newborn mice [188-191]. Basing on the route of administration, selective macrophages depletion in chosen body compartments can be achieved in otherwise non-immune deficient animals (www.clodronateliposomes.org).

To date, liposomal clodronate has been used for macrophages depletion in almost 1000 published studies and more that 3000 projects are registered. Several describe successful macrophages depletion in the skin through local or intraperitoneal injection (www.clodronateliposomes.org).

MATERIALS AND METHODS

Animals

A total of 16 male SKH1-E hairless mice aged 8 weeks (Charles River Laboratories, Wilmington, Mass.), were cared for and used at the animal facility of the Azienda Ospedaliera Universitaria of Padova under an approved experimental protocol.

Macrophages depletion

At 48 hours pre-EVE stimulation, 8 casually selected mice received an intraperitoneal injection of 0.3 ml of liposomal clodronate (Clodronate Liposomes, Nico van Rooijen, www.clodronateliposomes.com) along with

a subcutaneous 0.1 ml injection to the dorsum along the thoraco-lumbar midline. Further 0.2 ml were administered intraperitoneum 2 hours beore EVE stimulation. The 8 control animals received no treatment.

EVE stimulation

All animals were stimulated with EVE on one side of the dorsum for 2 hours according to our standard protocol. The contralateral side was left untreated and used as internal control. Mice were sacrificed at 48 hours and tissue samples were collected.

Immunohistochemistry

Sections were stained with Hematoxylin and Eosin, and for CD68p, CD45, Ki67, PECAM-1, Perilipin-A

Quantifications

- *For Ki63 and CD31, sections were digitalized with a Nikon D-Sight slide scanner (Menarini Diagnostics, Firenze); 4 casual fields per slide were then extracted. Ki67-positive nucleai in the epidermis were manually quantified and the data was normalized per lenght of the epidermis in the field. CD31 positive structures were quantified and expressed as n. vessels/field. Averages were calculated for each section.*

- *For CD68p three casual digital fields/section were acquired on a Nikon E200 microscope (Nikon Corp., Tokyo, Japan). Manual counting of CD68p positive cells was performed and data were expressed as density of CD68p+ cells per field. Averages were calculated for each section.*

- *For CD45 three casual digital fields/section were acquired on a Nikon E200 microscope (Nikon Corp., Tokyo, Japan). Manual counting of CD45 positive and total nucleai was performed and data were expressed as ratio of CD45+/total nucleai per field. Averages were calculated for each section.*

- *For Perilipin-A, positive staining adipocytes located superficial to the panniculus carnosus muscle were manually quantified over entire sections on a Olympus Vanox AHBT3 microscope. Values were normalized by section lenght measured on digital scan acquired with a Nikon D-Sight slide scanner, and expressed as adipocytes linear density per mm.*

Statistics

Means of treated and untreated within groups were compared using Student's t-test for paired samples. Means between groups were compared with unpaired Student's t-tests with equal variance.

RESULTS

Macroscopic observations and Histology

On Hematoxylin and eosin stained sections EVE treated samples exhibited a normal architecture and no edema at 48 hours from stimulation.

One animal in the control group and three animals in the clodronate group had to be excluded due to scratch wounds present at the stimulated site which caused major confounding bias in histological assessment.

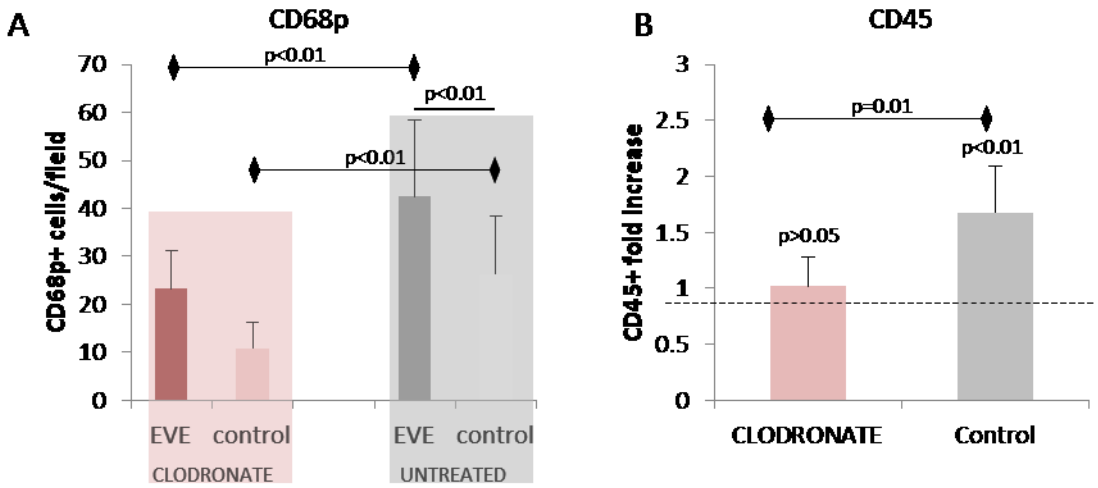

Fig. 36. (A) Clodronate treatment induced a significant reduction in the skin macrophages population and in macrophages accumulation following EVE. (B) The overall inflammatory response after EVE was reduced in clodronate treated animals.

Macrophage depletion and inflammatory response

Examination of CD68p stained sections revealed that clodronate pre-treatment did not result in complete elimination of macrophages. However, normal skin in clodronate treated animals exhibited none to very few macrophages with extremely rare foci of macrophages accumulation, while macrophage were widespreadely present and with frequent foci in the deep dermis in normal skin in the control group. Similarly, EVE treatment resulted in a still evident robust and diffuse macrophage infiltration in non clodronate-treated animals, while macrophage infiltration was greatly dampened in clodronate treated animals (fig. 36A).

At quantification of the global inflammatory response, clodronate treated animals had a similar percentage of CD45+ cells in EVE treated and untreated skin, while control animals displayed a still significant increase in CD45+ cells at 48h from EVE treatment (p<0.01). This corresponds to a 1.5 folds reduced inflammatory response to EVE in clodronate treated animals at comparison with control animals (p=0.01) (fig. 36B).

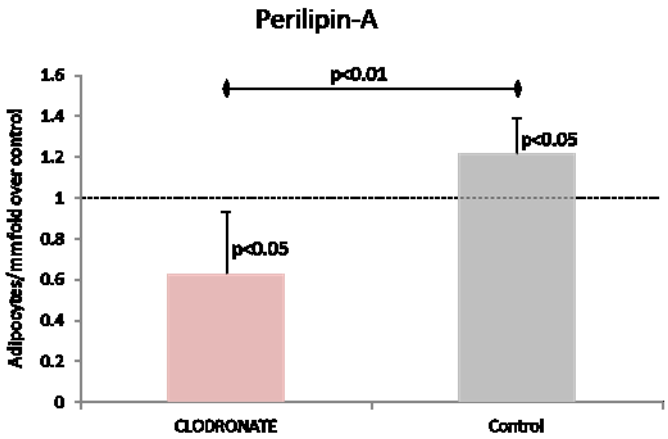

Figure 36: pretreatment with clodronate determined no adipogenic response after EVE stimulation.

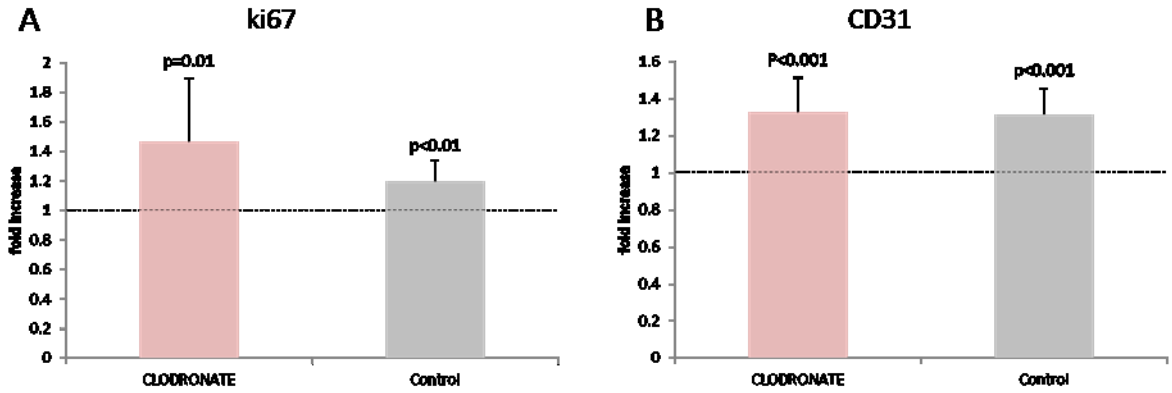

Figure 37: pretreatment with clodronate did not affect the pro-proliferative and pro-angiogenic effect of External Volume Expansion.

Perilipin-A

In control animals, EVE induced a significant increase in adipocytes linear density ($p<0.05$). In animals pre-treated with clodronate, a significantly decreased adipocyte linear density was observed after EVE treatment at comparison with the untreated skin ($p<0.05$), with a global significant difference in adipocytes density outcome after EVE between clodronate treated and control animals ($p<0.01$) (fig. 37).

Cell proliferation and vascular density

A significant increase in both epidermis cell proliferation rate and dermis vascular density resulted from EVE treatment independently from clodronate pre-treatment, with no differences between groups (fig. 38A and 38B).

DISCUSSION

We demonstrated the validity of the macrophages depletion model adopted showing that, albeit not completely absent, these cells were significantly less represented in normal animal skin and their accumulation following EVE stimulation was greatly decreased. The role of macrophages as pivot cells in tissue repair being well known, we observed that to this decreased migration into EVE-injured skin corresponded a decreased global inflammatory response.

As hypothesized basing on previously published studies by other groups [164], macrophages depletion also corresponded to a hampered accumulation of adipocytes following EVE stimulation. While it cannot be excluded with this model alone that liposomal clodronate has no direct effect on adipogenesis basing on available literature it seems reasonable to suggest that macrophages play a key role in driving the adipogenic response that follows EVE stimulation. Taking into account the low numerosity in our groups, further studies are needed to consolidate the results. An alternative model that would add further insight would be a repetition of the study in congenitally macrophage deficient mice. Interestingly, we did not observe either a reduced response in epidermis cell proliferation nor in angiogenesis in macrophages depleted animals. This suggests that differing from adipogenesis, cell proliferation and angiogenesis occur independently from inflammation. Alternatively that the reduced degree of inflammation observed in macrophage depleted animals is still above threshold to induce such effects. Cell strain and hypoxia/ischemia are alternative factors that we demonstrated occur in EVE and that could potentially stand alone as mechanisms for cell proliferation and angiogenesis.

If these observations were confirmed in further studies, modulation of inflammation might prove an additional route to control or stimulate fat deposition for tissue engineering purposes.

Next steps: EXTERNAL VOLUME EXPANSION AS A MODEL FOR STUDYING LYMPHEDEMA AND LIPEDEMA

A specific pathological condition goes under the name of lipedema. It consists in symmetrical enlargement of the extremities, more commonly the lower limbs, due to accumulation of adipose tissue not occurring in other body districts. Its pathogenesis is still unclear. It is considered a separate condition from lymphedema [192], but some similar features coexist. Even if, contrary to lymphedema, the main lymphatics are not disrupted, an increased interstitial pressure is observed in clinical lipedema[193-195].

Lymphedema is a pathologic condition characterized by deficient interstitial fluid drainage and its accumulation in the periphery. It is due to a malfunction of lymphatic vessels, a collector system that channels excessive fluids and carries them back into the blood stream. Malfunction can be acquired or congenital. Congenital cases are the result of malformation of the lymphatic system and can arise early or later in life. Acquired lymphedema is due to a stop in the drainage system. It can derive from parasitic infections (filariasis), inflammation, or mechanical compression and disruption during surgery. In either case, the outcome is deficient removal of fluids and catabolites that accumulate increasing interstitial pressure and widen the extracellular space.

If fluid stasis/accumulation is the most appreciated and primary effect in lymphedema, a key phenomenon is the stabilization of soft tissues swelling by transition from “pitting edema” to “non pitting edema”. In the earlier phase, fluids can be displaced from tissues by compression. Later on, tissues become hardened and uncompressible. Brorson showed how this is due to deposition of fat that accumulates in the spaces expanded by fluid stasis [138]. This transition from lymphedema to lipedema is of critical clinical importance. Cases in which development of lymphedema is diagnosed early can be treated by a combination of manual fluid drainage and surgical operations aiming at improving lymphatics function. Once transition occurs such approaches offer no significant benefit and treatment needs to focus primarily on elimination of the accumulated fat. How and when adipose tissue accumulates in lymphedema is not well understood. It is generally thought to be an overall late phenomenon occurring in chronic lymphedema.

Animal models to study lymphedema intrinsically accept this temporal relationship and expect to identify accumulation of adipose tissue at long term follow-up.

Our EVE model, as discussed before, shares many similarities with clinical lymphedema/lipedema and relative animal models such as those of Aschen and Zampell [141, 142]. And it shares many similarities with the models described by Morrison’s group which, even if not specifically directed at lymphedema, display many common features [145, 151, 166]. We observed how it stimulates deposition of adipose tissue, and this likely occurs as a result of an accumulation of extracellular fluid. Our data also suggest inflammation, and in particular macrophages play a primary role, similar to what observed by Morrison’s group and other authors [196, 197].

Interestingly, and likely due to the acute process by which the pro-adipogenic environment is induced, our model showed an unexpectedly very rapid and efficient promotion of adipogenesis, so that quantifiable effects are present in days rather than weeks or months. It is a peculiarity of our model which differentiates it from others available, and partly relates to the histological characteristics with physiologically poor hypodermis of mice skin that makes it suitable for precise quantification. It also suggests that fat deposition in lymphedema is likely to start at very early stage, and only take long to

become evident in much larger compartments such as human limds. On the other side, it leads to consider the hypothesis that in lipedema, similarly to lymphedema, lymph accumulation in the interstitial space might contribute to the mechanisms leading to fat accumulation. Our model appears as an interesting one in which to explore these issues, and potentially in which to test pharmacological approaches to control adipogenesis.

We are currently planning further studies to better delineate the similarities and differences between the local environment stimulated by EVE in our model and that induced in other animal models for lymphedema.

CONCLUSIONS

Mechanical forces are main determinants in the control of cell and tissue physiology. They act at multiple levels, either directly or by influencing the local environment. The responses to different mechanical stimulations vary in type and extent, and they can achieve effects as different as apoptosis, proliferation or differentiation. The understanding of the implications of mechanical stimulations is still incomplete, and the exploitation of mechanical forces in clinical settings is limited by the availability of devices that allow a practical use. The traditional use is restricted to the cases of distraction osteogenesis and tissue expansion. However, some techniques and devices are emerging in Plastic Surgery, as well as potential applications in the field of tissue engineering, which stimulates further exploration of these phenomena.

In our series of studies, we successfully designed a miniaturized animal model in which to test External Volume Expansion. We demonstrated that the hypotheses of stimulation of cell proliferation, angiogenesis, and expansion of tissue compartments on which it is proposed as a preparatory method to fat grafting was confirmed in experimental settings. We showed how mechanical stretch of tissues, hypoxia and ischemia, edema, and inflammation are all intervening factors that can contribute to these effects. We suggest that pre-stimulation with EVE is successful in achieving increased fat graft weight and volume retention, and that its beneficial effects are maintained also in the setting of recipient sites having sustained radiation injury. We also demonstrated that EVE has a potential for direct stimulation of adipogenesis, and gathered supportive results to a role for macrophages in this.

Our results validate the technique for its use in the preparatory phase to fat grafting, and can help moving towards making fat grafting a more effective and reliable procedure with improved outcomes for patients. We gathered evidence that help increasing our understanding of how EVE works and what it implies for tissues, which is the basis for optimizing the technique, make it safer, and increase patients compliance. For example, stimulation patterns can be improved, duration of treatment can be reduced, and practices such as continuation of EVE after fat grafting should be abandoned as detrimental. Our unexpected observations on adipogenesis also open interesting opportunities, such as that of re-starting EVE after fat grafting when this is at the peak of its remodeling phase. And linking this effect with the understanding of the similarity to other conditions in which adipogenesis is seen, both experimentally and in human disease, can expand the potential of our animal model to alternative fields.

References for the images used in the text

Fig. 2, 3, 6B: Lancerotto L, Orgill DP. Mechanoregulation of angiogenesis in wound healing. Advances in Wound Care. 2014; 3(10):626-34.

Fig. 4: Chin MS, Ogawa R, Lancerotto L, Pietramaggiori G, Schomacker KT, Mathews JC, Scherer SS, Van Duyn P, Prsa MJ, Ottensmeyer MP, Veves A, Orgill DP. In vivo acceleration of skin growth using a servo-controlled stretching device. Tissue Eng Part C Methods. 2010;16:397-405.

Fig. 5A: Lancerotto L, Bayer LR, Orgill DP. Mechanisms of action of microdeformational wound therapy. Semin Cell Dev Biol. 2012;23:987-992.

Fig. 6A: www.kennethsnelson.org

Fig. 7-11, 29: Heit YI, Lancerotto L, Mesteri I, Ackermann M, Navarrete MF, Nguyen CT, Mukundan S, Jr., Konerding MA, Del Vecchio DA, Orgill DP. External volume expansion increases subcutaneous thickness, cell proliferation, and vascular remodeling in a murine model. Plast Reconstr Surg. 2012;130:541-547.

Fig. 12-16: Lancerotto L, Chin MS, Freniere B, Lujan-Hernandez JR, Li Q, Valderrama Vasquez A, Bassetto F, Del Vecchio DA, Lalikos JF, Orgill DP. Mechanisms of action of external volume expansion devices. Plast Reconstr Surg. 2013;132:569-578.

Fig. 17-20: Khouri RK, Jr., Khouri RE, Lujan-Hernandez JR, Khouri KR, Lancerotto L, Orgill DP. Diffusion and perfusion: the keys to fat grafting. Plast Reconstr Surg Glob Open. 2014;2:e220.

Fig 22,23: Chin MS, Freniere BB, Bonney CF, Lancerotto L, Saleeby JH, Lo YC, Orgill DP, Fitzgerald TJ, Lalikos JF. Skin perfusion and oxygenation changes in radiation fibrosis. Plast Reconstr Surg. 2013;131:707-716.

Fig. 24: Chin MS, Freniere BB, Lancerotto L, Lujan-Hernandez J, Saleeby JH, Lo YC, Orgill DP, Lalikos JF, Fitzgerald TJ. Hyperspectral Imaging as an Early Biomarker for Radiation Exposure and Microcirculatory Damage. Front Oncol. 2015;5:232.

Fig. 25: Chin MS, Lujan-Hernandez J, Babchenko O, Bannon E, Perry DJ, Chappell AG, Lo YC, Fitzgerald TJ, Lalikos JF. External Volume Expansion in Irradiated Tissue: Effects on the Recipient Site. Plast Reconstr Surg. 2016;137:799e-807e.[130] *with permission*

Fig. 30-35: Lujan-Hernandez J, Lancerotto L, Nabzdyk C, Hassan KZ, Giatsidis G, Khouri RK, Jr., Chin MS, Bassetto F, Lalikos JF, Orgill DP. Induction of Adipogenesis by External Volume Expansion. Plast Reconstr Surg. 2016;137:122-131.

References

[1] Neuber F. Fettransplantation. *Chir Kongr Verhandl Dsch Geselsch Chir*. 1893;22:66.

[2] Czerny V. Drei Plastische Operationen. III. Plastischer Ersatz der Brustdruse durch ein Lipom. *Chir Kongr Verhandl Dsch Geselsch Chir*. 1895;2.

[3] Fournier P. Microlipoextraction et microlipoinjection. *Rev Chir Esthet Fr*. 1985;10:19-23.

[4] Illouz YG. The fat cell "graft": a new technique to fill depressions. *Plast Reconstr Surg*. 1986;78:122-123.

[5] Teimourian B. Repair of soft-tissue contour deficit by means of semiliquid fat graft. *Plast Reconstr Surg*. 1986;78:123-124.

[6] Report on autologous fat transplantation. ASPRS Ad-Hoc Committee on New Procedures, September 30, 1987. *Plast Surg Nurs*. 1987;7:140-141.

[7] Rubin E. Breast imaging considerations in fat grafting to the breast. *Plast Reconstr Surg*. 2011;128:570e-571e; author reply 571e-572e.

[8] Veber M, Tourasse C, Toussoun G, Moutran M, Mojallal A, Delay E. Radiographic findings after breast augmentation by autologous fat transfer. *Plast Reconstr Surg*. 2011;127:1289-1299.

[9] Rigotti G, Marchi A, Stringhini P, Baroni G, Galie M, Molino AM, Mercanti A, Micciolo R, Sbarbati A. Determining the oncological risk of autologous lipoaspirate grafting for post-mastectomy breast reconstruction. *Aesthetic Plast Surg*. 2010;34:475-480.

[10] Fraser JK, Hedrick MH, Cohen SR. Oncologic risks of autologous fat grafting to the breast. *Aesthet Surg J*. 2011;31:68-75.

[11] Delay E, Garson S, Tousson G, Sinna R. Fat injection to the breast: technique, results, and indications based on 880 procedures over 10 years. *Aesthet Surg J*. 2009;29:360-376.

[12] Gir P, Brown SA, Oni G, Kashefi N, Mojallal A, Rohrich RJ. Fat grafting: evidence-based review on autologous fat harvesting, processing, reinjection, and storage. *Plast Reconstr Surg*. 2012;130:249-258.

[13] Zheng DN, Li QF, Lei H, Zheng SW, Xie YZ, Xu QH, Yun X, Pu LL. Autologous fat grafting to the breast for cosmetic enhancement: experience in 66 patients with long-term follow up. *J Plast Reconstr Aesthet Surg*. 2008;61:792-798.

[14] Carpaneda CA, Ribeiro MT. Percentage of graft viability versus injected volume in adipose autotransplants. *Aesthetic Plast Surg*. 1994;18:17-19.

[15] Niechajev I, Sevcuk O. Long-term results of fat transplantation: clinical and histologic studies. *Plast Reconstr Surg*. 1994;94:496-506.

[16] Ersek RA. Transplantation of purified autologous fat: a 3-year follow-up is disappointing. *Plast Reconstr Surg*. 1991;87:219-227; discussion 228.

[17] Coleman SR, Saboeiro AP. Fat grafting to the breast revisited: safety and efficacy. *Plast Reconstr Surg*. 2007;119:775-785; discussion 786-777.

[18] Khouri RK, Schlenz I, Murphy BJ, Baker TJ. Nonsurgical breast enlargement using an external soft-tissue expansion system. *Plast Reconstr Surg*. 2000;105:2500-2512; discussion 2513-2504.

[19] Wilhelmi BJ, Blackwell SJ, Mancoll JS, Phillips LG. Creep vs. stretch: a review of the viscoelastic properties of skin. *Ann Plast Surg*. 1998;41:215-219.

[20] Ingber D. How cells (might) sense microgravity. *FASEB J*. 1999;13 Suppl:S3-15.

[21] Saxena V, Hwang CW, Huang S, Eichbaum Q, Ingber D, Orgill DP. Vacuum-assisted closure: microdeformations of wounds and cell proliferation. *Plast Reconstr Surg*. 2004;114:1086-1096; discussion 1097-1088.

[22] Chin MS, Ogawa R, Lancerotto L, Pietramaggiori G, Schomacker KT, Mathews JC, Scherer SS, Van Duyn P, Prsa MJ, Ottensmeyer MP, Veves A, Orgill DP. In vivo acceleration of skin growth using a servo-controlled stretching device. *Tissue Eng Part C Methods*. 2010;16:397-405.

[23] Saxena V, Orgill D, Kohane I. A set of genes previously implicated in the hypoxia response might be an important modulator in the rat ear tissue response to mechanical stretch. *BMC Genomics*. 2007;8:430.

[24] Chin MS, Lancerotto L, Helm DL, Dastouri P, Prsa MJ, Ottensmeyer M, Akaishi S, Orgill DP, Ogawa R. Analysis of neuropeptides in stretched skin. *Plast Reconstr Surg*. 2009;124:102-113.

[25] Zocchi ML, Zuliani F. Bicompartmental breast lipostructuring. *Aesthetic Plast Surg*. 2008;32:313-328.

[26] Del Vecchio D. Breast reconstruction for breast asymmetry using recipient site pre-expansion and autologous fat grafting: a case report. *Ann Plast Surg*. 2009;62:523-527.

[27] Del Vecchio DA, Bucky LP. Breast augmentation using preexpansion and autologous fat transplantation: a clinical radiographic study. *Plast Reconstr Surg*. 2011;127:2441-2450.

[28] Khouri RK, Eisenmann-Klein M, Cardoso E, Cooley BC, Kacher D, Gombos E, Baker TJ. Brava and autologous fat transfer is a safe and effective breast augmentation alternative: results of a 6-year, 81-patient, prospective multicenter study. *Plast Reconstr Surg*. 2012;129:1173-1187.

[29] Khouri RK, Rigotti G, Khouri RK, Jr., Cardoso E, Marchi A, Rotemberg SC, Baker TJ, Biggs TM. Tissue-engineered breast reconstruction with Brava-assisted fat grafting: a 7-year, 488-patient, multicenter experience. *Plast Reconstr Surg*. 2015;135:643-658.

[30] Lancerotto L, Orgill DP. Mechanoregulation of angiogenesis in wound healing. *Advances in Wound Care*. 2014; 3(10):626-34.

[31] Wolff J. Das Gesetz der Transformation der Knochen. Berlin: August Hirschwald 1892.

[32] Ilizarov GA. The tension-stress effect on the genesis and growth of tissues. Part I. The influence of stability of fixation and soft-tissue preservation. *Clin Orthop Relat Res*. 1989:249-281.

[33] Argenta LC, Marks M W. Principles of Tissue Expansion. In: Mathes SJ, ed. *Plastic Surgery*. 6 ed. Philadelphia, PA: Saunders Elsevier 2006:539-568.

[34] Radovan C. Breast reconstruction after mastectomy using the temporary expander. *Plast Reconstr Surg*. 1982;69:195-208.

[35] Austad ED, Rose GL. A self-inflating tissue expander. *Plast Reconstr Surg*. 1982;70:588-594.

[36] Austad ED, Pasyk KA, McClatchey KD, Cherry GW. Histomorphologic evaluation of guinea pig skin and soft tissue after controlled tissue expansion. *Plast Reconstr Surg*. 1982;70:704-710.

[37] Pasyk KA, Austad ED, McClatchey KD, Cherry GW. Electron microscopic evaluation of guinea pig skin and soft tissues "expanded" with a self-inflating silicone implant. *Plast Reconstr Surg*. 1982;70:37-45.

[38] Lew D, Fuseler JW. The effect of stepwise expansion on the mitotic activity and vascularity of subdermal tissue and induced capsule in the rat. *J Oral Maxillofac Surg*. 1991;49:848-853.

[39] Lorber M, Milobsky SA. Stretching of the skin in vivo. A method of influencing cell division and migration in the rat epidermis. *J Invest Dermatol*. 1968;51:395-402.

[40] Mackenzie IC. The effects of frictional stimulation on mouse ear epidermis. I. Cell proliferation. *J Invest Dermatol*. 1974;62:80-85.

[41] Bullough WS, Laurence EB. The control of epidermal mitotic activity in the mouse. *Proc R Soc Lond B Biol Sci*. 1960;151:517-536.

[42] Francis AJ, Marks R. Factors responsible for dermally induced epidermal hyperplasia. *Arch Dermatol Res*. 1977;258:275-280.

[43] Curtis AS, Seehar GM. The control of cell division by tension or diffusion. *Nature*. 1978;274:52-53.

[44] Squier CA. The stretching of mouse skin in vivo: effect on epidermal proliferation and thickness. *J Invest Dermatol*. 1980;74:68-71.

[45] Squier CA. The effect of stretching on formation of myofibroblasts in mouse skin. *Cell Tissue Res*. 1981;220:325-335.
[46] Brunette DM. Mechanical stretching increases the number of epithelial cells synthesizing DNA in culture. *J Cell Sci*. 1984;69:35-45.
[47] Ingber DE, Folkman J. How does extracellular matrix control capillary morphogenesis? *Cell*. 1989;58:803-805.
[48] Reinhart-King CA. How matrix properties control the self-assembly and maintenance of tissues. *Ann Biomed Eng*. 2011;39:1849-1856.
[49] Roca-Cusachs P, Sunyer R, Trepat X. Mechanical guidance of cell migration: lessons from chemotaxis. *Curr Opin Cell Biol*. 2013;25(5)543-9.
[50] Pietramaggiori G, Liu P, Scherer SS, Kaipainen A, Prsa MJ, Mayer H, Newalder J, Alperovich M, Mentzer SJ, Konerding MA, Huang S, Ingber DE, Orgill DP. Tensile forces stimulate vascular remodeling and epidermal cell proliferation in living skin. *Ann Surg*. 2007;246:896-902.
[51] Gurtner GC, Werner S, Barrandon Y, Longaker MT. Wound repair and regeneration. *Nature*. 2008;453:314-321.
[52] Langer K. Zur Anatomie und Physiologie der Haut. Über die Spaltbarkeit der Cutis. *Sitzungsbericht der Mathematisch-naturwissenschaftlichen Classe der Wiener Kaiserlichen Academie der Wissenschaften*. 1861;44.
[53] Lancerotto L, Bayer LR, Orgill DP. Mechanisms of action of microdeformational wound therapy. *Semin Cell Dev Biol*. 2012;23:987-992.
[54] Kairinos N, Solomons M, Hudson DA. The paradox of negative pressure wound therapy - in vitro studies. *J Plast Reconstr Aesthet Surg*. 2008;63(1)174-9.
[55] Wackenfors A, Sjogren J, Gustafsson R, Algotsson L, Ingemansson R, Malmsjo M. Effects of vacuum-assisted closure therapy on inguinal wound edge microvascular blood flow. *Wound Repair Regen*. 2004;12:600-606.
[56] Kairinos N, Solomons M, Hudson DA. Negative-pressure wound therapy I: the paradox of negative-pressure wound therapy. *Plast Reconstr Surg*. 2009;123:589-598; discussion 599-600.
[57] Kairinos N, Voogd AM, Botha PH, Kotze T, Kahn D, Hudson DA, Solomons M. Negative-pressure wound therapy II: negative-pressure wound therapy and increased perfusion. Just an illusion? *Plast Reconstr Surg*. 2009;123:601-612.
[58] Erba P, Ogawa R, Ackermann M, Adini A, Miele LF, Dastouri P, Helm D, Mentzer SJ, D'Amato RJ, Murphy GF, Konerding MA, Orgill DP. Angiogenesis in wounds treated by microdeformational wound therapy. *Ann Surg*.2011;253:402-409.
[59] Borgquist O, Ingemansson R, Malmsjo M. The influence of low and high pressure levels during negative-pressure wound therapy on wound contraction and fluid evacuation. *Plast Reconstr Surg*. 2011;127:551-559.
[60] Kairinos N, Hudson DA, Solomons M. The influence of different sizes and types of wound fillers on wound contraction and tissue pressure during negative pressure wound therapy. *Int Wound J*. 2011;8:656-657.
[61] Scherer SS, Pietramaggiori G, Mathews JC, Prsa MJ, Huang S, Orgill DP. The mechanism of action of the vacuum-assisted closure device. *Plast Reconstr Surg*. 2008;122:786-797.
[62] Ingber DE. The mechanochemical basis of cell and tissue regulation. *Mech Chem Biosyst*. 2004;1:53-68.
[63] Ingber DE. Mechanical control of tissue growth: function follows form. *Proc Natl Acad Sci U S A*. 2005;102:11571-11572.

[64] Lu F, Ogawa R, Nguyen DT, Chen B, Guo D, Helm DL, Zhan Q, Murphy GF, Orgill DP. Microdeformation of three-dimensional cultured fibroblasts induces gene expression and morphological changes. *Ann Plast Surg*. 2011;66:296-300.

[65] Heit YI, Dastouri P, Helm D, Pietramaggiori G, Younan G, Erba P, Munster S, Orgill DP, Scherer SS. Foam Pore Size is a Critical Interface Parameter of Suction-Based Wound Healing Devices. *Plast Reconstr Surg.* 2012;129:589-97.

[66] Fraccalvieri M, Zingarelli E, Ruka E, Antoniotti U, Coda R, Sarno A, Bocchiotti MA, Bruschi S. Negative pressure wound therapy using gauze and foam: histological, immunohistochemical and ultrasonography morphological analysis of the granulation tissue and scar tissue. Preliminary report of a clinical study. *Int Wound J*. 2011;8:355-364.

[67] Morykwas MJ, Argenta LC, Shelton-Brown EI, McGuirt W. Vacuum-assisted closure: a new method for wound control and treatment: animal studies and basic foundation. *Ann Plast Surg*. 1997;38:553-562.

[68] Argenta LC, Morykwas MJ. Vacuum-assisted closure: a new method for wound control and treatment: clinical experience. *Ann Plast Surg*. 1997;38:563-576; discussion 577.

[69] Malmsjo M, Gustafsson L, Lindstedt S, Gesslein B, Ingemansson R. The effects of variable, intermittent, and continuous negative pressure wound therapy, using foam or gauze, on wound contraction, granulation tissue formation, and ingrowth into the wound filler. *Eplasty*. 2012;12:e5.

[70] Dastouri P, Helm DL, Scherer SS, Pietramaggiori G, Younan G, Orgill DP. Waveform modulation of negative-pressure wound therapy in the murine model. *Plast Reconstr Surg*. 2011;127:1460-1466.

[71] Scherer SS, Pietramaggiori G, Mathews JC, Orgill DP. Short periodic applications of the vacuum-assisted closure device cause an extended tissue response in the diabetic mouse model. *Plast Reconstr Surg*. 2009;124:1458-1465.

[72] Chen SZ, Li J, Li XY, Xu LS. Effects of vacuum-assisted closure on wound microcirculation: an experimental study. *Asian J Surg*. 2005;28:211-217.

[73] Younan G, Ogawa R, Ramirez M, Helm D, Dastouri P, Orgill DP. Analysis of nerve and neuropeptide patterns in vacuum-assisted closure-treated diabetic murine wounds. *Plast Reconstr Surg*. 2010;126:87-96.

[74] Malmsjo M, Gustafsson L, Lindstedt S, Ingemansson R. Negative pressure wound therapy-associated tissue trauma and pain: a controlled in vivo study comparing foam and gauze dressing removal by immunohistochemistry for substance P and calcitonin gene-related peptide in the wound edge. *Ostomy Wound Manage*. 2011;57:30-35.

[75] Barker AR, Rosson GD, Dellon AL. Wound healing in denervated tissue. *Ann Plast Surg*. 2006;57:339-342.

[76] Ogawa R, Okai K, Tokumura F, Mori K, Ohmori Y, Huang C, Hyakusoku H, Akaishi S. The relationship between skin stretching/contraction and pathologic scarring: the important role of mechanical forces in keloid generation. *Wound Repair Regen*. 2012;20:149-157.

[77] Aarabi S, Bhatt KA, Shi Y, Paterno J, Chang EI, Loh SA, Holmes JW, Longaker MT, Yee H, Gurtner GC. Mechanical load initiates hypertrophic scar formation through decreased cellular apoptosis. *FASEB J*. 2007;21:3250-3261.

[78] Ogawa R. Mechanobiology of scarring. *Wound Repair Regen*. 2011;19 Suppl 1:s2-9.

[79] Mogili NS, Krishnaswamy VR, Jayaraman M, Rajaram R, Venkatraman A, Korrapati PS. Altered angiogenic balance in keloids: a key to therapeutic intervention. *Transl Res*. 2012;159:182-189.

[80] Kischer CW. The microvessels in hypertrophic scars, keloids and related lesions: a review. *J Submicrosc Cytol Pathol*. 1992;24:281-296.

[81] Gurtner GC, Dauskardt RH, Wong VW, Bhatt KA, Wu K, Vial IN, Padois K, Korman JM, Longaker MT. Improving cutaneous scar formation by controlling the mechanical environment: large animal and phase I studies. *Ann Surg*. 2011;254:217-225.

[82] Watt FM. Role of integrins in regulating epidermal adhesion, growth and differentiation. *Embo J*. 2002;21:3919-3926.
[83] Torsoni AS, Constancio SS, Nadruz W, Jr., Hanks SK, Franchini KG. Focal adhesion kinase is activated and mediates the early hypertrophic response to stretch in cardiac myocytes. *Circ Res*. 2003;93:140-147.
[84] Hamill OP, McBride DW, Jr. The pharmacology of mechanogated membrane ion channels. *Pharmacol Rev*. 1996;48:231-252.
[85] Vandenburgh HH. Mechanical forces and their second messengers in stimulating cell growth in vitro. *Am J Physiol*. 1992;262:R350-355.
[86] Takei T, Mills I, Arai K, Sumpio BE. Molecular basis for tissue expansion: clinical implications for the surgeon. *Plast Reconstr Surg*. 1998;102:247-258.
[87] Folkman J, Greenspan HP. Influence of geometry on control of cell growth. *Biochim Biophys Acta*. 1975;417:211-236.
[88] Folkman J, Moscona A. Role of cell shape in growth control. *Nature*. 1978;273:345-349.
[89] Ingber DE. Tensegrity I. Cell structure and hierarchical systems biology. *J Cell Sci*. 2003;116:1157-1173.
[90] Ingber DE. Tensegrity II. How structural networks influence cellular information processing networks. *J Cell Sci*. 2003;116:1397-1408.
[91] Chen CS, Mrksich M, Huang S, Whitesides GM, Ingber DE. Geometric control of cell life and death. *Science*. 1997;276:1425-1428.
[92] Heit YI, Lancerotto L, Mesteri I, Ackermann M, Navarrete MF, Nguyen CT, Mukundan S, Jr., Konerding MA, Del Vecchio DA, Orgill DP. External Volume Expansion Increases Subcutaneous Thickness, Cell Proliferation, and Vascular Remodeling in a Murine Model. *Plast Reconstr Surg*. 2012;130:541-547.
[93] Schultz K, Fanburg BL, Beasley D. Hypoxia and hypoxia-inducible factor-1alpha promote growth factor-induced proliferation of human vascular smooth muscle cells. *Am J Physiol Heart Circ Physiol*. 2006;290:H2528-2534.
[94] Yudovsky D, Nouvong A, Schomacker K, Pilon L. Monitoring temporal development and healing of diabetic foot ulceration using hyperspectral imaging. *J Biophotonics*. 2011;4:565-576.
[95] Yudovsky D, Nouvong A, Pilon L. Hyperspectral imaging in diabetic foot wound care. *J Diabetes Sci Technol*. 2010;4:1099-1113.
[96] McLean RA, Sanders WL, Stroup WW. A unified approach to mixed linear models. *The American Statistician*. 1991;45:54-64.
[97] Ingber DE. Tensegrity: the architectural basis of cellular mechanotransduction. *Annu Rev Physiol*. 1997;59:575-599.
[98] Del Vecchio D, Rohrich RJ. A classification of clinical fat grafting: different problems, different solutions. *Plast Reconstr Surg*. 2012;130:511-522.
[99] Carpaneda CA, Ribeiro MT. Study of the histologic alterations and viability of the adipose graft in humans. *Aesthetic Plast Surg*. 1993;17:43-47.
[100] Eto H, Kato H, Suga H, Aoi N, Doi K, Kuno S, Yoshimura K. The fate of adipocytes after nonvascularized fat grafting: evidence of early death and replacement of adipocytes. *Plast Reconstr Surg*. 2012;129:1081-1092.
[101] Rigamonti A, Brennand K, Lau F, Cowan CA. Rapid cellular turnover in adipose tissue. *PLoS One*. 2011;6:e17637.
[102] Suga H, Eto H, Aoi N, Kato H, Araki J, Doi K, Higashino T, Yoshimura K. Adipose tissue remodeling under ischemia: death of adipocytes and activation of stem/progenitor cells. *Plast Reconstr Surg*. 2010;126:1911-1923.

[103] Weijers EM, Van Den Broek LJ, Waaijman T, Van Hinsbergh VW, Gibbs S, Koolwijk P. The influence of hypoxia and fibrinogen variants on the expansion and differentiation of adipose tissue-derived mesenchymal stem cells. *Tissue Eng Part A*. 2013;17:2675-2685.
[104] Suga H, Eto H, Shigeura T, Inoue K, Aoi N, Kato H, Nishimura S, Manabe I, Gonda K, Yoshimura K. IFATS collection: Fibroblast growth factor-2-induced hepatocyte growth factor secretion by adipose-derived stromal cells inhibits postinjury fibrogenesis through a c-Jun N-terminal kinase-dependent mechanism. *Stem Cells*. 2009;27:238-249.
[105] Franko AJ, Sutherland RM. Oxygen diffusion distance and development of necrosis in multicell spheroids. *Radiat Res*. 1979;79:439-453.
[106] Franko AJ, Sutherland RM. Radiation survival of cells from spheroids grown in different oxygen concentrations. *Radiat Res*. 1979;79:454-467.
[107] Thomlinson RH, Gray LH. The histological structure of some human lung cancers and the possible implications for radiotherapy. *Br J Cancer*. 1955;9:539-549.
[108] Venkatasubramanian R, Henson MA, Forbes NS. Incorporating energy metabolism into a growth model of multicellular tumor spheroids. *J Theor Biol*. 2006;242:440-453.
[109] Chow DC, Wenning LA, Miller WM, Papoutsakis ET. Modeling pO(2) distributions in the bone marrow hematopoietic compartment. I. Krogh's model. *Biophys J*. 2001;81:675-684.
[110] Folkman J, Hochberg M. Self-regulation of growth in three dimensions. *J Exp Med*. 1973;138:745-753.
[111] Baran CN, Celebioglu S, Sensoz O, Ulusoy G, Civelek B, Ortak T. The behavior of fat grafts in recipient areas with enhanced vascularity. *Plast Reconstr Surg*. 2002;109:1646-1651; 1652.
[112] Guyton AC. Interstitial Fluid Presure. Ii. Pressure-Volume Curves of Interstitial Space. *Circ Res*. 1965;16:452-460.
[113] Milosevic MF, Fyles AW, Hill RP. The relationship between elevated interstitial fluid pressure and blood flow in tumors: a bioengineering analysis. *Int J Radiat Oncol Biol Phys*. 1999;43:1111-1123.
[114] Khouri RK, Rigotti G, Cardoso E, Khouri RK, Jr., Biggs TM. Megavolume autologous fat transfer: part I. Theory and principles. *Plast Reconstr Surg*. 2014;133:550-557.
[115] Khouri RK, Rigotti G, Cardoso E, Khouri RK, Jr., Biggs TM. Megavolume autologous fat transfer: part II. Practice and techniques. *Plast Reconstr Surg*. 2014;133:1369-1377.
[116] Khouri RK, Khouri RK, Jr., Rigotti G, Marchi A, Cardoso E, Rotemberg SC, Biggs TM. Aesthetic applications of Brava-assisted megavolume fat grafting to the breasts: a 9-year, 476-patient, multicenter experience. *Plast Reconstr Surg*. 2014;133:796-807; discussion 808-799.
[117] Reno F, Sabbatini M, Lombardi F, Stella M, Pezzuto C, Magliacani G, Cannas M. In vitro mechanical compression induces apoptosis and regulates cytokines release in hypertrophic scars. *Wound Repair Regen*. 2003;11:331-336.
[118] Sutcliffe MC, Davidson JM. Effect of static stretching on elastin production by porcine aortic smooth muscle cells. *Matrix*. 1990;10:148-153.
[119] Lancerotto L, Chin MS, Freniere B, Lujan-Hernandez JR, Li Q, Valderrama Vasquez A, Bassetto F, Del Vecchio DA, Lalikos JF, Orgill DP. Mechanisms of action of external volume expansion devices. *Plast Reconstr Surg*. 2013;132:569-578.
[120] Yamaguchi M, Matsumoto F, Bujo H, Shibasaki M, Takahashi K, Yoshimoto S, Ichinose M, Saito Y. Revascularization determines volume retention and gene expression by fat grafts in mice. *Exp Biol Med (Maywood)*. 2005;230:742-748.
[121] El-Sabawi B, Carey JN, Hagopian TM, Sbitany H, Patel KM. Radiation and breast reconstruction: Algorithmic approach and evidence-based outcomes. *J Surg Oncol*. 2016;113:906-912.

[122] El-Sabawi B, Sosin M, Carey JN, Nahabedian MY, Patel KM. Breast reconstruction and adjuvant therapy: A systematic review of surgical outcomes. *J Surg Oncol*. 2015;112:458-464.
[123] Fracol ME, Basta MN, Nelson JA, Fischer JP, Wu LC, Serletti JM, Fosnot J. Bilateral Free Flap Breast Reconstruction After Unilateral Radiation: Comparing Intraoperative Vascular Complications and Postoperative Outcomes in Radiated Versus Nonradiated Breasts. *Ann Plast Surg*. 2016;76:311-314.
[124] Zielins ER, Luan A, Brett EA, Longaker MT, Wan DC. Therapeutic applications of human adipose-derived stromal cells for soft tissue reconstruction. *Discov Med*. 2015;19:245-253.
[125] Shukla L, Morrison WA, Shayan R. Adipose-derived stem cells in radiotherapy injury: a new frontier. *Front Surg*. 2015;2:1.
[126] Luan A, Duscher D, Whittam AJ, Paik KJ, Zielins ER, Brett EA, Atashroo DA, Hu MS, Lee GK, Gurtner GC, Longaker MT, Wan DC. Cell-Assisted Lipotransfer Improves Volume Retention in Irradiated Recipient Sites and Rescues Radiation-Induced Skin Changes. *Stem Cells*. 2016;34:668-673.
[127] Chin MS, Freniere BB, Bonney CF, Lancerotto L, Saleeby JH, Lo YC, Orgill DP, Fitzgerald TJ, Lalikos JF. Skin perfusion and oxygenation changes in radiation fibrosis. *Plast Reconstr Surg*. 2013;131:707-716.
[128] Chin MS, Freniere BB, Lancerotto L, Lujan-Hernandez J, Saleeby JH, Lo YC, Orgill DP, Lalikos JF, Fitzgerald TJ. Hyperspectral Imaging as an Early Biomarker for Radiation Exposure and Microcirculatory Damage. *Front Oncol*. 2015;5:232.
[129] Garza RM, Paik KJ, Chung MT, Duscher D, Gurtner GC, Longaker MT, Wan DC. Studies in fat grafting: Part III. Fat grafting irradiated tissue--improved skin quality and decreased fat graft retention. *Plast Reconstr Surg*. 2014;134:249-257.
[130] Chin MS, Lujan-Hernandez J, Babchenko O, Bannon E, Perry DJ, Chappell AG, Lo YC, Fitzgerald TJ, Lalikos JF. External Volume Expansion in Irradiated Tissue: Effects on the Recipient Site. *Plast Reconstr Surg*. 2016;137:799e-807e.
[131] Kearney AM, Brown MS, Soltanian HT. Timing of radiation and outcomes in implant-based breast reconstruction. *J Plast Reconstr Aesthet Surg*. 2015;68:1719-1726.
[132] Chen TA, Momeni A, Lee GK. Clinical outcomes in breast cancer expander-implant reconstructive patients with radiation therapy. *J Plast Reconstr Aesthet Surg*. 2016;69:14-22.
[133] Satteson ES, Reynolds MF, Bond AM, Pestana IA. An Analysis of Complication Risk Factors in 641 Nipple Reconstructions. *Breast J*. 2016;22:379-383.
[134] Sultan SM, Stern CS, Allen RJ, Jr., Thanik VD, Chang CC, Nguyen PD, Canizares O, Szpalski C, Saadeh PB, Warren SM, Coleman SR, Hazen A. Human fat grafting alleviates radiation skin damage in a murine model. *Plast Reconstr Surg*. 2011;128:363-372.
[135] Mojallal A, Lequeux C, Shipkov C, Breton P, Foyatier JL, Braye F, Damour O. Improvement of skin quality after fat grafting: clinical observation and an animal study. *Plast Reconstr Surg*. 2009;124:765-774.
[136] Ranganathan K, Wong VW, Krebsbach PH, Wang SC, Cederna PS, Levi B. Fat grafting for thermal injury: current state and future directions. *J Burn Care Res*.2013;34:219-226.
[137] Rigotti G, Marchi A, Galie M, Baroni G, Benati D, Krampera M, Pasini A, Sbarbati A. Clinical treatment of radiotherapy tissue damage by lipoaspirate transplant: a healing process mediated by adipose-derived adult stem cells. *Plast Reconstr Surg*. 2007;119:1409-1422; discussion 1423-1404.
[138] Brorson H. Adipose tissue in lymphedema: the ignorance of adipose tissue in lymphedema. *Lymphology*. 2004;37:175-177.
[139] Brorson H, Ohlin K, Olsson G, Nilsson M. Adipose tissue dominates chronic arm lymphedema following breast cancer: an analysis using volume rendered CT images. *Lymphat Res Biol*. 2006;4:199-210.
[140] Harvey NL, Srinivasan RS, Dillard ME, Johnson NC, Witte MH, Boyd K, Sleeman MW, Oliver G. Lymphatic vascular defects promoted by Prox1 haploinsufficiency cause adult-onset obesity. *Nat Genet*. 2005;37:1072-1081.

[141] Zampell JC, Aschen S, Weitman ES, Yan A, Elhadad S, De Brot M, Mehrara BJ. Regulation of adipogenesis by lymphatic fluid stasis: part I. Adipogenesis, fibrosis, and inflammation. *Plast Reconstr Surg*. 2012;129:825-834.
[142] Aschen S, Zampell JC, Elhadad S, Weitman E, De Brot M, Mehrara BJ. Regulation of adipogenesis by lymphatic fluid stasis: part II. Expression of adipose differentiation genes. *Plast Reconstr Surg*. 2012;129:838-847.
[143] Bassetto F, Lancerotto L, Salmaso R, Pandis L, Pajardi G, Schiavon M, Tiengo C, Vindigni V. Histological evolution of chronic wounds under negative pressure therapy. *J Plast Reconstr Aesthet Surg*. 2012;65:91-99.
[144] Khouri R, Del Vecchio D. Breast reconstruction and augmentation using pre-expansion and autologous fat transplantation. *Clin Plast Surg*. 2009;36:269-280, viii.
[145] Cronin KJ, Messina A, Knight KR, Cooper-White JJ, Stevens GW, Penington AJ, Morrison WA. New murine model of spontaneous autologous tissue engineering, combining an arteriovenous pedicle with matrix materials. *Plast Reconstr Surg*. 2004;113:260-269.
[146] Dolderer JH, Abberton KM, Thompson EW, Slavin JL, Stevens GW, Penington AJ, Morrison WA. Spontaneous large volume adipose tissue generation from a vascularized pedicled fat flap inside a chamber space. *Tissue Eng*. 2007;13:673-681.
[147] Dolderer JH, Thompson EW, Slavin J, Trost N, Cooper-White JJ, Cao Y, O'Connor A J, Penington A, Morrison WA, Abberton KM. Long-term stability of adipose tissue generated from a vascularized pedicled fat flap inside a chamber. *Plast Reconstr Surg*. 2011;127:2283-2292.
[148] Abberton KM, Bortolotto SK, Woods AA, Findlay M, Morrison WA, Thompson EW, Messina A. Myogel, a novel, basement membrane-rich, extracellular matrix derived from skeletal muscle, is highly adipogenic in vivo and in vitro. *Cells Tissues Organs*. 2008;188:347-358.
[149] Kelly JL, Findlay MW, Knight KR, Penington A, Thompson EW, Messina A, Morrison WA. Contact with existing adipose tissue is inductive for adipogenesis in matrigel. *Tissue Eng*. 2006;12:2041-2047.
[150] Stillaert FB, Abberton KM, Keramidaris E, Thompson EW, Blondeel PN, Morrison WA. Intrinsics and dynamics of fat grafts: an in vitro study. *Plast Reconstr Surg*. 2010;126:1155-1162.
[151] Thomas GP, Hemmrich K, Abberton KM, McCombe D, Penington AJ, Thompson EW, Morrison WA. Zymosan-induced inflammation stimulates neo-adipogenesis. *Int J Obes (Lond)*. 2008;32:239-248.
[152] Findlay MW, Dolderer JH, Trost N, Craft RO, Cao Y, Cooper-White J, Stevens G, Morrison WA. Tissue-engineered breast reconstruction: bridging the gap toward large-volume tissue engineering in humans. *Plast Reconstr Surg*. 2011;128:1206-1215.
[153] Lujan-Hernandez J, Lancerotto L, Nabzdyk C, Hassan KZ, Giatsidis G, Khouri RK, Jr., Chin MS, Bassetto F, Lalikos JF, Orgill DP. Induction of Adipogenesis by External Volume Expansion. *Plast Reconstr Surg*. 2016;137:122-131.
[154] Brasaemle DL. Thematic review series: adipocyte biology. The perilipin family of structural lipid droplet proteins: stabilization of lipid droplets and control of lipolysis. *J Lipid Res*. 2007;48:2547-2559.
[155] Christodoulides C, Vidal-Puig A. PPARs and adipocyte function. *Mol Cell Endocrinol*. 2010;318:61-68.
[156] Farmer SR. Regulation of PPARgamma activity during adipogenesis. *Int J Obes (Lond)*. 2005;29 Suppl 1:S13-16.
[157] Rosen ED, Spiegelman BM. What we talk about when we talk about fat. *Cell*. 2014;156:20-44.
[158] Tang QQ, Lane MD. Activation and centromeric localization of CCAAT/enhancer-binding proteins during the mitotic clonal expansion of adipocyte differentiation. *Genes Dev*. 1999;13:2231-2241.
[159] Okuno A, Tamemoto H, Tobe K, Ueki K, Mori Y, Iwamoto K, Umesono K, Akanuma Y, Fujiwara T, Horikoshi H, Yazaki Y, Kadowaki T. Troglitazone increases the number of small adipocytes without the change of white adipose tissue mass in obese Zucker rats. *J Clin Invest*. 1998;101:1354-1361.

[160] Rosen ED, Sarraf P, Troy AE, Bradwin G, Moore K, Milstone DS, Spiegelman BM, Mortensen RM. PPAR gamma is required for the differentiation of adipose tissue in vivo and in vitro. *Mol Cell*. 1999;4:611-617.
[161] Hudak CS, Sul HS. Pref-1, a gatekeeper of adipogenesis. *Front Endocrinol (Lausanne)*. 2013;4:79.
[162] Sul HS. Minireview: Pref-1: role in adipogenesis and mesenchymal cell fate. *Mol Endocrinol*. 2009;23:1717-1725.
[163] Phipps KD, Gebremeskel S, Gillis J, Hong P, Johnston B, Bezuhly M. Alternatively Activated M2 Macrophages Improve Autologous Fat Graft Survival in a Mouse Model through Induction of Angiogenesis. *Plast Reconstr Surg*. 2015;135:140-149.
[164] Debels H, Galea L, Han XL, Palmer J, van Rooijen N, Morrison W, Abberton K. Macrophages play a key role in angiogenesis and adipogenesis in a mouse tissue engineering model. *Tissue Eng Part A*. 2013;19:2615-2625.
[165] Poon CJ, Pereira ECMV, Sinha S, Palmer JA, Woods AA, Morrison WA, Abberton KM. Preparation of an adipogenic hydrogel from subcutaneous adipose tissue. *Acta Biomater*. 2013;9:5609-5620.
[166] Lilja HE, Morrison WA, Han XL, Palmer J, Taylor C, Tee R, Moller A, Thompson EW, Abberton KM. An adipoinductive role of inflammation in adipose tissue engineering: key factors in the early development of engineered soft tissues. *Stem Cells Dev*. 2013;22:1602-1613.
[167] Levi B, Glotzbach JP, Sorkin M, Hyun J, Januszyk M, Wan DC, Li S, Nelson ER, Longaker MT, Gurtner GC. Molecular analysis and differentiation capacity of adipose-derived stem cells from lymphedema tissue. *Plast Reconstr Surg*. 2013;132:580-589.
[168] Shoham N, Gefen A. Mechanotransduction in adipocytes. *J Biomech*. 2012;45:1-8.
[169] Levy A, Enzer S, Shoham N, Zaretsky U, Gefen A. Large, but not small sustained tensile strains stimulate adipogenesis in culture. *Ann Biomed Eng*. 2012;40:1052-1060.
[170] Kato H, Suga H, Eto H, Araki J, Aoi N, Doi K, Iida T, Tabata Y, Yoshimura K. Reversible adipose tissue enlargement induced by external tissue suspension: possible contribution of basic fibroblast growth factor in the preservation of enlarged tissue. *Tissue Eng Part A*. 2010;16:2029-2040.
[171] Trayhurn P. Hypoxia and adipose tissue function and dysfunction in obesity. *Physiol Rev*. 2013;93:1-21.
[172] Mestas J, Hughes CC. Of mice and not men: differences between mouse and human immunology. *J Immunol*. 2004;172:2731-2738.
[173] Parekh C, Crooks GM. Critical differences in hematopoiesis and lymphoid development between humans and mice. *J Clin Immunol*. 2013;33:711-715.
[174] Suga H, Eto H, Aoi N, Kato H, Araki J, Doi K, Higashino T, Yoshimura K. Adipose tissue remodeling under ischemia: death of adipocytes and activation of stem/progenitor cells. *Plast Reconstr Surg*. 2010;126:1911-1923.
[175] Kato H, Mineda K, Eto H, Doi K, Kuno S, Kinoshita K, Kanayama K, Yoshimura K. Degeneration, Regeneration, and Cicatrization after Fat Grafting: Dynamic Total Tissue Remodeling during the First 3 Months. *Plast Reconstr Surg*. 2014;133:303e-313e.
[176] Khouri RK, Jr., Khouri RE, Lujan-Hernandez JR, Khouri KR, Lancerotto L, Orgill DP. Diffusion and perfusion: the keys to fat grafting. *Plast Reconstr Surg Glob Open*. 2014;2:e220.
[177] Khouri RK, Rigotti G, Cardoso E, Khouri RK, Jr., Biggs TM. Megavolume autologous fat transfer: part II. Practice and techniques. *Plast Reconstr Surg*. 2014;133:1369-1377.
[178] Morrison WA, Marre D, Grinsell D, Batty A, Trost N, O'Connor AJ. Creation of a Large Adipose Tissue Construct in Humans Using a Tissue-engineering Chamber: A Step Forward in the Clinical Application of Soft Tissue Engineering. *EBioMedicine*. 2016;6:238-245.

[179] Zhan W, Marre D, Mitchell GM, Morrison WA, Lim SY. Tissue Engineering by Intrinsic Vascularization in an In Vivo Tissue Engineering Chamber. *J Vis Exp*. 2016;30(111).
[180] Schlenz I, Kaider A. The Brava external tissue expander: is breast enlargement without surgery a reality? *Plast Reconstr Surg*. 2007;120:1680-1689; discussion 1690-1681.
[181] Fuentes-Felix C. BRAVA: Results did not meet expectations. *Aesthet Surg J*. 2003;23:42.
[182] Smith CJ, Khouri RK, Baker TJ. Initial experience with the Brava nonsurgical system of breast enhancement. *Plast Reconstr Surg*. 2002;110:1593-1595; author reply 1595-1598.
[183] Greco RJ. Nonsurgical breast enhancement--fact or fiction? *Plast Reconstr Surg*. 2002;110:337-339.
[184] Licata AA. Bisphosphonate therapy. *Am J Med Sci*. 1997;313:17-22.
[185] Frith JC, Monkkonen J, Auriola S, Monkkonen H, Rogers MJ. The molecular mechanism of action of the antiresorptive and antiinflammatory drug clodronate: evidence for the formation in vivo of a metabolite that inhibits bone resorption and causes osteoclast and macrophage apoptosis. *Arthritis Rheum*. 2001;44:2201-2210.
[186] van Rooijen N, van Kesteren-Hendrikx E. Clodronate liposomes: perspectives in research and therapeutics. *J Liposome Res*. 2002;12:81-94.
[187] van Rooijen N, van Kesteren-Hendrikx E. "In vivo" depletion of macrophages by liposome-mediated "suicide". *Methods Enzymol*. 2003;373:3-16.
[188] Konig S, Nitzki F, Uhmann A, Dittmann K, Theiss-Suennemann J, Herrmann M, Reichardt HM, Schwendener R, Pukrop T, Schulz-Schaeffer W, Hahn H. Depletion of cutaneous macrophages and dendritic cells promotes growth of basal cell carcinoma in mice. *PLoS One*. 2014;9:e93555.
[189] Wu X, Schulte BC, Zhou Y, Haribhai D, Mackinnon AC, Plaza JA, Williams CB, Hwang ST. Depletion of M2-like tumor-associated macrophages delays cutaneous T-cell lymphoma development in vivo. *J Invest Dermatol*. 2014;134:2814-2822.
[190] Stratis A, Pasparakis M, Rupec RA, Markur D, Hartmann K, Scharffetter-Kochanek K, Peters T, van Rooijen N, Krieg T, Haase I. Pathogenic role for skin macrophages in a mouse model of keratinocyte-induced psoriasis-like skin inflammation. *J Clin Invest*. 2006;116:2094-2104.
[191] Ward NL, Loyd CM, Wolfram JA, Diaconu D, Michaels CM, McCormick TS. Depletion of antigen-presenting cells by clodronate liposomes reverses the psoriatic skin phenotype in KC-Tie2 mice. *Br J Dermatol*. 2011;164:750-758.
[192] Warren Peled A, Kappos EA. Lipedema: diagnostic and management challenges. *Int J Womens Health*. 2016;8:389-395.
[193] Harwood CA, Bull RH, Evans J, Mortimer PS. Lymphatic and venous function in lipoedema. *Br J Dermatol*. 1996;134:1-6.
[194] Amann-Vesti BR, Franzeck UK, Bollinger A. Microlymphatic aneurysms in patients with lipedema. *Lymphology*. 2001;34:170-175.
[195] Zaugg-Vesti B, Dorffler-Melly J, Spiegel M, Wen S, Franzeck UK, Bollinger A. Lymphatic capillary pressure in patients with primary lymphedema. *Microvasc Res*. 1993;46:128-134.
[196] Avraham T, Zampell JC, Yan A, Elhadad S, Weitman ES, Rockson SG, Bromberg J, Mehrara BJ. Th2 differentiation is necessary for soft tissue fibrosis and lymphatic dysfunction resulting from lymphedema. *Faseb J*. 2013;27:1114-1126.
[197] Ghanta S, Cuzzone DA, Torrisi JS, Albano NJ, Joseph WJ, Savetsky IL, Gardenier JC, Chang D, Zampell JC, Mehrara BJ. Regulation of inflammation and fibrosis by macrophages in lymphedema. *Am J Physiol Heart Circ Physiol*. 2015;308:H1065-1077.